ANTAL KERPELY DOCTORAL SCHOOL OF MATERIALS SCIENCE & TECHNOLOGY

The Behavior of Noble Metals and Rare Earth Elements During Biomass Combustion

A PhD dissertation submitted to Antal Kerpely Doctoral School of Materials Science & Technology for the degree of Doctor of Philosophy in the subject of Materials Science and Technology

By

Truong Phi Dinh

MSc. Mechanical Engineering

Supervisors

Helga Kovács, PhD

Associate Professor

Zsolt Dobó, PhD

Senior Research Fellow

Institute of Energy, Ceramics and Polymer Technology

Faculty of Materials and Chemical Engineering

University of Miskolc

Miskolc, Hungary

2024

ACKNOWLEDGMENTS

First and foremost, I would like to express my sincerest and deepest gratitude to my supervisors, Dr. Helga Kovács and Dr. Zsolt Dobó, for their expert guidance, fruitful suggestions, and continuous encouragement during all stages of my PhD journey. I have been extremely lucky to get an opportunity to work with them. From them, I have learned a great deal which is essential for me to become an independent and critical-thinking researcher beyond my school life. Apart from the daily scientific support, they are the first people I think about knocking on the door in all circumstances.

I extend my appreciation to all the colleagues and staff members of the Institute of Energy, Ceramics and Polymer Technology for their generous help and assistance. The kind people and the friendly environment of my institute make me feel like it is my second home.

I would like to acknowledge the financial support of the Stipendium Hungaricum Scholarship Program from Tempus Public Foundation, which provided me with a golden opportunity to pursue my doctoral study at the University of Miskolc, Hungary.

Last but not least, my loving thanks go to my family, the biggest source of my strength and motivation. This work is a special dedication to my mother, Mrs. Le Thi Ngan for her constant love, endless care, and sacrifice. I owe my heartiest gratitude to my father Mr. Dinh Chinh Hanh, who has guided and inspired me devoutly throughout my life. I also thank my adorable nephew, Doan Nhat Minh, as well as my beloved sister, Dinh Thi Viet Hong, and her husband, Doan Van Quyen, for their unwavering inspiration and encouragement during the long journey of my PhD study. I am grateful for their unending support, without which my doctorate would not have been possible.

Truong Phi Dinh

Miskolc, 2024

TABLE OF CONTENTS

LIST OF ABBREVIATIONS

Nomenclature	Meaning
BA	Bottom ash
BF	Bioaccumulation factor
CB	Contaminated biomass
Ci	Contaminated biomass combustion experiment of "i" kW
DA	Deposited ash
EA	After heat exchanger ash
EF	Enrichment factor
FA	Fly ash
NB	Normal biomass or common market pellet
Ni	Normal biomass combustion experiment of "i" kW
NM	Noble metal
REE	Rare earth element
TF	Translocation factor
WB	Woody biomass

1. INTRODUCTION

In the context of industrialization and urbanization, the world is facing a series of issues such as environmental pollution, climate change, and the depletion of natural sources comprising fossil fuels and metal resources. These ongoing problems promote the utilization of biomass for thermal and electric energy production, as well as enforce the world to recover metals from secondary minerals. “The Behavior of Noble Metals and Rare Earth Elements During Biomass Combustion” is an innovative topic contributing to resolving the aforementioned global concerns, having impacts on multiple industries of waste management, energy production, and metal recovery. The main goal of my PhD research is to develop a suitable combustion and flue gas system for pelletized polluted biomass in order to investigate the fate of noble metals (NMs) and rare earth elements ($REEs$) during incineration. The experimental system aims to capture NMs and $REEs$ in solid remains to prepare for extraction and reduce their emission. Besides that, leaching of the combustion solid residues paving a potential pathway in reclaiming high-value metals is also the major interest of this study.

To achieve the main purposes of the study, the research work started with a literature review to identify the gaps of knowledge. This is followed by finding a possible location for contaminated biomass sampling based on the chemical analysis results of biomass ashes obtained from different sampling points. From the selected land, a bulk collection of ligneous plants was conducted alongside sample preparation steps such as drying, grinding, and pelletizing. Importantly, a combustion and flue gas system was built for contaminated biomass incineration. The development of the experimental system was carried out in several stages during my PhD research. Following the finalization of the system, a series of combustion experiments utilizing contaminated pellets and common market pellets was conducted under different operational conditions. Solid remains from different positions in the experimental system were collected and analyzed to investigate the fate of metals including NMs and $REEs$, as well as the influence of combustion parameters and feedstocks on the metal flows during biomass incineration. The combustion solid remains furtherly were subjected to SEM examinations to scrutinize the formation of the high-value metals. Additionally, a leaching procedure was proposed with the prospect of recovering valuable metals from the contaminated biomass ashes.

2. LITERATURE REVIEW

Reviewing the literature is essential to identify the gaps of knowledge as well as to clarify the directions of the PhD topic. The review concentrates on the distribution of metals during biomass combustion, and the overall concept of phytomining-enrichment-extraction to reclaim valuable metals. Based on the literature review, we published three review papers, and two of them were published in *Chemosphere* which is a D1 journal. The literature review presented in the following sub-sections is a base extracted knowledge of the PhD topic and the ground for all the experiments.

2.1. The behavior of metals in the burning system during biomass combustion

2.1.1. Biomass used for phytoextraction

Biomass is a renewable energy resource including plant and animal materials, its reservations are limitless. Biomass energy offers a variety of environmental advantages such as reducing climate change, mitigating acid rain, water pollution, soil erosion, etc. Therefore, biomass is a potential energy resource to diversify world fuel supplies and substantially decrease greenhouse gas emissions [1]. According to reported data, biomass made up 64% of renewable energy's contribution [2] and it is anticipated to rise around double to triple in 2050 [3]. Woody biomass has been known as an extensively used and the most plentiful resource of biomass. Statistically, more than one-third of the global lands are contaminated sites [4], called brownfields [5]. The real number even might be higher than what has been reported so far. Mineral oil and metals are the most contaminants contributing 60% to contaminated lands [6]. The mounting demand for metals in modern industry has stimulated a surge in mining activities, which has led to the release of these elements into the environment. Intensifying metal content in the environment adversely impacts the ecosystem and potentially threatens human health [7], [8]. On the other hand, the increasing metal concentration in soils provides the opportunity to recover metals from secondary resources to strengthen the circular economy.

Phytoextraction, using plants accumulating metals, is known as a feasible way to either remove metals (toxic metals) from contaminated soils (a process called phytoremediation) [9], [10] or to extract valuable metals (referred to as phytomining) [11]–[13]. During the phytoextraction process, plants accumulate metals from contaminated soils, transfer and store them into the roots and above-ground parts of the plants with various distributions [14]. Two types of plants can be efficiently used for phytoextraction, those are hyperaccumulators and

fast-growing species. Hyperaccumulators have been defined as plants that can accumulate huge amounts of metals in the soil without suffering [15]. Fast-growing species that have lower metal extracting ability than hyperaccumulators, however, their total biomass production is outstandingly higher such as poplar or willow [16], [17]. The lower limit for hyperaccumulation and studies corresponding to metals accumulated by plants are summarized in *Table 2.1*.

Table 2.1. Studies on metals accumulated by plants.

Element	Threshold (mg kg^{-1})	Plant species	Concentration in plant (mg kg^{-1})	Ref.
REEs	1000	*Dicranopteris linearis* (fern)	4438	[18]
		Dicranopteris dichotoma (fern)	2231	[19]
		Hickory	2296 (in leaves)	[20]
Ag	1	*Lupinus sp.* (blue lupin) - induced	126	[21]
		Amanita species (mushroom)	1253	[22]
		Tobacco - induced	54.3	[23]
Au	1	*Lupinus sp.* (blue lupin) - induced	6.3	[21]
		B. juncea (indian mustard) – induced	63	[24]
		Z. mays (corn) - induced	20	[24]
Pt	1	*Berkheya coddii* (flowering plant) - induced	0.183	[25]
		Berkheya coddii (flowering plant)	0.22 (in leaves) 0.14 (in roots)	[26]
Pd	1	*Berkheya coddii* (flowering plant) - induced	7.677	[25]
		Berkheya coddii (flowering plant)	0.71 (in leaves) 0.18 (in roots)	[26]
		Cannabis sativa (hemp)	30.336	[27]
Ni	1000	*Berkheya coddii* (flowering plant)	7880	[28]
		Alssum lesbiacum (flowering plant)	10000	[28]
Tl	100	*Iberis intermedia* (herbaceous plant)	4055	[29]
		Biscutella laevigata (flowering plant)	13768	[29]
Co	1000	*Berkheya coddii* (flowering plant)	290	[30]
		Haumaniastrum robertii (flowering plant)	4304 (in leaves)	[31]
Zn	10,000	*Thlaspi caerulescens* (alpine pennygrass)	43710	[32]
		Dichapetalum gelonioides (small semi-evergreen tree)	30000	[32]
Pb	1000	*Minuartia verna* (spring sandwort)	20000	[32]
		Agrostis tenuis (grass)	13490	[32]
Ca	100	*Thlaspi caerulescens* (alpine pennygrass)	2130	[32]
		Arabidopsis halleri (flowering plant)	267	[33]
Cu	1000	*Angiopteris sp. nov.* (fern)	3535	[34]
		Anisopappus davyi (sunflower)	3504	[34]
Mn	10,000	*Phytolacca acinosa* (herbaceous plant)	12180 (in leaves)	[35]
		Chengiopanax sciadophylloides (flowering tree)	23200 (in leaves)	[36]
Cr	300	*Leersia hexandra* (grass)	2978 (in leaves)	[37]
As	1000	*Pteris vittata* (brake fern)	3280–4980	[38]
		Pityrogramma calomelanos (fern)	8350 (in leaves)	[39]

2.1.2. The fate of metals during biomass combustion

Contaminated biomass used for phytoextraction requires appropriate management as it contains certain amounts of metals transferred from brownfields. Several methods of contaminated biomass treatments have been introduced including composting, compaction, direct disposal, leaching, and thermal conversion (pyrolysis, gasification, combustion) [40], [41]. Of these techniques, combustion is the most viable approach for the disposal of polluted biomass [42].

Table 2.2. Concentrations of metals in solid remains (mg kg^{-1}), adapted from [51].

Metal	Bottom ash			Cyclone ash		Filter ash			Flue dust
	[52]	[53]	[54]	[52]	[54]	[52]	[53]	[54]	[54]
As	9.2	<3	3	25.6	1.9	5.1	16	0.7	0.2
Ba	534.9	330	-	671.4	-	206.4	2000	-	-
Cd	1.1	<0.3	1.2	2.3	8.6	1.9	3	6.6	1.9
Co	6.7	2.5	9.7	11.5	3.7	6.4	8	0.6	0.2
Cr	24.6	15	187	128.1	50.7	10.1	24	15.2	4.6
Cu	12.8	<10	147.1	31.6	51.6	18.9	60	29.9	8.8
Fe	5230.9	-	11756.8	8136	4442.2	1988.3	-	384.1	116.9
Mn	4864	-	12293	7144	5700	5020	-	779	228
Ni	28.5	19	27.1	68.3	14.6	24.5	67	3.5	1.1
Pb	29	<3	43.4	36.1	22.5	23.4	49	27.5	8.2
Ti	160	-	-	179	-	982	-	-	-
V	-	95	32.2	-	10.3	-	140	2	0.6
Zn	99.2	160	485.9	252	946.7	61.7	480	511.1	150.8
Hg	0.005	<0.03	0.003	0.007	0.03	0.014	<0.3	0.283	0.084

During the combustion process, metals in biomass enter the combustion chamber and subsequently exit in one of the three major forms namely, solid residues in the combustion chamber (bottom ash), solid particles in the flue gas (fly ash), and the exhausted gas (flue gas). The distribution of metals during biomass combustion depends on various factors such as feedstock properties, type of boiler/furnace, operating conditions (combustion temperature, flue gas temperature, pressure, oxygen, residence time), the boiling point of metals/compounds, presence of chlorine, etc [43], [44]. During the incineration of contaminated biomass, metals were rather volatized and exited the combustion system in the gaseous form [45]. Some studies summarized in *Table 2.2* show that most of the metals were found in bottom ash and cyclone ash. Nonetheless, in another work, Vassilev et al. [46] concluded that more than 90% of Cd,

Hg, Sb, Se, and V are volatilized during biomass combustion, meanwhile, the volatilization rate is over 50% in the case of As, Cr, Pb, or Zn. Likewise, Kovacs et al. [45] revealed that more than 50% of the total metal input (except Ni) could not be detected in bottom ash and fly ash as seen in *Figure 2.1*. Several studies have been conducted focusing on the fate of heavy metals [46]–[50]. Meanwhile, the behavior of NMs and $REEs$ in the burning system during biomass combustion has been barely investigated. This gap of knowledge is the major interest of my doctoral research.

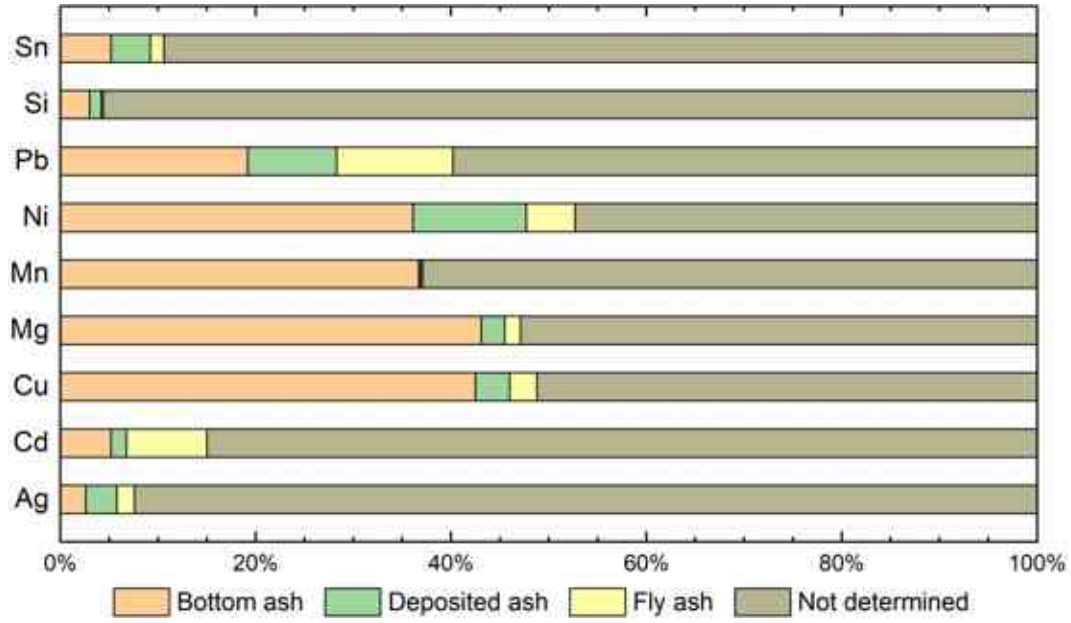

Figure 2.1. Metal flow during combustion of contaminated biomass [45].

2.2. The overall concept of noble metal and rare earth element phytomining

Besides traditional mining, producing of valuable metals from other sources is being explored such as the extraction of noble metals (NMs) and rare earth elements ($REEs$) from different waste streams, strengthening the circular economy concept while it provides economic value. Phytomining of noble metals and rare earth elements is another possibility to produce these metals offering high value with environmentally friendly methods and economic feasibility. Phytoextraction, using plants accumulating metals, is known as a feasible way to either remove metals from contaminated soils (a process called phytoremediation) or to extract valuable metals (referred to as phytomining) [11]–[13]. Phytomining is widely applied to recover for example nickel from brownfield lands [55], [56]. However, studies focusing on NM and REE accumulation in plants and extraction from plants are limited and therefore the overall concept needs to be investigated in more depth.

2.2.1. Noble metals and rare earth elements

The research topic focuses on noble metals and rare earth elements. This sub-section aims at giving a glimpse of these valuable metals. *Table 2.3* shows important information about NMs and $REEs$ as well as the other common metals for comparison purposes. The melting point and the boiling point are also included in that table as they influence the behavior of metals in the burning system. The higher boiling point leads to the lower volatilization of metal during combustion.

Noble metals

Noble metals (NMs) are a group of metals that are resistant to corrosion and oxidation even in humid air when heated [57]. Usually, noble metals are considered to comprise silver (Ag), gold (Au), and platinum sub-group metals including iridium (Ir), osmium (Os), palladium (Pd), platinum (Pt), rhodium (Rh), and ruthenium (Ru).

NMs are scarce and distributed in low concentrations in Earth's crust as seen in *Table 2.3*. NMs are widely known for their uses in jewelry and coinage (used as currency and investment), but they have a variety of applications in industry such as catalysts, metallurgy, electronic devices, or high-level technology. Industrial sectors of automotive catalysts, catalytic converters utilize valuable metals, namely Pd, Pt, and Rh. Other applications comprise electronic devices such as computers, laptops, and mobile phones, which use multiple NMs such as Ag, Au, Pt, and Pd. Furthermore, Pt and Ru are mainly used in the fuel cells area. The number of potential utilizations is anticipated to increase in the future with new methods and developments. In the economic aspect, noble metals are also called precious metals and receive increasing interest worldwide owing to their high economic value. NMs are supremely expensive, they are much more priced than common industrial metals and $REEs$, and their cost is escalating in general (*Table 2.3*).

The supply and demand of NMs are shown in *Figure 2.2*. The production and consumption of other noble metals tend to increase, which reflects their growing applications in recent years. The NMs market plummeted steeply in 2020 since the Covid-19 pandemic triggered temporary closures of mines and disruption in most end-use sectors, but it is snapping back after the slump. Based on the figure, even though the recycling of NMs has been rising gradually, this provision accounts for a smaller portion of the total metal supply (roughly 15–25%).

Table 2.3. The abundance in earth's crust [58], *properties* [57], [59], [60], *and recent price* [61]–[64] *of REEs, NMs, and base metals.*

Element	Name	Abundance	Melting point	Boiling point	Price (USD kg^{-1})					
		(mg kg^{-1})	(°C)	(°C)	Purity (%)	Jun-2019	Jan-2020	Jan-2021	Jan-2022	Jan-2023
Ag	Silver	0.075	962	2212	-	529.1	633.7	913.5	815.9	837.8
Au	Gold	0.004	1065	2807	-	47939	55051	65856	64084	66972
Ir	Iridium	0.001	2410	4130	-	47583	47587	102661	127956	149625
Os	Osmium	0.0015	3900	5510	99.9995	1341830	1392510	1621480	1853250	1919970
Pd	Palladium	0.015	1552	3141	-	46546	72465	77104	65183	56604
Pt	Platinum	0.005	1772	3825	-	26139	31915	35276	32102	34315
Rh	Rhodium	0.001	1976	3730	-	101714	274676	635399	529762	393702
Ru	Ruthenium	0.001	2310	3900	-	8151	8038	9181	17408	15045
Ce	Cerium	66.5	798	3426	99.9	5.15	4.66	-	-	-
Dy	Dysprosium	5.2	1412	2562	99.5	280.0	304.9	-	-	-
Er	Erbium	3.5	1529	2863	99.5	27.90	27.26	-	-	-
Eu	Europium	2	822	1597	99.999	32.70	33.00	-	-	-
Gd	Gadolinium	6.2	1313	3266	99.5	25.40	28.70	-	-	-
Ho	Holmium	1.3	1474	2695	99.5	58.80	58.83	-	-	-
La	Lanthanum	39	918	3457	99.9	5.30	4.88	-	-	-
Lu	Lutetium	0.5	1663	3395	99.99	610.0	647.2	-	-	-
Nd	Neodymium	41.5	1021	3068	99.5	48.05	52.66	-	-	-
Pr	Praseodymium	9.2	931	3512	99.5	103.0	93.27	-	-	-
Pm	Promethium	-	1042	-	-	-	-	-	-	-
Sm	Samarium	7.05	1074	1791	99.9	13.50	17.22	-	-	-
Sc	Scandium	22	1541	2831	99.99	3194	3487	-	-	-
Tb	Terbium	1.2	1356	3223	99.99	770.0	645.0	-	-	-
Tm	Thulium	0.52	1545	1947	-	-	-	-	-	-
Yb	Ytterbium	3.2	819	1194	99.999	30.50	33.72	-	-	-
Y	Yttrium	33	1522	3338	99.99	15.70	17.94	-	-	-
Al	Aluminium	82300	660	2470	-	1.75	-	-	29.99	25.21
Cu	Copper	60	1085	2562	-	5.87	-	-	97.47	90.19
Ni	Nickel	84	1455	2913	-	11.97	-	-	220.1	284.8
Pb	Lead	14	328	1749	-	1.89	-	-	23.28	21.89
Zn	Zinc	70	420	907	-	2.60	-	-	35.79	32.69

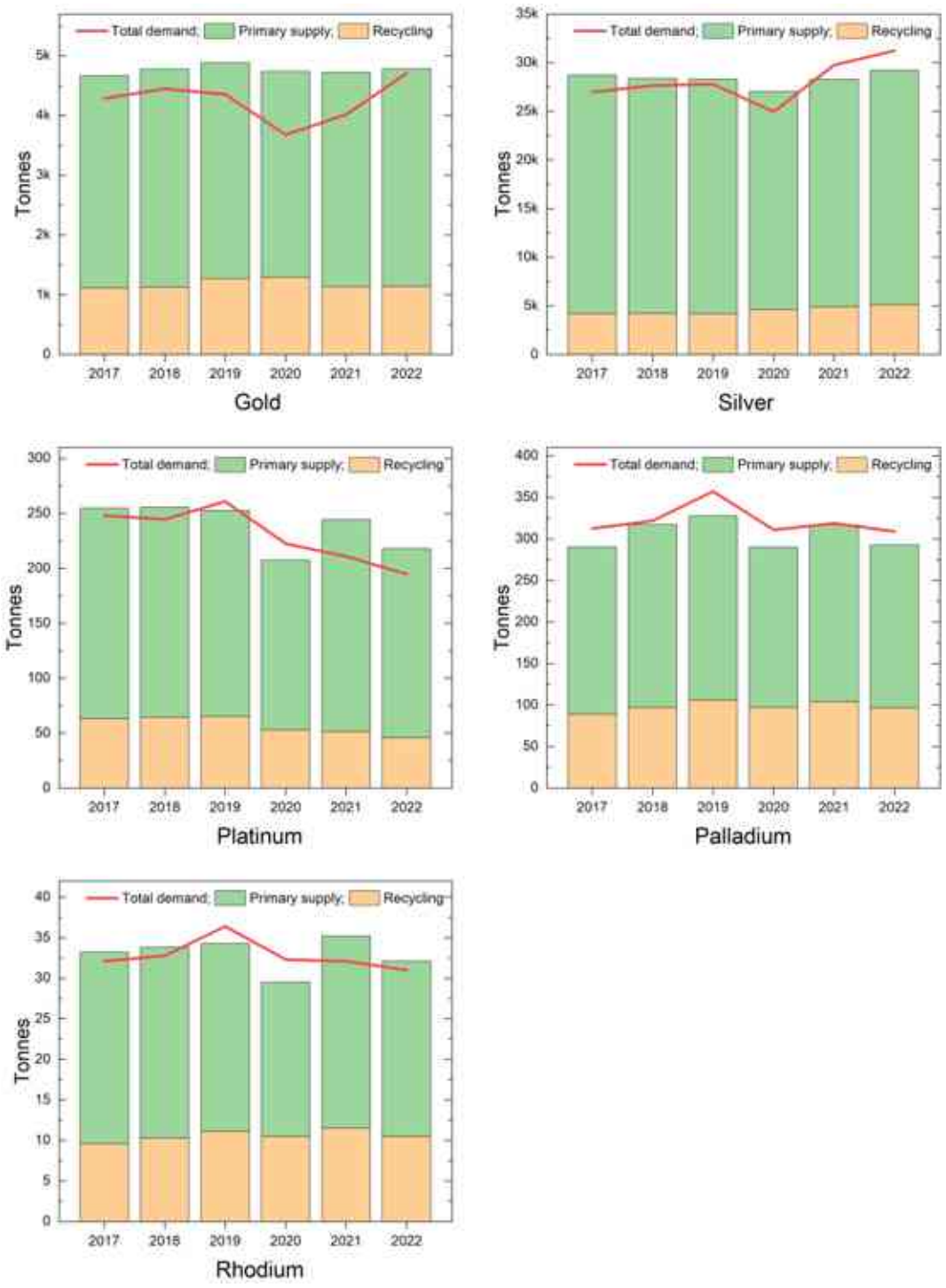

Figure 2.2. Supply and demand of some noble metals in recent years (Sources: [64]–[66]*).*

Rare earth elements

Rare earth elements ($REEs$) are a group of 17 chemically similar metallic elements in the periodic table, including scandium (Sc), yttrium (Y), and 15 "lanthanides" elements, from lanthanum (La) to lutetium (Lu). The terms rare earths (REs) and rare earth metals or minerals

($REMs$) are also used. $REEs$ are divided into two groups, which are light rare earth elements ($LREEs$) and heavy rare earth elements ($HREEs$). $LREEs$ are lanthanum (La), cerium (Ce), promethium (Pm) praseodymium (Pr), neodymium (Nd), samarium (Sm), europium (Eu), and scandium (Sc). The elements gadolinium (Gd), terbium (Tb), dysprosium (Dy), holmium (Ho), erbium (Er), thulium (Tm), ytterbium (Yb), lutetium (Lu), and yttrium (Y) are defined as $HREEs$ [67].

Rare earth elements are not as rare as their name suggests; the term "rare" relates to the complex and challenging metallurgical isolation processes needed to obtain the individual metal species. $REEs$ are in reasonable abundance in the Earth's crust. Cerium (Ce) is the most abundant rare earth element; its concentration (66.5 mg kg^{-1}) is even higher than that of common metals like lead (Pb, 14 mg kg^{-1}) or copper (Cu, 60 mg kg^{-1}) [58]. Nonetheless, $REEs$ are mostly dispersed throughout the Earth's crust at low levels, as shown in *Table 2.3*. Especially, promethium (Pm) only presents in very minute amounts in natural materials since it has no long-lived or stable isotopes [68]. The rarest metal is best known as an artificial element, and no concentration in Earth's crust has been reported so far. $REEs$ occur in nature in their oxidized form in minerals and salts because of their electropositive nature and high affinity for oxygen.

The applications of $REEs$ vary in multiple industrial areas. They are playing an increasingly vital role in industry, especially in green high-technology applications, such as wind turbines, hybrid cars, electric cars, batteries, etc. [69]. Moreover, these valuable elements are also widely utilized as fertilizers in agriculture to enhance the production and quality of crops [70], [71]. Despite high demand, the supply of $REEs$ is limited and dominated by China, the source of up to 97% of global rare earth production [72]. Furthermore, the recycling rate of $REEs$ is still extremely limited at only approximately 1% of end-products [69].

The price of rare earth elements is not widely available; it is presented in *Table 2.3*. $REEs$ are quite valuable and more expensive than base metals. Some $REEs$ such as scandium (Sc), lutetium (Lu), and terbium (Tb) are relatively high-priced. That can be explained by the importance of these rare earth metals.

NMs and $REEs$ are considered critical strategic resources [73]–[75] according to supply risk, economic importance, and cruciality to the progress of science and technology [76]. The demand for these valuable metals has dramatically increased, while their natural ores are limited and unevenly distributed. Therefore, recovery of NMs and $REEs$ from urban mines such as

tailings, waste catalysts, electronic wastes, slag, ashes, etc. is crucial, it assists to secure resources for sustainable development.

2.2.2. Phytomining of NMs and $REEs$

Hyperaccumulators are usually chosen for phytomining; these plants accumulate vast quantities of NMs and $REEs$ in their aerial parts without substantial adverse effects. Their metal concentration is 100 times higher than "normal" plants (non-accumulators) growing in the same environment [77]. The lower limit for hyperaccumulators shown in *Table 2.1* has not been thoroughly defined. The suggested threshold concentration for REE hyperaccumulators could range from 100 to 1000 mg kg^{-1} [78]. Meanwhile, the lower limit is 1 mg kg^{-1} for the hyperaccumulation of NMs [77].

During the phytoextraction process, plants accumulate NMs and $REEs$ from contaminated lands and transport them in roots and other plant parts. Hyperaccumulators actively transfer NMs and $REEs$ from roots to shoots, and storage of the metals in root parts is generally limited. The distribution of NMs and $REEs$ within the major components of plants varies substantially, depending on the plant species and metals. Several studies have verified that the concentration of NMs and $REEs$ in the below-ground parts is usually higher than in the above-ground parts (stems, leaf) [79]–[82]. This can be explained by the accumulation rate of NMs and $REEs$ from the substrate to root being higher than the translocation rate from root to aerial tissues [83]. Contrarily, in other investigations, the highest concentration of NMs and $REEs$ was observed in the above-ground parts (stem, leaf) due to substantial translocation of these metals from root to shoot [19], [84], [85]. The difference in $REEs$ concentration among plants might reflect the disparate mobility of these elements in various plants.

The bioaccumulation factor (BF) and translocation factor (TF) are utilized to describe the bioaccumulative properties of hyperaccumulators. The bioaccumulation factor is the quotient of metal concentration in shoots to that in soils. This index is used to depict the capability of plants to accumulate NMs and $REEs$ from substrates and translocate them into their aerial tissues. The translocation factor is the ratio of metal concentration in shoots to that in roots. The higher the TF, the better the ability of the plant to transfer NMs and $REEs$ from below-ground plant parts to above-ground plant parts. This index is crucial for the application of phytomining because usually only the above-ground plant parts are harvested. BF and TF higher than 1 is the pre-requisite for hyperaccumulators [86]. The definitions of the two factors are seen in the equations below.

$$Bioaccumulation\ factor\ (BF) = \frac{Metal\ concentration\ in\ shoot}{Metal\ concentration\ in\ soil} \quad (1)$$

$$Translocation\ factor\ (TF) = \frac{Metal\ concentration\ in\ shoot}{Metal\ concentration\ in\ root} \quad (2)$$

Some notable studies on NMs and $REEs$ accumulated by plants are summarised in *Table 2.4* and *Table 2.5*. *Brassica juncea* (Indian mustard) and *Berkheya coddii* (Asteraceae) are commonly used in the phytomining of NMs. Meanwhile, REE phytomining employs *Phytolacca americana* (pokeweed) and fern species. The BF and TF of those plants usually are higher than one, proving their ability to accumulate and translocate NMs and $REEs$.

Table 2.4. Studies on NMs accumulated by plants.

Element	Plant species	Substrate	Accumulation	Ref.
Au	- *B. juncea* (Indian mustard)	- Disseminated Au in sand: 5 mg kg^{-1} Au - Treatment: NH_4SCN 0, 80, 160, 320, and 640 mg kg^{-1}	- In aerial parts of the plants: up to 57 mg kg^{-1} Au	[87]
Au	- Five crops (carrot, red beet, onion, and two cultivars of radish) - Induced hyperaccumulator	- Artificial substrate: 3.8 mg kg^{-1} Au - Treatment: NH_4SCN (1.0 g kg^{-1}) and $(NH_4)_2S_2O_3$ (2.0 g kg^{-1})	- In roots of Carrot: 48.3 mg kg^{-1} Au - In roots of Salad radish: 113 mg kg^{-1} Au - In roots of Oriental radish: 102 mg kg^{-1} Au	[80]
Au	- *Brassica juncea* (Indian mustard), *Berkheya coddii* (Asteraceae), and *Cichorium intybus* (chicory) - Induced hyperaccumulator	- Artificial gold-bearing soil: 5 mg kg^{-1} Au - Treatment: KCN, NaSCN, KI, KBr, $(NH_4)_2S_2O_3$	- *Brassica juncea*: 88, 46, 326 mg kg^{-1} Au in root, stem, leaf respectively (treated by KCN) - *Berkheya coddii*: 36, 94, 97 mg kg^{-1} Au in root, stem, leaf respectively (treated by KCN) - *Cichorium intybus*: 164 mg kg^{-1} Au in the whole plant (treated by KCN)	[84]
Au	- *Brassica juncea* (Indian mustard) and *Zea mays* (corn) - Induced hyperaccumulator	- Oxidized ore pile: 0.6 mg kg^{-1} Au - Treatment: NaCN, KCN	- *Brassica juncea*: 39 mg kg^{-1} Au in plant (treated by NaCN) - *Zea mays*: 20 mg kg^{-1} Au in plant (treated by NaCN)	[24]
Au	- Australian native plant species and exotic agricultural species - Induced hyperaccumulator	- Oxide ore: 1.75 mg kg^{-1} Au - Treatment: NaCN (0.1 and 1 mg kg^{-1})	- *Trifolium repens* cv. Prestige stems: 26.87 mg kg^{-1} Au (treated by 1 mg kg^{-1} NaCN) - *Bothriochloa macra* (red grass) leaves: 23.78 mg kg^{-1} Au (treated by 1 mg kg^{-1} NaCN)	[88]
Au, Ag	- *Brassica juncea* (Indian mustard)	- Artificial soil: 48 mg kg^{-1} Au and 31 mg kg^{-1} Ag - Treatment: KCN	- Au: 760 mg kg^{-1} in plant - Ag: 730 mg kg^{-1} in plant	[89]
Au	- *Helianthus annuus L.* (sunflower) and *Kalanchoe serrata L.* (magic tower) - Induced hyperaccumulator	- Mine tailing: 2.35 mg kg^{-1} Au - Treatment: NaCN, NH_4SCN, $(NH_4)_2S_2O_3$, and $SC(NH_2)_2$	- *H. annuus* added NaCN: 14.9, 21.5, 19.2 mg kg^{-1} Au in root, stem, leaf respectively - *K. serrata*: 4.3–10.15 mg kg^{-1} Au in plant	[85]
Au	- *Lindernia crustacea* (Scrophulariaceae), *Paspalum conjugatum* (carabao grass), *Cyperus kyllingia* (nut grass) - Induced accumulation	- Cyanidation tailings: 1.68 mg kg^{-1} Au - Treatment: $(NH_4)_2S_2O_3$ (2 g kg^{-1}), NaCN (1 g kg^{-1})	- In the shoot of *Paspalum conjugatum* plant induced by $(NH_4)_2S_2O_3$: 0.602 mg kg^{-1} Au	[90]
Au, Ag	- Tobacco - Induced hyperaccumulator	- Cyanidation tailing: 1.03 mg kg^{-1} Au and 18.2 mg kg^{-1} Ag - Treatment: NaCN (0.05 g kg^{-1} of tailing)	- Au: 1.2 mg kg^{-1} in plant - Ag: 54.3 mg kg^{-1} in plant	[23]

Element	Plant species	Substrate	Accumulation	Ref.
Au, Ag	- *Brassica napus* (Rapeseed) - Induced hyperaccumulator	- Mine tailings: 0.5164 mg kg^{-1} Au and 22.1 mg kg^{-1} Ag - Treatment: NH_4SCN (1 g kg^{-1}), $(NH_4)_2S_2O_3$ (2 g kg^{-1}), inoculation of *Aspergillus niger* (fungus)	- Au (treated by NH_4SCN): in stems 1.5 mg kg^{-1}, in roots 10 mg kg^{-1} - Ag (treated by $(NH_4)_2S_2O_3$ and inoculated by *Aspergillus niger* fungus): around 50000, 30000, 15000 mg kg^{-1} in roots, stems, and leaves respectively	[91]
Ag	- Terrestrial plants: *Euphorbia macroclada* (spurge), *Verbascum cheiranthifolium Boiss* (Mullein flowering plant), *Astragalus gummifer* (leguminous) - Natural accumulation	- Polluted mining area	- In spurge twig: up to 0.97 mg kg^{-1} Ag - In spurge root: up to 3.12 mg kg^{-1} Ag	[92]
Ag	- *Amanita* species (mushroom), *A. strobiliformis*, and *A. solitaria* - Natural accumulation	- Soil: non-argentiferous areas (0.07–1.01 mg kg^{-1} Ag)	- *Amanita* species: mostly in the range of 200–700 mg kg^{-1} Ag - Highest Ag concentration: 1253 mg kg^{-1}	[22]
Au, Ag	- *Lupinus sp.* (blue lupin) - Induced hyperaccumulation	- Base-metal mine tailings - Chemical treatment	- Au: 6.3 mg kg^{-1} - Ag: 126 mg kg^{-1}	[77]
Ag	- *Brassica juncea* (Indian mustard) and *Medicago sativa* (alfalfa) - Artificial accumulation	- Aqueous substrate: 500–10000 mg kg^{-1} $AgNO_3$	- *Brassica juncea*: up to 124000 g kg^{-1} Ag (12.4%) in plant - *Medicago sativa*: up to 136000 g kg^{-1} Ag (13.6%) in plant	[93]
Pd	- *Pinus flexilis* (limber pine) - Natural accumulator	- Soil: 3.1 mg kg^{-1} Pd	- In the twig ash: 285 μg kg^{-1} Pd	[94]
Pd	- *Quercus chrysolepsis* (oak) - Natural accumulation	- Soil: 140 μg kg^{-1} Pd	- In plant ash: 400 μg kg^{-1} Pd	[95]
Pt, Pd	- *Berkheya coddii* (Asteraceae) - Natural accumulation	- Contaminated soil: 0.04 mg kg^{-1} Pt and 0.07 mg kg^{-1} Pd	- In leaf: 0.22 mg kg^{-1} Pt and 0.71 mg kg^{-1} Pd - In root: 0.14 mg kg^{-1} Pt and 0.18 mg kg^{-1} Pd	[26]
Pt, Pd, Au	- *Berkheya coddii* (Asteraceae) - Induced hyperaccumulator	- Mine tailing: 315 μg kg^{-1} Pd and 61.4 μg kg^{-1} Au - Treatment: KCN (10 g L^{-1})	- Pt: 183 μg kg^{-1} in plant - Pd: 7677 μg kg^{-1} in plant - Au: 1580 μg kg^{-1} in plant	[25]
Pd, Au	- *Cannabis sativa* (hemp) - Induced hyperaccumulator	- Gossan (rock): 205.5 μg kg^{-1} Pd, 20 μg kg^{-1} Au - Treatment: KCN (8 g L^{-1})	- Pd in aerial biomass: mean value 30336 μg kg^{-1}, highest value 62420 μg kg^{-1} - Au in aerial biomass: mean value 4528 μg kg^{-1}, highest value 7635 μg kg^{-1}	[27]
Pd	- *Salix purpurea* willow (Green Dicks) - Induced accumulation	- Synthetic ore medium: 50 mg kg^{-1} Pd - Treatment: KCN	- In leaf: 820 mg kg^{-1} Pd	[96]
	- *Miscanthus* (silver grass) - Induced accumulation	- Synthetic ore medium: 100 mg kg^{-1} Pd - Treatment: KCN	- In leaf: 505 mg kg^{-1} Pd	
Pd	- *Sinapis alba L.* (mustard), M*iscanthus* (silver grass), and Green dicks (willow) - Induced accumulation	- Synthetic tailings medium: 50 mg kg^{-1} Pd - Treatment: KCN (100 mg kg^{-1})	- Aerial plant of mustard: 500 mg kg^{-1} Pd - *Miscanthus*: 1500 mg kg^{-1} Pd - Leaf of willow: 800 mg kg^{-1} Pd	[97]
Ag, Pt	- Trees (oak, pine, birch, poplar, etc) - Natural accumulation	- Contaminated brownfield land	- Ag: 11.9 mg kg^{-1} in plant - Pt: 3.06 mg kg^{-1} in plant	[45]
Pt	- Grass species - Natural accumulation	- Soil: vicinity of a motorway	- In leaf: 19–42 μg kg^{-1} Pt - In root: 59–137 μg kg^{-1} Pt	[98]
Pt, Pd, Rh	- *Daucus carota* (wild carrot) - Natural accumulation	- Soil: vicinity of the heavy traffic locations	- Pt: 14.6 mg kg^{-1} (mean value in plant) - Pd: 10.2 mg kg^{-1} (mean value in plant) - Rh: 0.7 mg kg^{-1} (mean value in plant)	[99]
Pt, Pd, Rh	- *Sinapis alba* (white mustard) - Artificial accumulation	- Nutrient solution: 1.0 mg L^{-1} of Pt, Pd, Rh	- In aboveground parts: 95.8, 30.6, 145 mg kg^{-1} of Pt, Pd, Rh respectively - In roots: 5973, 1958, 74.2 mg kg^{-1} of Pt, Pd, Rh respectively	[100]
Rh	- *Phragmites australis* (common reed) - Natural accumulation	- River side affected by massive urbanization	- In plant: 1.11–1.13 mg kg^{-1} Rh	[101]

Table 2.5. Studies on REEs accumulated by plants.

Element	Plant species	Substrate	Accumulation	BF, TF	Ref.
$REEs$	Hickory (tree)	- Mining area	- Total rare earth oxides in dry leaf: 2000 mg kg^{-1}	–	[102]
$REEs$	Hickory (tree)	- Chester loam	- $\sum REEs$ in dry leaf: 2296 mg kg^{-1} - $\sum REEs$ in leaf ash: more than 25000 mg kg^{-1}	–	[20]
All $REEs$ except Pm, Sc	Hickory (tree)	- Non-mining area	- $\sum REEs$ in dry leaf: 2300 mg kg^{-1}	–	[103]
All $REEs$ except Pm, Sc, Y	Mockernut hickory (tree)	- Silt loam	- $\sum REEs$ in dry foliage: 136 mg kg^{-1} - $\sum REEs$ in foliage ash: 1350 mg kg^{-1}	–	[104]
$REEs$	*Phytolacca americana* (pokeweed)	- Non-mining area andesite soil - $\sum REEs$ in soil: 399.4 mg kg^{-1}	- $\sum REEs$ in dry leaf: 581.5 mg kg^{-1}	- BF = 1.5	[105]
$REEs$	*Phytolacca americana* (pokeweed)	- Mining region - $\sum REEs$ in soil: 303 to 691 mg kg^{-1}	- Highest $\sum REEs$ in leaf: 1040 mg kg^{-1} - In root: 70.6 to 386 mg kg^{-1} - In stem: 27.5 to 154 mg kg^{-1}	- BF = 1.5–3.4 - TF = 2.7–14.7	[106]
All $REEs$ except Pm	*Salix* (willow)	- Hydroponically grown in a greenhouse	- $\sum REEs$ in plant: 5678 mg kg^{-1}	–	[107]
2 $REEs$: La, Ce	*Dryopteris erythrosora* (fern) *Asplenium ruprechtii* (fern)	- Non-mining area	- $\sum REEs$ in leaf mesophyll tissue: 62 mg kg^{-1} - $\sum REEs$ in leaf mesophyll tissue: 54 mg kg^{-1}	– –	[108]
All $REEs$ except Pm, Sc	*Pronephrium simplex* (fern)	- Semi-tropical rainforest - $\sum REEs$ in soil: 34 mg kg^{-1}	- $\sum REEs$ in dry leaf: 1234 mg kg^{-1}	- BF = 36.3	[109]
All $REEs$ except Pm, Sc	*Pronephrium simplex* (fern)	- Semi-tropical rain forest	- $\sum REE$ in leaf: 3000 mg kg^{-1}	–	[110]
5 $REEs$: Ce, Eu, La, Sc, Sm	*Alsophila sternbergii* (tree fern)	- Atlantic forest - $\sum REEs$ in soil: 111.07 mg kg^{-1}	- $\sum REEs$ in plant: 57 mg kg^{-1}	- BF = 0.5	[111]
6 $REEs$: La, Ce, Sm, Gd, Yb, Y	*Onoclea sensibilis* (sensitive fern)	- Pot experiment - Artificial substrate containing 333 mg kg^{-1} of La, Ce, Sm, Gd, Yb, and Y	- $\sum REEs$ in plant: more than 200 mg kg^{-1}	- BF = 0.6	[112]
8 $REEs$: La, Ce, Nd, Sm, Eu, Tb, Yb, Lu	*Dicranopteris linearis* fern (formerly known as *Dicranopteris dichotoma)*	- Rare earth ore area	- $\sum REEs$ in dry leaf, root, stem: 3358, 38.6, 41.0 mg kg^{-1} respectively	- TF = 87.0	[113]
All $REEs$ except Pm, Sc	*Dicranopteris linearis* (fern)	- $LREE$-enriched mining area (SCD): 1224 mg kg^{-1} $\sum REEs$	- $\sum REEs$ in leaf, root, stem: 2271, 1570, 459 mg kg^{-1} respectively	- BF = 1.9 - TF = 1.4	[18]
		- $HREE$-enriched mining area (SDG): 195 mg kg^{-1} $\sum REEs$	- $\sum REEs$ in leaf, root, stem: 977, 1296, 401 mg kg^{-1} respectively	- BF = 5.0 - TF = 0.8	
		- Both $LREE$ and $HREE$-enriched mining area (SHG): 342 mg kg^{-1} $\sum REEs$	- $\sum REEs$ in leaf, root, stem: 1412, 1028, 313.1 mg kg^{-1} respectively	- BF = 4.1 - TF = 1.4	
		- Non-mining area (SG): 15 mg kg^{-1} $\sum REEs$	- $\sum REEs$ in leaf, root, stem: 1121, 134, 107 mg kg^{-1} respectively	- BF = 14.7 - TF = 8.4	
4 $LREEs$: La, Ce, Pr, Nd	*Dicranopteris linearis* (fern)	- REE contaminated mined area - $\sum LREEs$ in soil: 946.95 mg kg^{-1}	- $\sum LREEs$ in leaf: 6946.45 mg kg^{-1} - $\sum LREEs$ in root: 1079.5 mg kg^{-1}	- BF = 7.3 - TF = 6.4	[114]
All $REEs$ except Pm, Sc	*Dicranopteris linearis* (fern)	- $LREE$-enriched mining area (GX): 330.68 (mg kg^{-1}) $\sum REEs$	- $\sum REEs$ in leaf: 2648.8 mg kg^{-1}	- BF = 8.0	[115]

Element	Plant species	Substrate	Accumulation	BF, TF	Ref.
		- $HREE$-enriched mining area (ZD): 207.02 (mg kg^{-1}) $\sum REEs$	- $\sum REEs$ in leaf: 2090.3 mg kg^{-1}	- BF = 10.1	
		- Non-mining area (NM)	- $\sum REEs$ in leaf: 1494.5 mg kg^{-1}	–	
All $REEs$ except Pm, Sc, Y	*Dicranopteris linearis* (fern)	- Gold deposit including 299 mg kg^{-1} $\sum REEs$	- $\sum REEs$ in leaf, root, stem: 1964, 222, 44.7 mg kg^{-1} respectively	- BF = 6.6 - TF = 8.8	[19]
7 $REEs$: La, Nd, Ce, Pr, Sm, Y, Gd	*Dicranopteris linearis* (fern)	- REE mine tailings	- $\sum REEs$ in plant (including leaf and stem) ranged from 1715 to 3898 mg kg^{-1}	–	[116]
4 $REEs$: La, Ce, Nd, Pr	*Dicranopteris linearis* (fern)	- Former REE mine tailings	- $\sum REEs$ in plant (including leaf and stem): 3580 mg kg^{-1}	–	[117]
$REEs$	*Dicranopteris linearis* (fern)	- REE mine tailings and unmined sites - $\sum REEs$ in soil: 283–651 mg kg^{-1}	- $\sum REEs$ in young, middle, and mature leaf: 479, 1560, 2750 mg kg^{-1} respectively	- BF = 0.7–9.7	[118]
All $REEs$ except Lu, Pm, Sc	*Dicranopteris linearis* (fern)	- Abandoned rare earth ores: 454.42 mg kg^{-1} $\sum REEs$ - Noncontaminated soil: 94.84 mg kg^{-1} $\sum REEs$	- $\sum REEs$ in plant: 1948.67 mg kg^{-1} - $\sum REEs$ in plant: 203.87 mg kg^{-1}	- BF = 4.3 - BF = 2.1	[119]
7 $REEs$: La, Ce, Nd, Pr, Sm, Gd, Y	*Dicranopteris linearis* (fern)	- Abandoned mining area - $\sum REEs$ in soil: 300–700 mg kg^{-1}	- $\sum REEs$ in plant (including leaf and stem): 3890 mg kg^{-1}	- BF = 5.6–13.0	[120]
All $REEs$ except Pm, Sc	*Dicranopteris linearis* (fern)	- Four rare earth mines - $\sum REEs$ in soil: 310.42 to 801.34 mg kg^{-1}	- $\sum REEs$ in leaf: 1142.99 to 1965.67 mg kg^{-1} - $\sum REEs$ in underground biomass (rhizome and root): 392.59 to 1877.65 mg kg^{-1}	- BF = 1.4–6.5 - TF = 0.6–5.0	[121]
All $REEs$ except Pm, Sc	*Dicranopteris linearis* (fern)	–	- $\sum REEs$ in plant: 2032 mg kg^{-1}	–	[122]
All $REEs$ except Pm, Sc	*Dicranopteris linearis* (fern)	- $LREE$-enriched mining area (ML1): 556 mg kg^{-1} $\sum REEs$ - $HREE$-enriched mining area (TAH): 286 mg kg^{-1} $\sum REEs$ - Non-mining area (NMGZ): 309 mg kg^{-1} $\sum REEs$	- $\sum REEs$ in leaf: 3473 mg kg^{-1} - $\sum REEs$ in leaf: 520 mg kg^{-1} - $\sum REEs$ in leaf: 831 mg kg^{-1}	- BF = 6.2 - BF = 1.8 - BF = 2.7	[123]
$REEs$	*Dicranopteris linearis* (fern)	- Former mine tailings	- $\sum REEs$ in leaf: 2700 mg kg^{-1}	–	[124]

BF: Bioaccumulation factor, TF: Translocation factor.

NMs and $REEs$ are promising candidates for phytomining due to their high value and manifold applications. However, considerable data are only available on the concentration of $REEs$ and Au in plants. In contrast, the information about other noble metals accumulated by plants is scanty (Ag, Pd, Pt, Rh) or even zero (Ru, Ir, Os). Presently the concept of NM and REE phytomining is discussed on a rather theoretical basis, with few relationships to the "real world" depicted in *Table 2.4* and *Table 2.5*.

Gold

Gold has been known as the most promising candidate for phytomining of noble metals due to its high economic value. Since the twentieth century, there have been many studies corresponding to the ability of plants to accumulate gold [125], [126]. Plants accumulating more

than 1 mg kg^{-1} of gold are considered hyperaccumulators; this limit is based on the normal gold concentration in plants of 0.01 mg kg^{-1} [127]. Plants do not normally accumulate gold due to the low solubility of gold in most soils. Hence, chemicals are often applied to enhance phytoextraction [128].

The first true gold phytomining experiment was carried out in 1998 [87]. In this greenhouse study, *Brassica juncea* (Indian mustard) was treated with ammonium thiocyanate (NH_4SCN) at the rate of 0, 80, 160, 320, and 640 mg kg^{-1} in sand substrate containing disseminated gold at a concentration of 5 mg kg^{-1}. *Brassica juncea* plants accumulated gold in their aerial parts up to 57 mg kg^{-1}. Msuya et al. (2000) [80] induced hyperaccumulation in five crops (carrot, red beet, onion, salad radish, and oriental radish) with chelating agents ammonium thiocyanate NH_4SCN and ammonium thiosulfate $(NH_4)_2S_2O_3$ in the same artificial substrate consisting of 3.8 mg kg^{-1} gold. The results revealed that gold concentrations in the roots of all the five crops were higher than in the above-ground plant parts. Additionally, the average gold concentrations of carrot roots, salad radish roots, and oriental radish roots were 48.3, 113, and 102 mg kg^{-1}, respectively.

In 2001, Lamb and colleagues [84] conducted a trial in which artificial gold-bearing soil containing 5 mg kg^{-1} was used to study the viability of *Brassica juncea* (Indian mustard), *Berkheya coddii* (Asteraceae), and *Cichorium intybus* (chicory) to accumulate gold upon treatment with NaCN (sodium cyanide), KCN (potassium cyanide), KI (potassium iodide), KBr (potassium bromide), and $(NH_4)_2S_2O_3$ (ammonium thiosulphate). The highest gold concentration was observed in the case of KCN. Specifically, 36, 94, and 97 mg kg^{-1} of gold were detected in the root, stem, and leaf of *Berkheya coddii* plant, respectively. Content in *Brassica juncea* plant could reach up to 326 mg kg^{-1} in leaf and 46, 88 mg kg^{-1} in the cases of stem and root, respectively. *Chicory* plant induced via KCN also gave the highest accumulation of 164 mg kg^{-1}Au for the whole plant. Moreover, concentrations of gold in leaves are generally higher than in roots. This element was actively accumulated by *Berkheya coddii* and *Brassica juncea*, expressed by high bioaccumulation and translocation factor ($BF \approx 19.1$, $TF \approx 2.7$ for *Berkheya coddii*, and $BF = 9.2–65.5$, $TF = 0.5–3.7$ in the case of *Brassica juncea*).

In 2005, the first gold phytoextraction field trial from mine tailings was carried out [24]. In this work, *Brassica juncea* (Indian mustard) and *Zea mays* (corn) plants grown on an oxidized ore pile containing 0.6 mg kg^{-1} gold were treated with chemicals (KCN, NaCN) to induce gold hyperaccumulation. The highest gold concentrations of 20 and 39 mg kg^{-1} in *Zea mays* and *Brassica juncea* plants were achieved after the application of KCN, respectively [24]. Two years later, another study on gold phytoextraction was reported [88]. An oxide ore presenting a

mean gold grade of 1.75 mg kg^{-1} was collected as the substrate of this research. The selected plants comprising *Acacia decurrens* (Black Wattle), *Trifolium repens* (White clover cvs. Tribute and Prestige), *Eucalyptus polybractea* (Blue Mallee), *Sorghum bicolor* (Sorghum), *Bothriochloa macra* (Red grass), *Microlaena stipoides* (Weeping grass), and *Austrodanthonia caespitosa* (Wallaby grass) were induced by NaCN (sodium cyanide) at the rates of 0.1 and 1 mg kg^{-1}. The most significant result was found in the white clover Prestige plant, which presented a stem gold concentration of 26.87 mg kg^{-1} under the application of 1 g kg^{-1} NaCN. Concentrations of gold in the stems and older leaves were higher than in the younger leaves of the plants. This investigation also demonstrated the possibility of using plants to extract and concentrate gold from low-grade ore and waste products [88].

A study published in 2011 [85] showed that *Helianthus annus* (sunflower) plants could accumulate average gold concentrations of 14.9, 21.5, and 19.2 mg kg^{-1} in roots, stems, and leaves, respectively. In this study, mine tailings substrate had a gold concentration of 2.35 mg kg^{-1}, and NaCN (sodium cyanide) was added at the rate of 1 mg kg^{-1} to promote gold solubility and enhance gold accumulation in the plants. The bioaccumulation factor and translocation factor of the sunflowers were greater than one ($BF \approx 8.7$, $TF \approx 1.4$), showing its potential for gold phytomining [85]. A 2014 experiment tested the ability of three plant species namely *Cyperus kyllingia* (nut grass), *Lindernia crustacea* (Scrophulariaceae), *Paspalum conjugatum* (carabao grass) to accumulate gold from cyanidation tailings containing 1.68 mg kg^{-1} Au [90]. Sodium cyanide NaCN (1 g kg^{-1}) and ammonium thiosulfate $(NH_4)_2S_2O_3$ (2 g kg^{-1}) were added to induce accumulation in the plants. However, the gold concentration only reached a maximum value of 0.602 mg kg^{-1} in the shoot of *Paspalum conjugatum* under the amendment of ammonium thiosulfate [90].

Another phytoextraction field trial was reported in 2016 [23]. Tobacco grown on cyanidation tailing substrate consisting of 1.03 mg kg^{-1} Au and 18.2 mg kg^{-1} Ag was treated with 0.05 g kg^{-1} of NaCN (sodium cyanide). Under field conditions, mean concentrations of gold and silver in Tobacco could achieve levels of 1.2 and 54.3 mg kg^{-1}, respectively [23]. Recently in 2018, González-Valdez et al. [91] evaluated the viability of *Brassica napus* (Rapeseed) for extracting gold from mine tailings containing 0.5164 mg kg^{-1} Au. The gold concentration could reach levels of 1.5 mg kg^{-1} in stems and 10 mg kg^{-1} in roots under the effect of NH_4SCN (ammonium thiocyanate). The concentration of gold in roots is approximately seven times higher than in the shoots of the plant.

Gold is the most promising candidate for phytomining. It has lured worldwide attention and has been extensively studied. Base metal ore tailings containing less than 1 mg kg^{-1} of gold seem not to have sufficient Au to justify economic phytomining. Nevertheless, substrates with more than 1 mg kg^{-1} should be targets for development [85]. Gold phytomining is much closer to practical applications than other precious metals. However, all phytomining experiments on this element are based on induced hyperaccumulation.

Silver

Natural silver accumulation into native plants including *Euphorbia macroclada* (spurge), *Verbascum cheiranthifolium Boiss* (Scrophulariaceae), *Astragalus gummifer* (leguminous) was reported by Sagiroglu et al. (2006) [92]. The terrestrial plants coming from a polluted mining area contained the maximum silver concentrations of 0.97 mg kg^{-1} in twigs and 3.12 mg kg^{-1} in roots of the spurge plant. In another work, Borovička et al. (2007) [22] revealed that macrofungal Amanita species, namely *A. strobiliformis* and *A. solitaria* could naturally hyperaccumulate silver from non-argentiferous areas containing 0.07–1.01 mg kg^{-1} Ag. Concentrations of silver in the Amanita species were commonly in the range of 200–700 mg kg^{-1} with the highest value of 1253 mg kg^{-1} Ag. The natural phytomining of silver seems viable, but its feasibility under more realistic natural conditions still needs to be demonstrated.

Lupinus sp. (blue lupin) grown on base-metal mine tailings could accumulate 126 mg kg^{-1} of silver in aerial tissues after applying induced accumulation [77]. Harris and Bali (2008) [93] investigated the accumulation of silver by *Brassica juncea* (Indian mustard) and *Medicago sativa* (alfalfa). *Brassica juncea* could accumulate 12.4% silver when exposed to an aqueous substrate containing 1000 mg L^{-1} $AgNO_3$ for 72 h. While *Medicago sativa* plant accumulated as high as 13.6% of silver when exposed to an aqueous substrate containing 10000 mg L^{-1} $AgNO_3$ for 24 h. Silver was stored as discrete nanoparticles in both cases, with an average size of around 50 nm. It has been suggested that using plants to synthesize a huge number of metallic nanoparticles is viable.

Palladium

Among the platinum metal group, palladium has received substantial attraction, probably owing to its higher abundance than others (*Table 2.3*). Fuchs and Rose (1974) [94] are likely to be the first authors to provide evidence of the accumulation of this valuable metal in plants when 285 µg kg^{-1} Pd was detected in the twig ash of *Pinus flexilis* (limber pine). Five years later, Kothny

(1979) [95] observed 400 µg kg^{-1} Pd in the ash of *Quercus chrysolepsis* (oak) collected from a sampling site containing 140 µg kg^{-1} Pd. In another work, Nemutandani et al. (2006) [26] assessed the feasibility of the native plant *Berkheya coddii* (Asteraceae) for phytoextraction from a contaminated area containing 70 µg kg^{-1} Pd. Under natural conditions, palladium was obtained in the roots and leaves of this plant at a concentration of 180 and 710 µg kg^{-1}, respectively. *Berkheya coddii* performed a high ability to accumulate and transport Pd via its elevated bio-indices (BF = 10.1, TF = 3.9).

Like gold, other noble metals such as Pt and Pd also have low solubility in the natural environment. Therefore, amendments are often applied to soil to make these elements soluble and enhance their accumulation in plants. Although hyperaccumulators of such metals have not been defined yet, the threshold level of hyperaccumulation of these precious elements in plants would be expected at 1 mg kg^{-1} based on their low concentration in normal plants. The first study on induced palladium hyperaccumulation in plants was reported in [25]. In this greenhouse trial, *Berkheya coddii* (Asteraceae) grown on mine tailings containing 315 µg kg^{-1} Pd was treated with KCN (potassium cyanide) at a rate of 10 g L^{-1} to induce palladium accumulation. The data showed palladium levels of 7677 µg kg^{-1} in the plant. Another phytomining pot trial was carried out by Aquan (2015) to evaluate the accumulation of palladium in *Cannabis sativa* (hemp) [27]. Gossan rock consisting of 0.206 mg kg^{-1} Pd was picked as the substrate of this study. The average palladium level in the aerial part of the plant reached 30.336 mg kg^{-1} with the highest value of 62.420 mg kg^{-1} under the application of KCN (potassium cyanide). More recently, in a Ph.D. dissertation, Harumain (2016) [96] induced hyperaccumulation in *Salix purpurea* willow (Green Dicks) and *Miscanthus* (silver grass) by KCN (potassium cyanide). Synthetic ore presenting 50–100 mg kg^{-1} Pd was used as the medium in this work. Palladium was detected in leaves of *Salix purpurea* and *Miscanthus* at the levels of 820 and 505 mg kg^{-1}, respectively. Another study assessing the capability of plants in accumulating palladium was conducted by Harumain et al. (2017) [97]. *Miscanthus* (silver grass), Indian mustard, and 16 willow species and cultivars were grown on synthetic tailings consisting of 50 mg kg^{-1} Pd, dosed with 100 mg kg^{-1} cyanide in the form of KCN. As a result, aerial tissues of Indian mustard, *Miscanthus*, and leaves of *Salix purpurea* willow (Green Dicks) could attain 500 mg kg^{-1}, 1500 mg kg^{-1}, and 800 mg kg^{-1} palladium, respectively.

The concept of palladium phytomining is somewhat novel, it has been monitored in recent decades. The viability of the phytoextraction approach on this valuable element has been barely demonstrated.

Platinum

Although the ability of plants to accumulate platinum has been mentioned since the twentieth century [94], many studies about that have just been reported in the last decades. Nemutandani et al. (2006) [26] revealed that *Berkheya coddii* (Asteraceae) sampled from contaminated sites containing 0.04 mg kg^{-1} Pt could concentrate 0.22 and 0.18 mg kg^{-1} platinum in leaves and roots, respectively. The bioaccumulation factor and translocation factor of *Berkheya coddii* were higher than one (BF = 5.5, TF = 1.2), demonstrating its capability to accumulate and transfer platinum. In another study, Walton (2002) found 0.183 mg kg^{-1} of platinum from the same *Berkheya coddii* plant grown on mine tailings [25]. Recently, a concentration of 3.06 mg kg^{-1} Pt in terrestrial plants collected from contaminated brownfield land was reported in 2018 [45]. There have been several studies focusing on platinum accumulated by plants in the vicinity of roads [79], [98]. Diehl and Gagnon (2007) [99] found the highest platinum concentration of 14.6 mg kg^{-1} in *Daucus carota* (wild carrot) gathered along a country highway with heavy traffic. Kińska and Kowalska (2019) [100] assessed the accumulation of platinum by *Sinapis alba* (white mustard). The platinum concentration in the root of white mustard could reach as high as 5973 mg kg^{-1} when this plant was cultivated in a nutrient solution containing 1 mg L^{-1} Pt for 2 weeks. In spite of many reports about platinum in plants, platinum accumulation in phytomining experiments has not been conducted.

Rhodium

The occurrence of rhodium in plants has been monitored in recent years [79]. Diehl and Gagnon (2007) provided evidence of rhodium accumulation in plants when 0.7 mg kg^{-1} Rh was identified in roadside *Daucus carota* (wild carrot) collected from four heavy traffic locations [99]. In 2011, a range of 1.11–1.13 mg kg^{-1} Rh was detected in *Phragmites australis* (common reed) sampled along a riverside affected by massive urbanization [101]. Generally, investigations of rhodium in plants are scarce, probably due to its low abundance. Nevertheless, rhodium has been found to be the most soluble platinum group element in soil sorption studies [129], providing the potential of this element in phytomining.

Rare earth elements

The first outstanding discoveries of $REEs$ accumulation in plants were accidentally detected by Robinson and his associates [20], [102], [103]. In 1938, Robinson et al. [102] reported an extraordinary concentration of 2000 mg kg^{-1} total rare earths observed in the leaves of hickory

(a woody tree) grown on a mining area in the United States. Five years later, hickory leaves were harvested from a non-mining area (granite and gneiss soils) containing as much as 2296 mg kg^{-1} $REEs$ [20]. The ash of these woody leaves concentrated more than 2.5%, corresponding to 25000 mg kg^{-1} rare earth metals. Likewise, Thomas (1975) identified 136 and 1350 mg kg^{-1} of rare earths within the foliage and the foliage ash, respectively of hickory planted on silt loam soil [104]. In other studies, a flowering herbaceous species, *Phytolacca americana*, had high $REEs$ accumulation capability. The grade of rare earth metals in the leaves of this plant harvested from a forest zone reached up to 581.5 mg kg^{-1} [105]. Recently, a field survey was conducted in an REE mining area consisting of 303 to 691 mg kg^{-1} $REEs$. The results indicated that *Phytolacca americana* (pokeweed) could achieve 1040 mg kg^{-1} of rare earths in their leaves. The levels of $REEs$ in this plant follow the decreasing order of leaf > root > stem [106]. The bioaccumulation factor and translocation factor of *Phytolacca americana* were higher than one (BF = 1.5–3.4, TF = 2.7–14.7), showing its elevated capability in accumulating and transferring $REEs$.

Among the plants with an unusual accumulation of $REEs$, the fern has been known as the majorly potential hyperaccumulator. Diversifying genera (*Asplenium* in *Aspleniaceae*, *Polystichum* and *Dryopteris* in *Dryopteridaceae*, and *Diplazium* in *Woodsiaceae*) were reported to accumulate remarkable concentrations of lanthanides (La and Ce) in a Japanese investigation comprehending 96 species of ferns [108]. Generally, most studies have focused on *Dicranopteris linearis* formerly known as *Dicranopteris dichotoma*, a fern species commonly found in tropical and sub-tropical climatic regions. The first report of exceptional $REEs$ concentration in this plant likely was published in 1997 [113]. The paper showed that the fern leaves harvested from plants growing in a rare earth ore area could contain 3358 mg kg^{-1} of 8 rare earth metals, including La, Ce, Nd, Sm, Eu, Tb, Yb, and Lu. Four years later, Zhenggui and his colleagues analyzed *Dicranopteris linearis* plants sampled from four different substrates, such as a light REE-enriched mining area, a heavy REE-enriched mining area, both heavy and light REE-enriched mining areas, and a non-mining area [18]. The highest entire REE levels of 2271, 1570, and 459 mg kg^{-1} were identified in leaf, root, and stem, respectively of the biomass collected from the area with the most rare-earth metals pollution, which was a light REE-enriched mining area consisting of 1224 mg kg^{-1} $REEs$. Their article also revealed that the fern gathered from a noncontaminated site containing 15 mg kg^{-1} $REEs$ could accumulate up to 1121 mg kg^{-1} of $REEs$ in its leaves [18]. Conclusively, the higher number of $REEs$ in soils reflects the greater grade of $REEs$ in plants; however, elevated concentrations of

$REEs$ might be enriched in pteridophyte species (ferns) even those growing in unpolluted locations. These outcomes are in complete agreement with the other investigations [115], [119], [123]. Findings on the exceptionally extraordinary occurrence of $REEs$ in plants were published by Shan et al. (2003) [114]. The scholars disclosed that 6946.45 mg kg^{-1} of approximately 0.7% light $REEs$ comprising La, Ce, Pr, and Nd was determined in leaves of a natural perennial fern *Dicranopteris linearis* growing in acidic soil in southern China. In recent years, many studies have been carried out indicating massive accumulation of $REEs$ in the fern *Dicranopteris linearis* [19], [118], [120]–[122], [124]. The results of these studies are briefly depicted in *Table 2.5*. Many of them are carried out in China, which can be explained by the superior abundance of $REEs$ in the nation. The two indices BF and TF were greater than one in almost all studies, clearly indicating the ability of the fern *Dicranopteris linearis* to accumulate and translocate $REEs$.

In addition, another fern species, *Pronephrium simplex*, gathered from a semi-tropical rainforest, presented up to 3000 mg kg^{-1} total $REEs$ in its dry leaves [110]. This fern demonstrated an outstanding ability to accumulate and transport $REEs$ via its high bioaccumulation factor (BF = 36.3) [109]. In a recent pot experiment, a type of fern called *Onoclea sensibilis* was planted on an artificial substrate containing 333 mg kg^{-1} of six rare earths, namely La, Ce, Sm, Gd, Yb, and Y. Consequently, more than 200 mg kg^{-1} of those six metals were detected in the biomass [112]. Another work showed that the fern *Alsophila sternbergii* is able to accumulate $REEs$ [111]. However, $REEs$ were not actively accumulated by this plant, as shown by its bioaccumulation factor of less than one.

2.2.3. Enrichment of NMs and $REEs$ from contaminated biomass prior to metal extraction

During the phytoextraction process, plants accumulate NMs and $REEs$ from contaminated soils and then translocate and store these metals in their roots and shoots. NMs and $REEs$ accumulated in woody biomass can be recovered by applying extraction techniques. Prior to extracting NMs and $REEs$, the bulky contaminated plants should be lessened to a manageable amount and volume; the metal grade is then elevated in the solid residues called bio-ores. Enrichment of NMs and $REEs$ is crucial in the entire pathway of phytomining; it not only lowers the transportation costs but also minimizes the size of the downstream processing apparatus. The treatment of biomass used for phytoextraction has been mentioned previously. In this section, the enrichment of metals is discussed.

2.2.3.1. Enrichment techniques

Several enrichment approaches including thermal conversion (ashing, pyrolysis, gasification, combustion), composting, or compaction have been introduced [41]. Concentrating technologies, with their positives and negatives from the enrichment point of view, are briefly depicted in *Table 2.6*. Of these methods, combustion is considered the most promising manner because of its superior volume reduction and efficient metal enrichment [42].

Composting technology has been deemed a post-harvest biomass treatment used to substantially lower the weight of contaminated plant material. The volume and water content reductions are the main benefits of this method, leading to a decrease in transportation costs. Metals are mainly enriched in decomposed biomass material, but these are also presented in water-soluble forms. Therefore, the composting process must be implemented under strict monitoring to evade undesirable leachates. Other downsides of this technique are that it is time-consuming (a couple of months are required) and has special equipment requirements. For the reasons above, composting has been conducted only at the laboratory scale so far [130]–[132].

Compaction provides another solution to diminish the volume of contaminated plants and enhance metal levels in compacted products. A container equipped with a press and a leachate collection system is used in the compaction process. The compacted product is generated by compression, and the leachate containing metals is captured via the collecting system. The benefits of this method are similar to composting; total dry mass loss of contaminated plants is lessened by compaction varying from species to species. In comparison, compaction of the same quantity of biomass requires less time than composting. Nevertheless, information regarding compaction of contaminated biomass is difficult to find [41].

The thermal biomass conversion process is one of the more conventional and attainable methods to significantly lessen harvested biomass quantities and elevate metals into solid remains. Techniques include ashing, pyrolysis, gasification, and combustion occurring at elevated temperatures (ranging from 300 to 1000 °C) in a fast reaction. This process lowers the high amount of contaminated plants and allows carbon-neutral energy to be produced. The end-products of thermal biomass conversions such as syngas, biochar, and bio-oil are deemed the advantages of these techniques. It is worth mentioning that besides carbon-neutral energy generation, the conception of negative carbon emission is also a feasible approach that reinforces the worldwide endeavors to counter climate change.

Table 2.6. Technologies for enriching metals from contaminated biomass [43].

Process	Main principle	Advantages	Disadvantages
Composting	- Decomposing organic materials by microorganisms	- Reduces volume and water content - Lowers the costs of handling and transportation	- Time-consuming (2–3 months) - At laboratory scale
Compaction	- Compression	- Volume reduction leads to cost transportation reduction - Shorter time compared to composting	- Special equipment is required - Metals enriched in the product of leachates
Pyrolysis	- 350–700 °C - Absence of oxygen	- High volume reduction, metals concentrated in bio-char - Useful end-products such as biochar, bio-oil, fuel gas	- Complex and requires elevated costs for operation and investment
Gasification	- 700–1000 °C - Partial oxidation of compounds using steam, air, or oxygen	- High volume reduction, metals enriched in solid residual - Lowering harmful climate change via CO_2 mitigation - Useful end-product of flue gas	- Undesired products such as tar are formed - Technical and environmental problems during the utilization of syngas produced from contaminated biomass
Combustion	- Over 900 °C - In the presence of excess oxygen/air	- High volume reduction, metals enriched in solid residual - Produces energy	- Undesirable emissions of CO, NOx, fly ash, gaseous metal compounds
Ashing	- 300–550 °C	- High volume reduction, metals enriched in solid residual	- Estimations of the cost or feasibility of such a process are not available

Pyrolysis is a thermal conversion process for degrading metal-containing biomass at moderate temperatures (350–700 °C) in the absence of oxygen conditions. The products of pyrolysis can be classified into a solid fraction (bio-char), a liquid fraction (bio-oil), and a gaseous fraction consisting of carbon monoxide, carbon dioxide, hydrogen, and methane [133],

[134]. In terms of contaminated biomass pyrolysis, the major purpose is to obtain the highest metal concentrations in the solid residual, and the lowest in the pyrolytic fluid oil and the gaseous portion. Due to the low operating temperature, metals from contaminated plants tend to be contained in biochar. Since the process of pyrolysis is utterly hermetic, there is no emission into the air. This pathway enhances the energy density of biomass and reduces the volume of polluted plants as well as transportation costs [135]. However, high installation and operation costs are the limitations in the pyrolysis of plant material.

Gasification degrades contaminated biomass and converts it into organic material and/or syngas (H_2, CO, CH_4, etc.) at high temperatures (700–1000 °C) through partial oxidation of compounds using steam, air, or oxygen [136], [137]. Using this technique, an enormous mass reduction of harvested material can be attained, with metals concentrated in the solid remains (ashes), which is easy to mobilize and handle. The utilization of synthesis gas for energy recovery is advantageous, but the generation of value-added fuels or chemicals is an achievable approach as well. However, the combustive gas might contain contaminants; robust gas cleaning is also necessary.

Combustion is another thermal conversion process to decompose harvested plant materials at temperatures greater than 900 °C under the presence of excess oxygen/air [138], [139]. More than 90% of the contaminated woody biomass is transformed into flue gas and heat throughout the combustion process. Metals are substantially concentrated in the products of bottom ash and fly ash. Combustion is considered the most rational treatment used after phytoextraction due to the excellent mass diminution. This pathway offers the opportunity to associate the enrichment manner with a somewhat simple energy production with completely developed techniques. On the other hand, the incineration of polluted plants leads to severe environmental problems such as undesirable emissions of carbon monoxide (CO) or nitrogen oxides (NO_x). Nonetheless, the carbon-neutral operation provides a restful resolution of greenhouse gas emissions. Negative carbon emission is also an attainable concept, for instance, with oxy-fuel combustion integrated with carbon capture and storage.

According to some studies [23], [122], [140], the ashing process disintegrates polluted plant materials at reasonably low temperatures of 300–550 °C. During this thermal degradation, harvested biomass is decreased in a smaller amount of ash containing greater metal concentrations. The ashing process is quite similar to combustion but occurs at lower temperatures.

2.2.3.2. Enrichment of NMs and $REEs$ from contaminated biomass

Thermal conversions are feasible approaches to enrich metals from polluted woody biomass. The viability of these enrichment technologies has been demonstrated in terms of heavy metals [141]. However, the information on heightening NMs and $REEs$ of biomass used for phytoextraction is extremely sparse, with only a couple of investigations carried out so far. The feasibility of these enrichment techniques has been demonstrated in the cases of heavy metals [141]. The behavior of heavy metals [51], [142] as well as the influence factors on metal flows [143] during thermal conversions have been intensively investigated. However, the information on the enrichment of NMs and $REEs$ from polluted biomass is scanty, with only a few investigations having been conducted so far (*Table 2.7*).

Table 2.7. Enrichment of NMs and REEs from contaminated biomass.

Element	Material	Technique	Condition	Result	Ref.
Au	Contaminated biomass: 30 mg kg^{-1} Au	Ashing	550 °C, 15–20 h	- Au was enriched in ash	[140]
Au, Ag	Tobacco: 1.2 mg kg^{-1} Au and 54.3 mg kg^{-1} Ag	Air drying, ashing	300 °C	- Mass reduction: 94.46%	[23]
Au, Ag, Pt	Contaminated biomass: 11.9 mg kg^{-1} Ag and 3.06 mg kg^{-1} Pt	Combustion	Firing rate: 34 kW	- In bottom ash: 2.81 mg kg^{-1} Au, 22 mg kg^{-1} Ag, and 2.51 mg kg^{-1} Pt - In deposited ash: 4.1 mg kg^{-1} Au, 26.5 mg kg^{-1} Ag, and 20.8 mg kg^{-1} Pt - In fly ash: 545 mg kg^{-1} Ag, and 46.4 mg kg^{-1} Pt	[45]
All $REEs$ except Pm, Sc	*Dicranopteris linearis* (fern): 2032 mg kg^{-1} $\sum REEs$	Ashing	500 °C, 2 h	- In ash: 15956 mg kg^{-1} $\sum REEs$ - Retention rate: 93%	[122]
$REEs$	*Dicranopteris linearis* (fern): 2700 mg kg^{-1} $\sum REEs$	Ashing	550 °C, 3 h	- Mass reduction: 92.3% - In ash: 30000 mg kg^{-1} $\sum REEs$	[124]
All $REEs$ except Lu, Pm, Sc	*Dicranopteris linearis* (fern): 1948.67 mg kg^{-1} $\sum REEs$	Pyrolysis	Vacuum-pyrolysis-condensation	- In pyrolysis ash: 6160 mg kg^{-1} $\sum REEs$	[119]
All $REEs$ except Pm	*Salix* (willow): 5678 mg kg^{-1} $\sum REEs$	Combustion	800 °C	- Ash content: 6.6% (equating to 93.4% mass reductio) - In bottom ash: 70000 mg kg^{-1} $\sum REEs$ - Retention rate: > 80%	[107]
			1000 °C	- Ash content: 6.3% (equating to 93.7% mass reductio) - In bottom ash: 80000 mg kg^{-1} $\sum REEs$ - Retention rate: > 80%	

In one, harvested plants were incinerated at 550 °C to remove organics as the first step of extraction of gold from biomass [140]. After ashing at approximately 300 °C, 100 kg of tobacco used for Au phytomining was reduced to 5.54 kg of ash, equating to 94.46% mass reduction [23]. In another study regarding biomass combustion, 11.9 mg kg^{-1} Ag and 3.06 mg kg^{-1} Pt in gathered plants resulted in concentrations of 545 and 46.4 mg kg^{-1}, respectively, in the fly ash [45]. It was observed that Au was not detectable in the biomass, but its concentration became high enough to be identified in the solid remain (4.10 mg kg^{-1}) as a result of the enrichment process. The authors also investigated the influence of flue gas temperature on the behavior of metals including NMs during biomass combustion. The concentration of Ag was significantly higher in the fly ash sample collected at 150 °C flue gas temperature compared to the 250 °C case, indicating a strong temperature dependence. Minor temperature dependence was observed in deposited ash and fly ash samples for other NMs. Probably this was the first investigation on the effect of the flue gas temperature on the metal fallout including NMs during contaminated woody biomass combustion.

In terms of $REEs$, by incinerating the harvested *Dicranopteris linearis* fern at 500 °C, 2032 mg kg^{-1} $REEs$ in the plant was elevated to 15956 mg kg^{-1} in the ash, and 93% of REE input from the biomass was converted into the solid remains [122]. Likewise, 92.3% weight of the collected *Dicranopteris linearis* fern was lessened after ashing at 550 °C [124]. As a result, $REEs$ is concentrated in the ash at the level of 30000 mg kg^{-1}, which is over eleven times higher than in the fern (2700 mg kg^{-1}). In another study, an environmentally friendly approach of vacuum-pyrolysis-condensation was proposed for concentrating $REEs$ from contaminated biomass [119]. The pyrolytic product derived from *Dicranopteris linearis* containing 1948.67 mg kg^{-1} rare earths reached a level of 6160 mg kg^{-1} $REEs$ after treatment. In another study, a mixture of roots, stems, and leaves of hydroponically grown *Salix* (willow) samples containing 5678 mg kg^{-1} of $REEs$ were combusted at two reaction temperatures, 800 °C and 1000 °C, in a fixed-bed, batch, tube reactor [107]. Yields of ash following the combustion of the homogenized *Salix* sample were 6.6% and 6.3% at combustion temperatures of 800 °C and 1000 °C, respectively. It was observed that the concentration of $REEs$ in bottom ash formed at 1000 °C (8% equating to 80000 mg kg^{-1}) was higher than at 800 °C (7% equating to 70000 mg kg^{-1}). Furthermore, the retention rate for $REEs$ in the bottom ash at 1000 °C combustion temperature was also greater than at 800 °C. In both cases, the numbers of retention rates were greater than 80%, indicating that the volatilization of $REEs$ is minor during combustion. To my best knowledge, this is the first information concerning REE enrichment from *Salix* by a

combustion process as well as the influence of combustion temperature on the behavior of rare earth metals.

2.2.4. Extraction of NMs and $REEs$

Extraction is the eventual step in the phytoextraction-enrichment-extraction chain to recover NMs and $REEs$ from brownfields. This section provides an overview of extraction techniques and details the studies pertaining to the recovery of NMs and $REEs$ from bio-ores.

2.2.4.1. Extraction techniques

Basically, conventional and newly developed methods could be used to recover metals from urban mines. Together with their pros and cons, these methods are briefly presented in *Table 2.8*.

Table 2.8. Technologies for recovery of metals from secondary resources [43].

Technology		Advantages	Disadvantages
Conventional	Pyrometallurgy	- Simplicity - Large capacity - Wide range of applications	- Emission of toxic gases - Poor selectivity of the target element - Expensive equipment required - High energy consumption
	Hydrometallurgy	- Superior recovery efficiency - Low cost of required equipment	- Waste-water generation - Corrosion of equipment
	Biometallurgy	- Most environmental friendly - Affordable cost	- Time-consuming - Poor leaching rate - At laboratory scale
Emerging	Ionic liquid Mechanochemical Supercritical fluid Electrochemical	- Efficiency - Ecological amiability	- At laboratory scale

Traditional technologies for recovering metals are pyrometallurgy, hydrometallurgy, and bio-metallurgy [144]. Previously, mechanical or physical techniques were typically employed as a pre-treatment process to segregate metals from non-metallic components. However,

applying only one single approach could not completely separate and purify metals. Thus, a collaboration of two or more approaches is commonly used to carry out metal recycling.

Pyrometallurgy is a well-known thermal method comprising incineration, vacuum carbon-thermal reduction, and chlorination volatilization for reclaiming metals from waste streams under elevated temperatures [145]. Essentially, it is an effective preconcentration pathway for dispersed metals in low-grade minerals; other sequential refinement processes are necessary for further metal recycling. This technique has been in practice for years because of its wide-range applications, simplicity, and huge capacity. On the other side, pyrometallurgy requires high energy consumption and has encountered some challenges from environmental concerns like toxic smoke or the liberation of noxious volatile organic compounds. This process is characterized by poor selectivity of the individual target metal and high energy consumption. It is not appropriate for small and medium-sized enterprises due to the requirements of costly apparatus and remarkable initial investment.

Hydrometallurgy is a chemical method that can be used to recover metals from secondary minerals. This technology has two main steps: (1) dissolution and leaching of metals and (2) separation and purification of metals [146], [147]. In the first stage, refuse bearing metals is subjected to mineral acids to dissolve metals. The leaching process can be affected by various factors such as solid-to-liquid ratio, pH, lixiviant type, particle size, agitation speed, temperature, time, etc. In the second phase, the resulting leached solution is separated and purified through separation and purification processes: solvent extraction, ion adsorption, ion exchange, or precipitation. For most metals, a leaching operation is commonly followed by solvent extraction in practice. In comparison, the hydro-metallurgical pathway has many benefits over pyrometallurgy, such as high metal recovery rates, good selectivity of target elements, low production costs, and less emission of disastrous gases (CO, CO_2, NO_x, SO_x). Therefore, hydrometallurgy has attracted global attention in recent decades and become the prevalent approach for recycling metals from low-grade resources since the mid-1980s. However, hydro-processes still have various limitations and shortages due to sludge generation, toxicity, and equipment corrosion.

Recycling metals by bio-metallurgy has been one of the most promising pathways in the last decade. There are two major areas of biotechnology for recovering metals from urban mines, namely bioleaching and biosorption [148]. Bioleaching refers to using bacteria, microorganisms, fungi, algae, or their metabolites to interact with metals [149]. This technique is featured by environmental friendliness, inexpensive costs, and simplicity. Nevertheless,

research studies on biological leaching are mainly at the laboratory scale because of the poor leaching rate and long operation time [150]. The biosorption-based process relates to a passive physico-chemical interaction between metal ions in solution and the charged surface groups of biological materials called bio-sorbents [151], [152]. Biosorbents consist of multiple microorganisms, yeasts, bacteria, fungi, algae, and biowaste materials, which can be used to actively accumulate metals [153]. Biosorption has been known as the following purification process after metal leaching; it offers an affordable-cost choice to extract metal ions from an aqueous phase. This technology provides a variety of advantages compared to other traditional methods of pyrometallurgy and hydrometallurgy. These encompass cost-effectiveness, high efficacy in detoxifying effluents, and minimizing chemical and/or biological sludge [154].

In addition to conventional extraction techniques, alternative methods to extract metals from waste streams bearing metals, including the mechanochemical approach, electro-chemical technology, ionic liquid method, and supercritical fluid pathway have been constantly developed [154]. The emerging technologies provide potentially efficient, ecologically sound, and novel options for recovering metals from secondary minerals. These newly developed approaches have received appreciable attraction and been the subject of certain laboratory applications recently.

To sum up, various pathways have been examined and developed for reclaiming metals from secondary ores to strengthen the circular economy concept. The pyrometallurgical method has been commonly used for ages due to its simplicity and large capacity. Nevertheless, this approach has raised environmental concerns about generating harmful gases. Its applications are also limited by the expensive apparatus requirement. In recent decades, attraction has turned to hydrometallurgy for the extraction of metals from low-grade minerals. Compared to pyrometallurgy, the hydrometallurgical technique requires an affordable investment cost, is easy to operate, and shows a high recovery efficiency of metals. On the other side, wastewater generation and equipment corrosion are the main drawbacks of this manner. Biometallurgy appears to be the most promising extraction technology to reclaim metals from urban mines because of its ecological friendliness and reasonable cost. However, the long operation times and poor leaching efficiency have restricted the utilization of biotechnology. Currently, several newly developed approaches such as ionic liquid, electrochemical, mechanochemical, and supercritical fluid provide other possibilities to recover metals. These alternatives have attracted significant attention and attained some notable achievements at the laboratory scale. Collectively, only one single process alone can hardly extract metals perfectly due to the

intricacy of waste streams. Thus, integrating various methods is necessary to recover metals from secondary resources with high recovery efficacy and low pollution.

2.2.4.2. Extraction of NMs and $REEs$ from bio-ores

Table 2.9 presents a summary of the literature pertaining to the recovery of NMs and $REEs$ from bio-ores ores comprising biomass and biomass-derived ashes. One of the first routes for the extraction of gold from woody biomass has been published by Lamb et al. in 2001 [140]. First, the biomass was ashed and dissolved in a 2 M HCl leaching agent. The process was followed by solvent extraction utilizing MIBK (methyl isobutyl ketone). Afterward, the addition of $NaBH_4$ (sodium borohydrate as a reducing agent) to the organic layer resulted in the formation of a black precipitate at the boundary between the layers. Eventually, this precipitate yielded metallic gold by heating at 800 °C. Nevertheless, this pathway presents a variety of issues. Specifically, the greatly reactive reducing agent generates gas during the reaction and probably deteriorates the solvent. The use of solvent gives superior expense and environmental problems. It is difficult to separate the precipitate from the boundary layer. The utilization of both thermal reduction and a reducing agent needs two stages. The authors then worked on these problems and made some improvements to provide a cost-effective method for the extraction of gold from biomass. In the following pathway, 30 g of harvested plants consisting of 30 mg kg^{-1} Au was ashed at 550 °C and the ash was dissolved in 300 mL HCl. This is followed by extracting the aqueous phase into 50 mL MIBK and contacted with the same volume of $C_6H_8O_6$ (ascorbic acid). After 3.5 h, the solution was filtered, and 85% of Au was recovered into the precipitate. Although this extraction technique has been simplified to reduce the costs and save reagents, it still presents the environmental restriction of waste stream acid generation and high price. Hence, this method requires significant work before it is feasible for scale-up. Recently, another technology relating to the recovery of NMs from plant material has been implemented [23]. Dried tobacco containing 54.3 mg kg^{-1} Ag and 1.2 mg kg^{-1} Au was ashed at approximately 300 °C. The ash samples were added with borax ($Na_2B_4O_7.10H_2O$), and then the silver was smelted at temperature greater than 1000 °C. During this process, borax and silver were used as collector metals, and NMs contained in biomass ash were recovered into the final smelted product called bullion. Despite the inconclusive results, this study has offered a technically viable approach for the extraction of NMs from woody biomass.

Table 2.9. A summary of studies on the recovery of NMs and REEs from bio-ores.

Element	Sample	Technology, mechanism, condition	Result	Ref.
Au	Contaminated biomass: 30 mg kg^{-1} Au	Hydrometallurgy: ashing, leaching, solvent extraction, precipitating - Ashing: at 550 °C between 15–20 h → ash - Leaching: 300 mL 2M HCl → aqueous phase - Solvent extraction: 50 mL methyl isobutyl ketone (MIBK) → gold-bearing MIBK - Precipitating: 50 mL $C_6H_8O_6$ (ascorbic acid) in 3.5 h → precipitate	- 85% of Au was recovered into the precipitate.	[140]
Au, Ag	Tobacco: 1.2 mg kg^{-1} Au and 54.3 mg kg^{-1} Ag	Incineration: ashing, smelting - Ashing: around 300 °C → ash - First smelting: Ash and added borax ($Na_2B_4O_7.10H_2O$) were smelted at greater than 1000 °C, in 30 min → slag - Second smelting: Slag, added borax, and silver pieces were smelted at greater than 1000 °C, in 1.5 h → bullion	- Au and Ag were recovered into bullion. - Inconclusive results, but offers a technically viable approach	[23]
$REEs$	*Dicranopteris linearis* (fern): 2700 mg kg^{-1} $\sum REEs$	Hydrometallurgy: ashing, alkaline leaching, traditional acid leaching - Ashing: 550 °C, 3 h → $REEs$ from biomass are enriched into ash which is subjected to extraction - Alkaline leaching (pre-treatment): 6 M NaOH, 80 °C → $REEs$ in solid concentrate - Acid leaching (dissolution step): HNO_3, pH 4.8, 25 °C → $REEs$ in leachate	- Final product: $REEs$ in pregnant solution (acid leachate) - The overall efficiency of the extraction process: 74%	[124]
7 $REEs$: La, Nd, Ce, Pr, Sm, Y, Gd	*Dicranopteris linearis* (fern): 3350 mg kg^{-1} $\sum REEs$	Ion-exchange leaching (hydrometallurgy and bio-metallurgy: chemical leaching, biosorption, desorption) - Ion-exchange leaching: 0.5 M HNO_3 with the presence of resin in 2 h → $REEs$ in biomass were leached and adsorbed into the resin - Desorption: +Washing with water, followed by 0.75 M nitric acid +Elution step using 3 M nitric acid	- 81.4% REE purity and 78% recovery	[116]
4 $REEs$: La, Ce, Nd, Pr	*Dicranopteris linearis* (fern): 3580 mg kg^{-1} $\sum REEs$	Hydrometallurgy: leaching, precipitation - Leaching: biomass was leached by 0.05 M EDTA solutions, solid-liquid ratio of 30 g/L, for 2 h → $REEs$ in leachate (efficiency of 85%) - Precipitation: the leachate was precipitated by using oxalic acid, pH 2.3, the molar ratio of 8:0.37 → $REEs$ in the precipitate	- Final product: $REEs$ in the precipitate after the precipitation process - The recovery rate of the whole process: 70%	[117]
7 $REEs$: La, Ce, Nd, Pr, Sm, Gd, Y	*Dicranopteris linearis* (fern): 3890 mg kg^{-1} $\sum REEs$	Hydrometallurgy: leaching, precipitation, calcination - Leaching: 0.25 M H_2SO_4, solid:liquid ratio of 3 g/100 mL, for 2 h → $REEs$ in leachate (efficiency of 79%) - Precipitation: the leachate was precipitated by using oxalic acid, pH 2.6, the molar ratio of 8:0.37 → $REEs$ in the precipitate (efficiency more than 90%) - Calcination: the precipitate was burnt at 700 °C for 2 h → REE-oxides	- Final product: rare earth oxides - The recovery rate of the whole process: 72%	[120]

There is only one study aiming at reclaiming $REEs$ in biomass ashes so far [124]. In this research, the collected plant *Dicranopteris linearis* was initially incinerated at 550 °C for 3 h in a muffle furnace to secure complete oxidation. Then the fern ash was subjected to an extraction procedure consisting of two stages, namely pre-treatment and dissolution. The pre-processing step aimed to render rare earths available for extraction and eliminate aluminum as much as possible by using 6 M sodium hydroxide (NaOH) at an average temperature of 80 °C. Following that, the $REEs$ were extracted by employing diluted nitric acid (HNO_3) at ambient temperature. The recovery rate of the extraction procedure was reported at 74% under optimal conditions. Alternatively, a few approaches to extract $REEs$ directly from polluted plants have been proposed. The first research based on the ion exchange leaching process was published in 2018 [116]. In this paper, harvested fern *Dicranopteris linearis* was initially leached in 0.5 M nitric acid solution with the presence of exchange resin. Consequently, rare earth metals in the plants were dissolved and absorbed into the resin. This was followed by washing the resin with water and 0.75 M HNO_3. Ultimately, $REEs$ are eluted using 3 M nitric acid, which provides a solution containing 81.4% $REEs$ purity. This procedure resulted in an overall recovery rate of 78%. In another work, Laubie et al. (2018) [117] reported a hydrometallurgical pathway to recycle $REEs$ from natural fern growing on former mine tailings. The manner includes a direct leaching step using an EDTA solution (Ethylenediaminetetraacetic acid), followed by precipitation with acid oxalic. The optimal conditions of the process are given in *Table 2.9*, leading to an overall recovery yield of 70% $REEs$. More recently, a relatively comprehensive hydrometallurgical pathway for reclaiming $REEs$ from a hyperaccumulator *Dicranopteris linearis* was revealed [120]. In the beginning, collected fern was leached in 0.25 M sulphuric acid at a solid-liquid ratio of 3:100 (g mL^{-1}). Following this, rare earth metals were precipitated by utilizing oxalic acid at a molar ratio of 8:0.37 after pH adjustment to 2.6. Eventually, the precipitate was calcinated at 700 °C for 2 h in order to convert it to rare earth oxide as the final product of the procedure. As a result, 72% of $REEs$ in the plant were reclaimed via this recovery route.

Generally, the investigations regarding the extraction of NMs and $REEs$ bio-ores especially biomass solid remains are extremely scant and inadequate, although reclaiming valuable metals from these secondary resources has great potential. This scientific gap might stem in part from the novelty; it brings opportunities and challenges to researchers.

2.2.5. Concentration limits, the potential of NM and REE phytomining

The concentration of NMs and $REEs$ in biomass or solid remains is essential to the economic feasibility of the extraction, but this threshold value is not completely defined yet. It is suggested that the extraction of materials containing 300 mg kg^{-1} $REEs$ may be profitable [155]. Meanwhile, these numbers are 4, 6, and 1000 mg kg^{-1} for Pt, Au, and Ag respectively [156], [157], and range from 5 to 15 mg kg^{-1} in the cases of other NMs (Ir, Os, Pd, Rh, Ru) [158]. The profitable concentrations might be lower due to the development of extraction technologies and the increase in metal prices. The economic levels together with the concentration factor defined as the quotient of economic levels to metal grades in the Earth's crust are given in *Table 2.10*. The commercial metal grades are reachable in many of the cases presented earlier in *Table 2.4* and *Table 2.5*, where the high NM and REE concentrations in plants are observed.

Table 2.10. Profitable grade, concentration factor, and economic concentration in biomass of NMs and $REEs$.

Element	Abundance in Earth's crust (mg kg^{-1})	Economic concentration (mg kg^{-1})	Concentration factor (times)	Economic proposed concentration in biomass (mg kg^{-1})	Ref.
Ag	0.0750	1000	13333	10–100	[157]
Au	0.0040	6	1500	0.06–0.6	[157]
Ir	0.0010	5–15	5000–15000	0.05–1.5	[158]
Os	0.0015	5–15	3333–10000	0.05–1.5	[158]
Pd	0.0150	5–15	333–1000	0.05–1.5	[158]
Pt	0.0050	4	800	0.04–0.4	[156]
Rh	0.0010	5–15	5000–15000	0.05–1.5	[158]
Ru	0.0010	5–15	5000–15000	0.05–1.5	[158]
$\sum REEs$	241.87	300	1.24	3–30	[155]

Furthermore, if the enrichment process is considered, then the levels of NMs and $REEs$ in the solid residuals may surpass the economic limits. For instance, once woody biomass is combusted, its mass is assumed to lessen by 90–99%. As a result, the concentration of NMs and $REEs$ in solid remains would be 10–100 times higher than that in plants. This means the

grades of metals in biomass of ten to a hundred times less than the economic limits might reap the benefit if ashes are subjected to the extraction process. The profitable metal concentrations in biomass are proposed as in *Table 2.10*, which are absolutely achievable in hyperaccumulators or even in ordinary biomass gathered from contaminated land.

The economic viability of NM and REE phytomining is basically dependent on several factors. These are the concentration of NMs and $REEs$ in soil and plant matter, biomass production, and the effectiveness of enrichment and extraction processes. More importantly, metal prices play a paramount role in the commercial aspect of the operation. Rare earth elements are relatively valuable, precious metals are extremely costly, and their market prices tend to increase consistently *Table 2.3*. Therefore, the conception of NM and REE phytomining could be feasible on a commercial basis if ample amounts of biomass and profitable concentrations in plants are attained. Additionally, the energy produced by the enrichment process of biomass combustion can strengthen the economic facet of the NM and REE phytomining pathway. On the whole, the results found in this review of the literature indicate that the phytomining of NMs and $REEs$ is potentially viable from both economic and technical points of view.

Phytomining has been widely applied to reclaim nickel from contaminated soils [55], [56]. To date, more than five hundred plant species have been reported to hyper-accumulate this metal [159]. The agronomic processes as well as extraction techniques have been developed to produce Ni-based products such as metal, salts, and oxide [160], [161]. When compared with NMs and $REEs$, the phytomining of nickel has been intensively investigated and is much closer to practical applicability. However, the common application of nickel phytomining can lay a foundation for the evolution of this technology in terms of NMs and $REEs$.

Collectively, phytomining-enrichment-extraction is an innovative approach to reclaiming metals from secondary resources in this era of industrialization and metal reserve depletion. The enrichment process is a vital stage in the overall concept of phytomining to recover high-value metals such as NMs and $REEs$, however, the available information about the method is sparse and scanty. This research investigates the combustion process of biomass containing valuable metals, and the behavior of metals as well as the influence factors on the metal flows, focusing on NMs and $REEs$.

3. SELECTION OF A LOCATION FOR CONTAMINATED BIOMASS SAMPLING

The selection of a location containing considerable metal-concentrations is paramount for the investigation. A brownfield land situated in Gyöngyösoroszi, Hungary (Mátra Mountains, Northern Hungary) is a potential candidate as many studies [162]–[164] indicate that the area is highly metal-contaminated. In fact, Gyöngyösoroszi is an abandoned mining area where lead and zinc industrialized mining started in 1926 and closed in 1986 after 40 years of operation. The common ligneous plant species living there include poplar, oak, birch, pine, walnut, wattle, and bushes. Four locations in Gyöngyösoroszi namely A, B, C, and D were examined to find the biomass sampling point, their exact positions are presented in *Figure 3.1*. From those locations, different woody biomass comprising root and trunk were collected as chemical elements are not distributed evenly in plant parts.

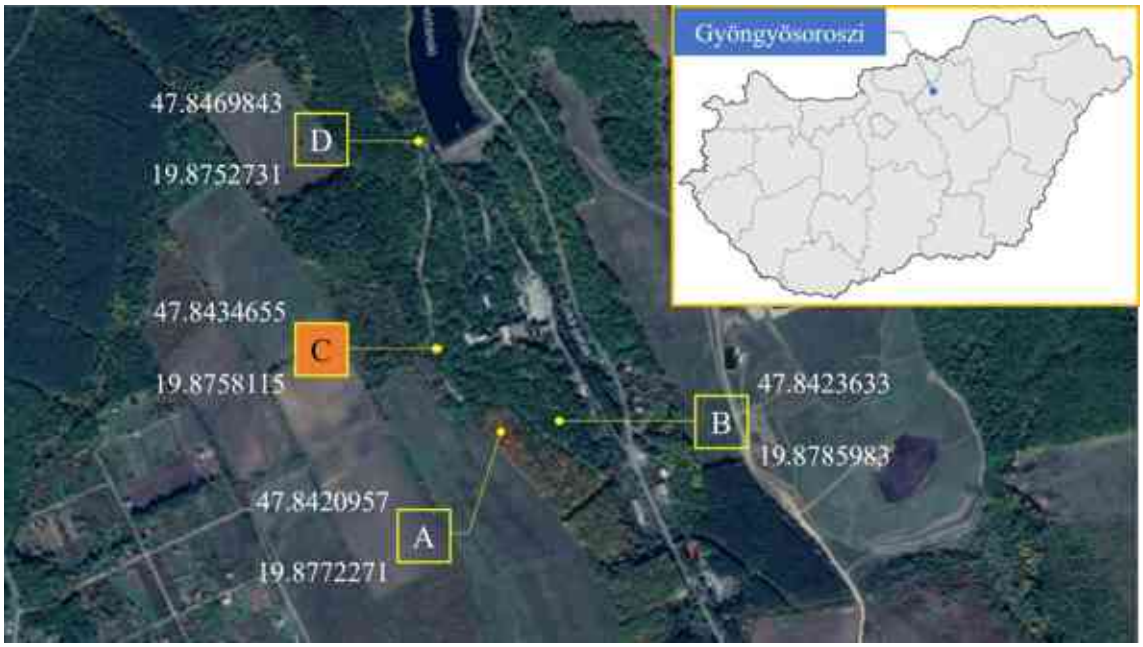

Figure 3.1. Sampling sites in Gyöngyösoroszi, Hungary.

The harvested biomass was cleaned and rinsed in the case of root samples. Then, the biomass was left in the laboratory under natural conditions for several weeks for air drying. Afterward, the collected samples were incinerated by a two-stage ashing process. In the first step, the dried biomass was heated at 250 °C, for 2 h. In the second stage, the process was carried out under the conditions of 500 °C, 4 h. The operation was conducted two times to ensure carbon-free ash samples. The ashing temperature applied for the polluted biomass is based on previous publications [23], [140].

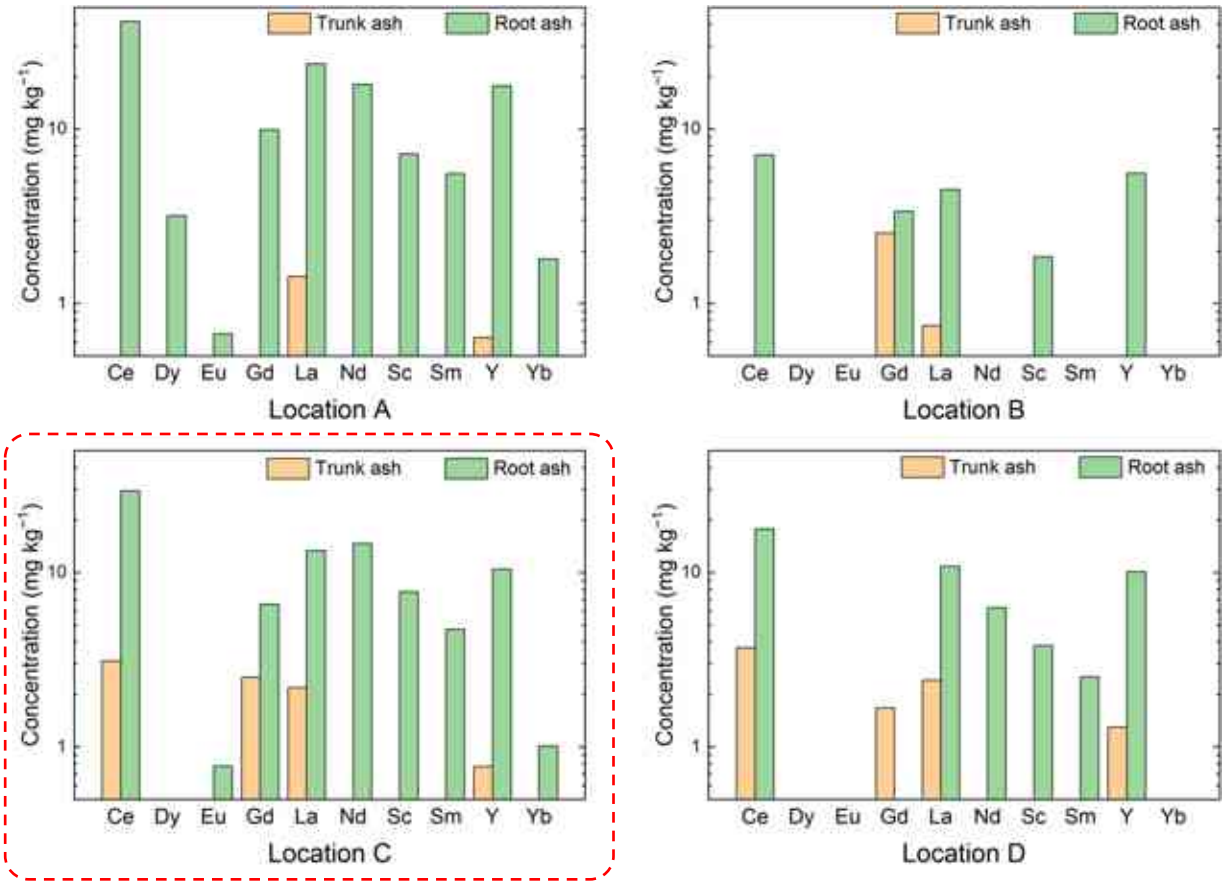

Figure 3.2. The concentration of REEs in the trunk ash and root ash samples of biomass gathered from different contaminated sites.

The derived ash samples were analyzed via the ICP (Inductively Coupled Plasma) technique to determine the possible sampling location. Although *NMs* were not found in this preliminary analysis. It is worth noting that, in another study [45], *NMs* were detectable in the combustion solid remains of biomass gathered from the same area. Despite the results are not fully comparable, it suggests that with lower detection limits, *NMs* can be detected in solid residues obtained from the combustion of biomass.

Meanwhile, several rare earth elements were observed, and the outcomes were visualized in the graphs in *Figure 3.2*. In terms of trunk ash and root ash together, *REEs* were most identified in the samples collected from the C site. To be specific, four elements comprising Ce, Gd, La, and Y were found in both trunk and root ash samples, and five more *REEs* (Eu, Nd, Sc, Sm, Yb) were detected in root ash of biomass coming from this area. In addition, the concentration of *REEs* in the solid remains derived from metal-polluted site C is relatively high compared to that in other sampling points. Because of the mentioned reasons, site C was chosen as the location of contaminated biomass sampling.

4. MATERIALS AND METHODS

4.1. Materials

From the selected site C, bulk biomass collection was done including the necessary sample preparation steps. The harvested plant parts including the trunk, branches (branch and twig), and leaf were left in a laboratory under natural conditions for a few weeks for air drying. The different parts of the biomass were individually shredded and then mixed in the proportion of 75% trunk, 16% branches, and 9% leaf corresponding to the mass ratio of a real tree. Afterward, the contaminated biomass mixture was pelletized to the required dimensions to provide fuel for the boiler operation. The pelletizing process was done by the Faculty of Earth and Environmental Sciences and Engineering, at the University of Miskolc.

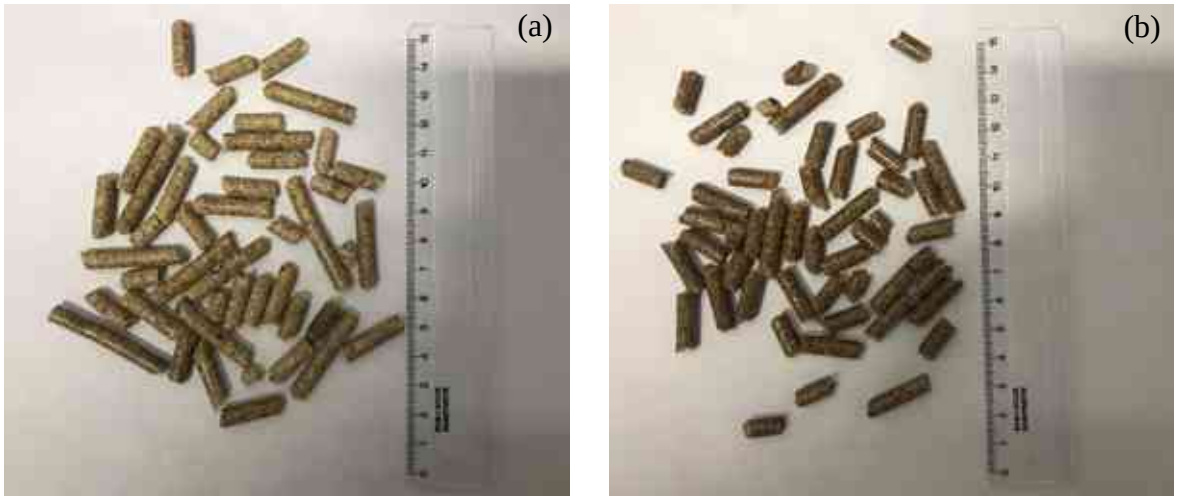

Figure 4.1. Biomass samples. (a) Contaminated pellet, (b) Common market pellet.

In addition to contaminated biomass gathered from brownfield land, a common market pellet was also analyzed and tested in this study for comparison purposes (*Figure 4.1*). The common market pellet (also called, common biomass or normal biomass) was provided by MBH Zrt (Hungary) company. Both of the pellets are 10–30 mm in length and 6 mm in diameter. The general properties of the contaminated pellet and the common market pellet are given in *Table 4.1*, where CB and NB stand for contaminated biomass and normal biomass, respectively. The proximate analysis outcomes were determined through the thermogravimetric measurement. The thermal measurement was performed by MOM Derivatograph C/PC with a heating rate of 10 °C min^{-1} in an air atmosphere. The TG and DTG curves as a function of temperature during the thermogravimetric analysis are presented in *Figure 4.2*. The thermal behaviors of the two biomass samples perform similarities. The initial weight loss, typically occurring between 60

and 150 ℃, is attributed to the evaporation process of moisture content. Subsequently, the devolatilization process ensues, involving the release of volatile content. Eventually, combustion of the fixed carbon content is the final process that primarily occurs within the temperature range of 350 to 700 ℃.

Table 4.1. Properties of biomass samples.

Properties		CB	NB
Ultimate,	N_{db}	0.40	0.27
% by weight	C_{db}	46.75	47.19
	H_{db}	6.05	5.94
	S_{db}	0.01	0.02
	O^*_{db}	37.78	35.66
Proximate,	Fixed carbon	38.82	37.18
% by weight	$Volatile_{db}$	52.17	51.91
	$Moisture_{db}$	6.81	6.92
	Ash	2.20	4.00
HHV_{db}, MJ/kg		18.2	19.1
Density, kg m^{-3}		422	636

CB: Contaminated biomass, NB: Normal biomass, HHV: Higher heating value, db: dry basis, *: by difference.

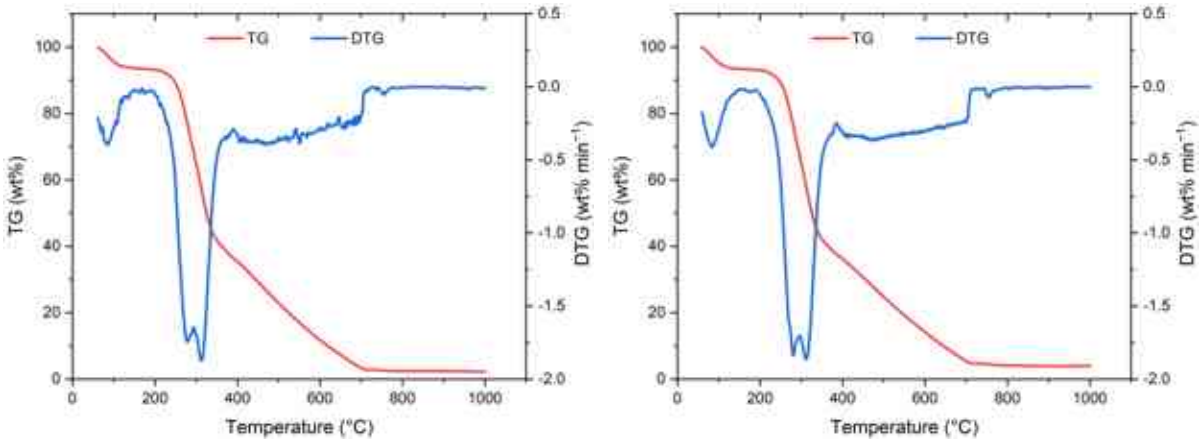

(a) Contaminated pellet (b) Common market pellet

Figure 4.2. Thermogravimetric analysis of biomass samples.

4.2. Experimental system

It is crucial to develop suitable combustion and flue gas system for contaminated biomass. The experimental system was installed and finalized in several stages during the PhD study. The schematic illustration of the measurement setup is shown in *Figure 4.3*.

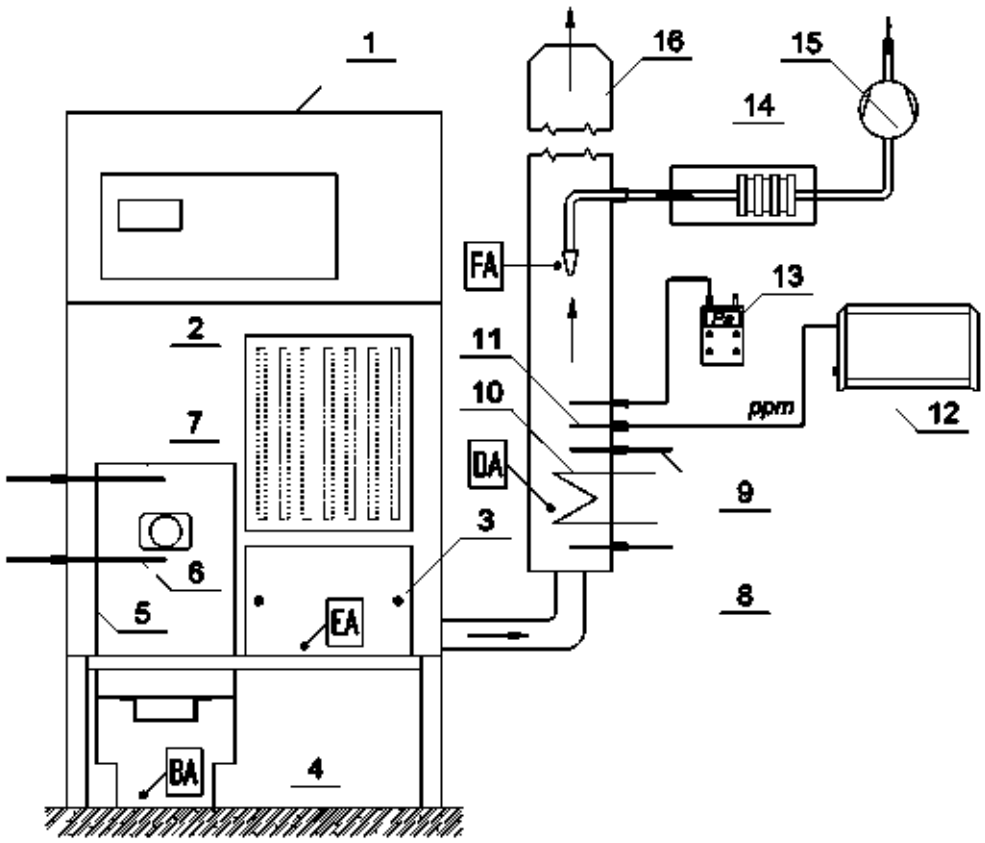

Figure 4.3. Schematic illustration of the measurement setup: (1) boiler body, (2) water heat exchanger, (3) chamber after the water heat exchanger, (4) ashtray, (5) combustion chamber door, (6, 7, 8, and 9) thermocouples, (10) air heat exchanger, (11) gas sampling probe, (12) portable flue gas analyzer, (13) manometer, (14) impactor, (15) pump, and (16) stack. Ash samples: BA – bottom ash, EA – after heat exchanger ash, DA – deposited ash, FA – fly ash.

Basically, the experimental system comprises three main components namely the boiler, water system, and flue gas system. The biomass is supplied from the fuel storage of the boiler into the grate by a screw conveyor. The combustion air passes through the grate in the combustion chamber, where the biomass combustion process takes place. Solid fuels are combusted, and their products comprise hot flue gas and bottom ash. The bottom ash dropped down to the bottom of the boiler is sampled at the end of the combustion process. The high-temperature flue gas leaves the chamber and goes through the water heat exchanger and the air

heat exchanger in sequence. In which, flue gas transfers thermal energy to the water and the cooling air moving between the pipes of the water heat exchanger and the air heat exchanger respectively. After the heat exchangers, flue gas with a lower temperature including gaseous components and particulate matter content (fly ash) is transported to the stack by a centrifugal fan. An isokinetic fly ash sampling system is used to separate and collect fly ash from the flue gas before it emits into the environment.

4.2.1. Boiler

The combustion experiments are carried out in a fixed-grate pilot-scale boiler located at the Department of Combustion Technology and Thermal Energy at the University of Miskolc. This boiler was developed and manufactured by MBH Hungarian Biomass Recycling Company as a hot water heating appliance. It can be operated with solid biofuel in the form of pellets or chips. The main components and dimensions of the boiler are presented in *Figure 4.4*. The major technical parameters of the boiler are given in *Appendix 1*.

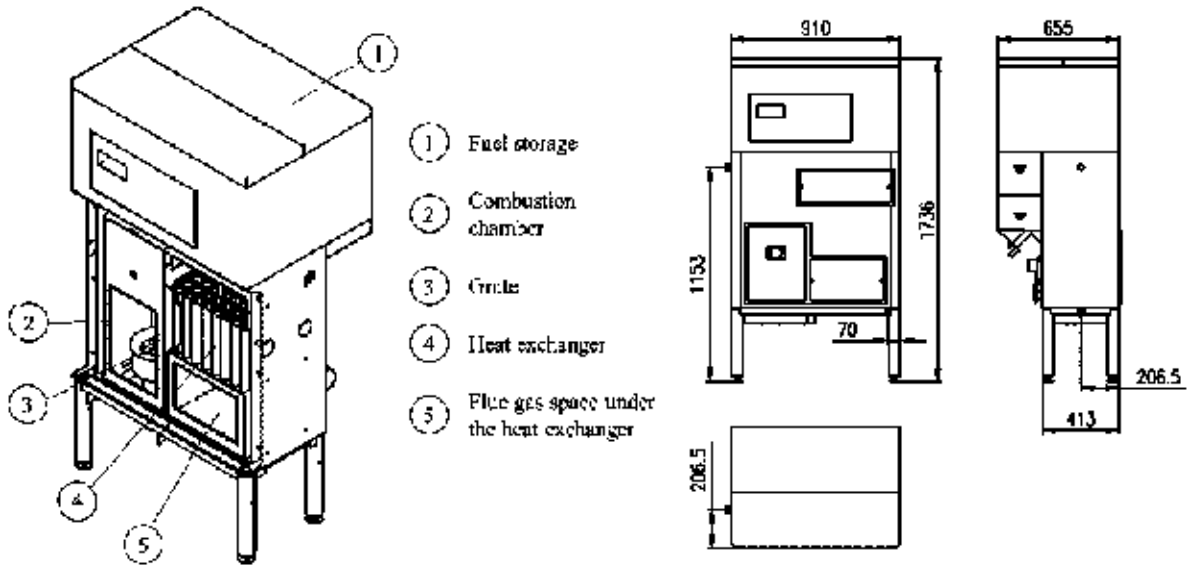

Figure 4.4. Sketch of the boiler with major components and main dimensions (mm) [165].

4.2.2. Water system

The schematic illustration as well as the principle of the water system are shown in *Figure 4.5*. Generally, the water inlet from the water supply goes through a ball valve and a regulating valve to the boiler. Regulating valve (2) is used to control the volume flow of the raw water. In the water heat exchanger of the boiler, the inlet water receives thermal energy from flue gas. After the boiler, the water outlet with elevated temperature is transported to the tank (6). From there,

the water then partly flows to drainage, and another part of this hot water via the regulating valve (8) is returned to the boiler. By applying the regulating valves, the temperature difference between the water inlet and the water outlet can be adjusted. In other words, with the designed system we can control the temperatures before and after the boiler.

During operation, the temperatures of upstream the boiler, water inlet, and water outlet are determined by thermocouples. Moreover, the volume flow rate of water is also measured. In this system, the water is transported by using a circulation pump (7). There are 2 valves installed between the boiler for maintenance purposes. Besides that, the discharge valve (10) is located at the bottom to exhaust all the water from the system.

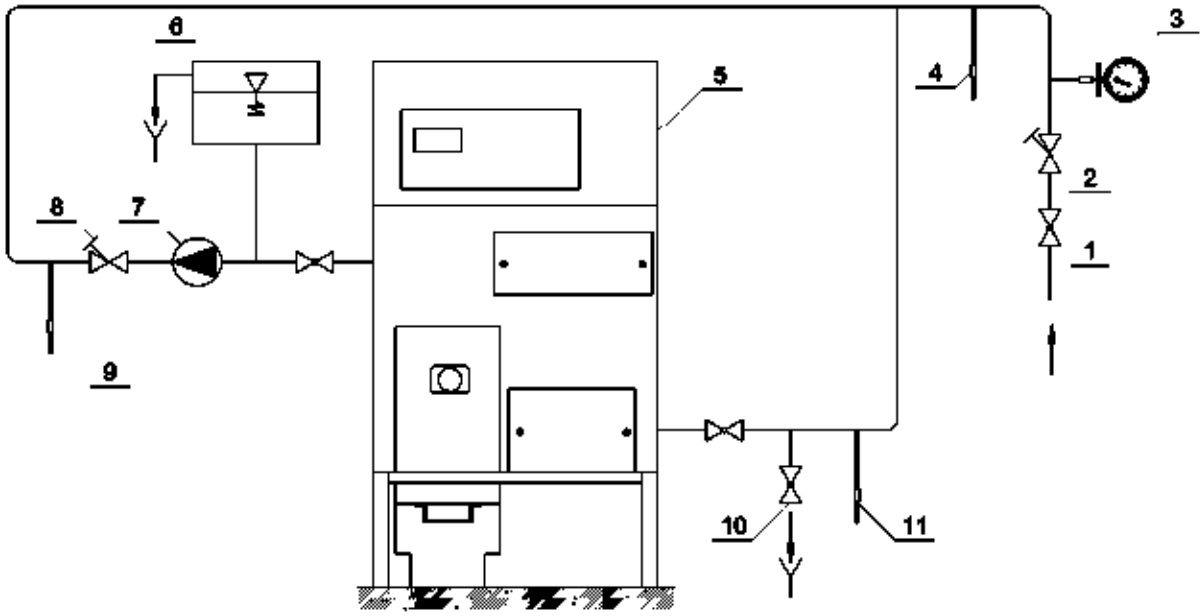

Figure 4.5. Schematic illustration of the water system: (1) ball valve, (2 and 8) regulating valves, (3) water flow meter, (4, 9, and 11) thermocouples, (5) boiler, (6) tank, (7) pump, (10) discharge valve.

By knowing the water inlet temperature, the boiler outlet temperature, and the flow rate of the tap water, the heat removal or the heat transfer in the heat exchanger of the boiler is calculated in equation (3).

$$Q = \dot{m}.C_p.\Delta T = \dot{V}.\rho_w.C_p.(T_{in} - T_{out}) \quad (3)$$

Where:

- Q: heat removal of flue gas in the boiler (W)
- $\dot{m}$: mass flow rate of the water (kg s^{-1})

- C_p: specific heat at a constant pressure of water depending on temperature and pressure (J kg K^{-1})
- ΔT: difference in temperature of the inlet and outlet water (K)
- $\dot{V}$: volume flow rate of the water (m^3 s^{-1})
- ρ_w: density of water depending on temperature and pressure (kg m^{-3})
- T_{in}: water inlet temperature upstream of the boiler (raw water) (°C)
- T_{out}: water outlet temperature (°C)

4.2.3. Isokinetic fly ash sampling system

The main purpose of isokinetic sampling is to capture particles that pass through a defined area for a defined time without disturbing their paths. The isokinetic fly ash sampling system (*Figure 4.6*) contains an impactor that has a three-stage cascade for determining particles of flue gas in the stack in the size fractions of PM10, PM2.5, and PM1. Setting up the impactor for measurements of PM10 and PM2.5 (option to add PM1 in the same instrument) follows ISO23210 standard [166]. The sample collection is started after the boiler reaches quasi-steady-state operational conditions. The fly ash sampling method meets the regulations of the ISO23210 standard.

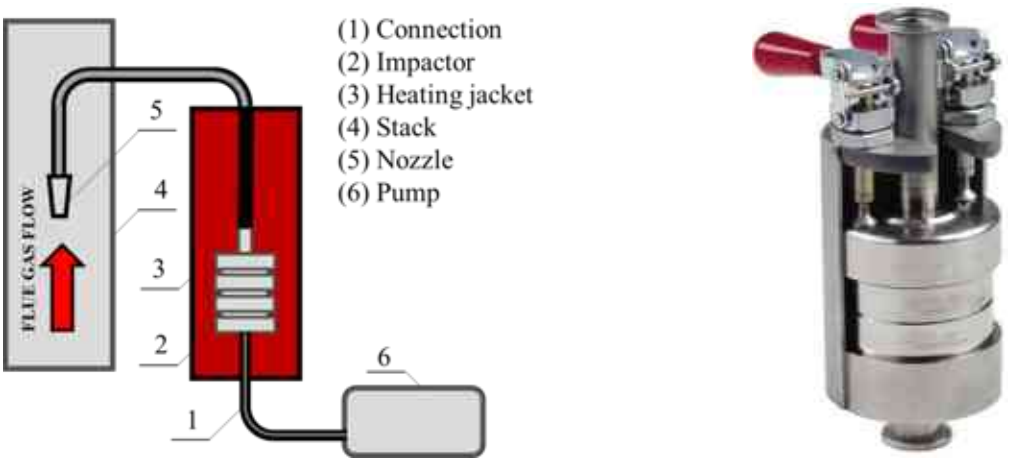

(a) Isokinetic fly ash sampling system (b) Impactor

Figure 4.6. Isokinetic fly ash sampling system employing an impactor.

Dekati® PM10 impactor has three-stage cascades to determine particle gravimetric mass size distribution. It is operated based on inertial size classification and gravimetric or chemical analysis of the collected size-classified particle samples. The impactor has cut points of 10, 2.5,

and 1 μm for PM10, PM2.5, and PM1.0 measurements. This impactor is manufactured of stainless steel for operation even in harsh environments and can be heated up to 200 °C.
It is worth noting that the Dekati® PM10 impactor is capable of separating various particle sizes, including PM10, PM2.5, and PM1.0. However, in this study, these separation stages are intentionally omitted, and only the isokinetic feature is employed as this is a critical part in fly ash sampling. The main reason for that is to collect all the fly ash samples together and handle the samples together. Later, the separation of different fly ash particle sizes (PM10, PM2.5, and PM1.0) could potentially offer valuable scientific insights into the behavior of different metals across divergent particle sizes.

4.3. Experiment and methodology

A series of combustion experiments were conducted to investigate the behavior of metals in the burning system as well as the influence factors on the metal flows during biomass incineration. The operational procedure of the experiment is detailed in *Appendix* 2. During the combustion process, several parameters were observed which are given in *Table 4.2*.

Table 4.2. Parameters observed during combustion experiments.

Symbol	Unit	Parameter
T_1	°C	Water inlet temperature upstream of the boiler (raw water)
T_2	°C	Circulation water temperature (mixture of return and raw water)
T_3	°C	Water outlet temperature
T_4	°C	Flue gas temperature in the stack
T_5	°C	Temperature after the water heat exchanger
T_6	°C	Temperature at the edge of the combustion chamber
T_7	°C	Temperature in the middle of the combustion chamber
$\dot{V}$	$m^3\ s^{-1}$	The volume flow rate of inlet water
f_{vfd}	Hz	Frequency of variable frequency drive (VFD)
p	Pa	The pressure of flue gas controlled by VFD
ΔT	K	The temperature difference between inlet and outlet water
Q	kW	Heat removal of flue gas in the boiler
f	$kg\ h^{-1}$	Feeding rate
O_2	vol %	Oxygen content in flue gas
CO_2	vol %	Carbon dioxide in flue gas
CO	vol ppm	Carbon monoxide in flue gas
NO_x	vol ppm	Nitrogen oxide in flue gas

To preliminarily investigate the fate of metals as well as the reproducibility of the combustion experiments, three experiments utilizing contaminated biomass were conducted in a fix-grate pilot-scale boiler under similar operational circumstances. The average values of the major parameters are given as follows: firing rate Q = 12.8 kW, fuel feed rate f = 4.9 kg h^{-1}, typical combustion chamber temperature T_7 = 664 °C, and a typical flue gas temperature T_4 = 118 °C. The influence of combustion parameters on the metal flows was also researched. Three contaminated biomass incineration experiments with different firing rate levels of 10 kW ($C10$), 20 kW ($C20$), and 30 kW ($C30$) were carried out. Differing boiler performances result in different combustion temperatures (T_7 = 693 °C, 840 °C, and 924 °C for 10 kW, 20 kW, and 30 kW, respectively) and different flue gas temperatures (T_4 = 83 °C, 106 °C, and 149 °C for 10 kW, 20 kW, and 30 kW, respectively). These parameters are expected to have impacts on the combusted solid remains and the metal flows during the biomass incineration process. Additionally, an incineration experiment utilizing the common market pellet ($N20$) was implemented under similar operational conditions to the 20-kW contaminated biomass combustion experiment $C20$. The common pellet combustion was conducted for the purpose of comparison with contaminated biomass combustion aiming to study the effect of feedstocks on metal distributions in order to better understand the behavior of metals during biomass incineration.

4.4. Collection of biomass combustion solid remains

Combustion solid remains were collected from different points in the experimental system *Figure 4.3*. After the experiments, bottom ash and after heat exchanger ash were respectively taken from the ashtray and from the chamber after the water heat exchanger. The deposited ash was captured from the surface of the flue gas system at the end of the combustion process. The collection of fly ash was performed by an isokinetic fly ash sampling system employing a Dekati® PM10 three-stage cascades impactor. The fly ash sampling was started after the boiler reached steady-state operational conditions, and the capturing method meets the regulations of the ISO23210 standard. An example of the collected solid remains is given in *Figure 4.7*.

Figure 4.7. An example of ash samples collected from 20-kW contaminated biomass combustion experiment C20. (a) Bottom ash, (b) After exchanger ash, (c) Deposited ash, (d) Fly ash.

4.5. Leaching of biomass combustion solid remains

Following the combustion process, leaching experiments were conducted as the first step to predominately reclaim gold alongside other high-value metals from biomass-derived ashes. The leaching process aims to remove impurity substances and primarily recover gold along with other valuable metals in the leaching residues. The flow chart of the proposed procedure is depicted in *Figure 4.8* including three major leaching stages namely water leaching, acid leaching, and alkaline leaching.

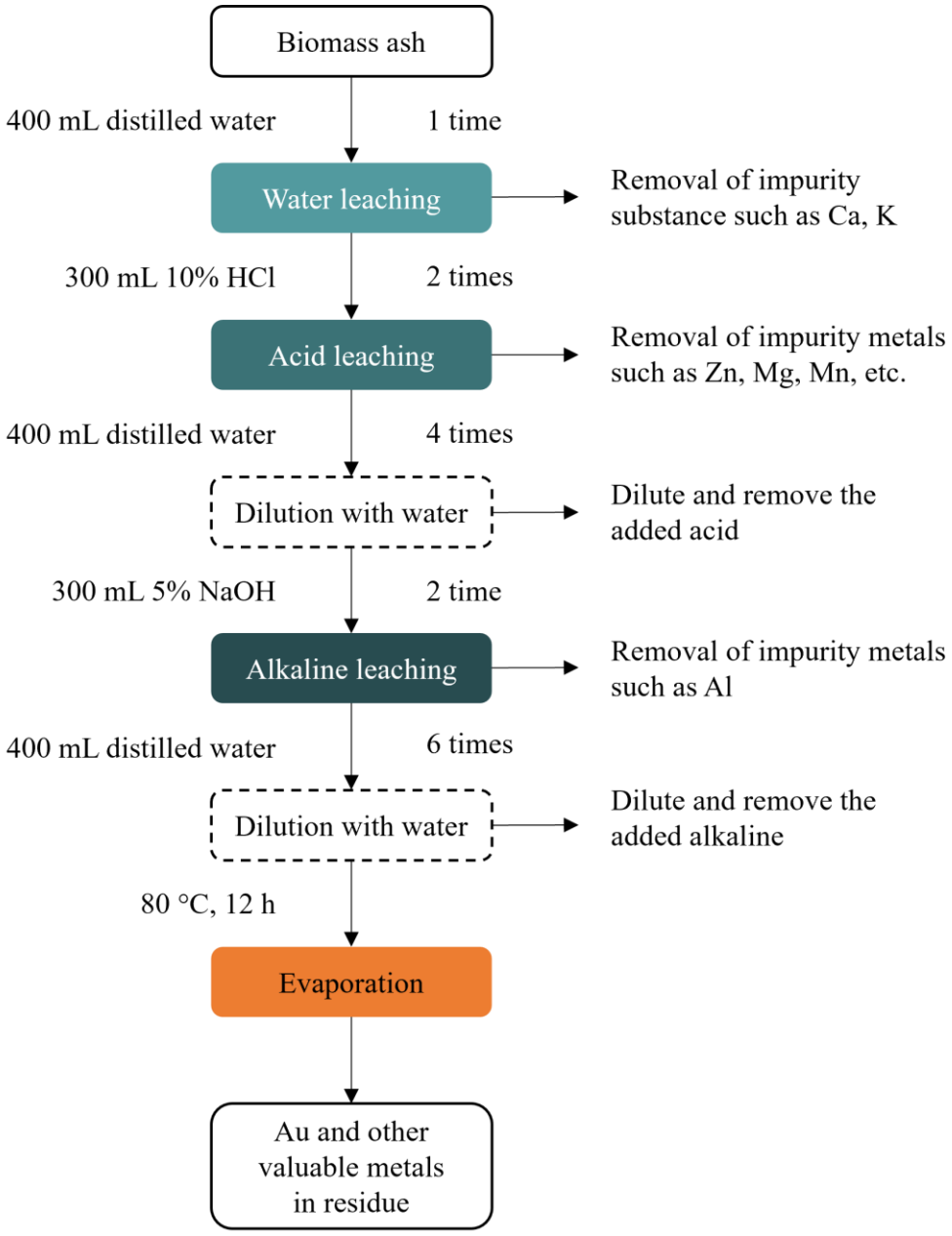

Figure 4.8. Flow chart of leaching procedure for biomass ash samples.

Water leaching is the first phase in the leaching approach. The biomass-derived ashes are leached in 400 mL of distilled water at ambient temperature. In this process, the impurity elements such as K and Ca are dissolved and removed with the leachate. The remaining material (in the solid phase) containing Au and other valuable metals furtherly undergoes an acid-leaching process.

Following the water leaching, two times of hydrochloric acid leaching is applied to eliminate certain metals such as Zn, Mn, and Mg, etc. from the ash samples. The solution of 300 mL 10% HCl is utilized which is prepared by pouring 93.75 mL 32% HCL into 206.25 mL distilled

water. Gold and other targeted metals are insoluble in the acid solution and remain in the solid phase. After acid leaching, 400 mL of distilled water is used to dilute and then remove the added acid. The addition and removal of distilled water are conducted four times to purge the acid remnant.

Alkaline leaching is the last leaching step aiming to selectively dissolve and remove the impurities of Al while leaving gold and other high-value metals in the sediment. This is repeated two times to enhance the efficiency of the process. To prepare the alkali leaching solution, at first 15 g of sodium hydroxide in solid form is added into 100 mL distilled water. Following that, 100 mL NaOH is mixed with 200 mL distilled water to make a 300 mL solution of 5% NaOH used for the alkaline leaching. Similar to acid leaching, 400 mL of distilled water is added and removed to dilute and eliminate the used alkaline. This purging step is repeated six times as alkali leaching is the final leaching stage.

The sediment or slurry derived from the leaching of ash samples is dried in a furnace at a temperature of 80 °C for 12 h. As a result of the leaching process, a significant amount of impurities was eliminated accounting for more than 97% of ash samples. Gold and other valuable metals are expected to be enriched in the obtained leaching residues.

4.6. ICP analysis

The woody biomass, the combustion ashes, and the leaching residues were taken for the elemental analysis to investigate the behavior of metals in the burning system and the efficiency of the leaching process. Woody biomass (WB) refers to common market pellets (or normal biomass NB) and contaminated biomass (CB) which were used for all the combustion experiments. The combustion ashes comprise four types of ash samples namely bottom ash (BA), after heat exchanger ash (EA), deposited ash (DA), and fly ash (FA) captured from the incineration experiments. The leaching residues were derived from the leaching of the combustion ashes. The chemical composition of the solid samples identified by ICP (Inductively Coupled Plasma) spectrometry was performed by an individual company in Hungary. Perkin Elmer Avio 200 inductively coupled plasma-optical emission spectrometer (ICP-OES) and ICP mass spectrometry (ICP-MS) are employed for the analysis. The samples were prepared based on the Hungarian standard MSZ EN 13346:2000. The procedure of sample preparation for analysis is described below. The concentrations of all NMs (Ag, Au, Ir, Os, Pd, Pt, Rh, Ru), and most $REEs$ (15 elements namely Ce, Dy, Er, Eu, Gd, Ho, La, Nd, Pr, Sc, Sm, Tb, Tm, Y, Yb) and other metals (Cd, Co, Cr, Cu, Fe, Mg, Mn, Ni, Pb, Th, Ti, U, V, Zn) were

selected to be measured due to their importance, high economic value, and toxicity (for heavy metals).

- In the case of the FA sample, a royal water solution was used (2 ml cc. HNO_3 and 6 ml cc. HCl) for 30 minutes at 180 °C. From 0.1 to 0.4 g of FA were taken, according to how much material was available. The standard used was Lu at 1 mg L^{-1}, applied to the sample before the extraction process.
- In the case of the WB samples: nitric acid-hydrogen peroxide extraction was used (5 mL cc. HNO_3 + 4.5 mL 30% H_2O_2) at 190 °C for 15 min. 0.35 g samples were measured three times and applied to the extraction vessel. After the extraction process, the three parallel samples were filtered and washed into a 50 mL measuring flask, then filled to the sign. The standard used was Lu at 1 mg L^{-1}, applied to the sample before the extraction process. The blank tests were prepared the same way, without putting the samples in.
- In the case of the FA samples: a royal water solution was used (2 mL cc. HNO_3 and 6 mL cc. HCl) at 180 °C for 30 min. From 0.1 to 0.4 g of FA were taken, according to how much material was available. The standard used was Lu at 1 mg L^{-1}, applied to the sample before the extraction process. The blank tests were prepared the same way, without putting the samples in.
- In the case of the BA, EA, and DA samples: a royal water solution was used (2 mL cc. HNO_3 and 6 mL cc. HCl) at 180 °C for 30 min. From each sample, 0.5 g was measured three times into three extraction vessels. After the extraction process, the three parallel samples were filtered and washed into a 50 mL measuring flask, then filled to the sign. In the case of the samples where it was not possible to measure the 1.5 g, less material was used, thus the detection limits were increased. The standard used was Lu at 1 mg L^{-1}, applied to the sample before the extraction process. The blank tests were prepared the same way, without putting the samples in.

4.7. SEM analysis

Biomass combustion solid remains and leaching residues were characterized by using scanning electron microscopy (SEM) and energy dispersive spectroscopy (EDS). SEM examinations of biomass-derived ashes aim to investigate forms of valuable metals in the contaminated ashes as well as to find evidence for the ICP measurement outcomes. Meanwhile, the major purpose of the leaching residue scanning is to evaluate the efficiency of the leaching process in

reclaiming valuable metals from unconventional resources. SEM technique is widely used to study the occurrence of NMs and $REEs$ in coal-derived ashes [167]–[172]. It is deemed the best method for the characterization of coal ashes [173]. On the other hand, investigations regarding the formation of NMs and $REEs$ in biomass-derived materials are sparse and scanty. Therefore, characteration of biomass ashes and leaching residues via SEM analyses is nessesarry that can open new insights into the holistic phytomining concept.

SEM-EDS technique provides detailed imaging information about surface morphology and elemental composition of the samples. The analysis was conducted by using a scanning electron microscope of ZEISS EVO MA10 equipped with backscattered and secondary electron detectors coupled with EDS. This scanning electron microscope employs high-energy electron beams scanning on a sample surface area of 3 µm, going below 1 µm depth of the surface. To prepare for SEM-EDS analysis, representative portions of the samples were either sprinkled onto double-sided carbon tapes or suspended onto aluminum plates or glass plates. Suspension of the samples on aluminum plates looked like the best preparation method for SEM-EDS analysis of biomass ashes and leaching residues. Noble metals and rare earth elements are major interests of the scanning.

The visual information is provided based on gray-scale intensity between chemical phases of backscattered electron imaging. Backscattered electrons are the electrons reflected directly from the specimen surface; these electrons correlate to the atomic number. For instance, a particle of gold (atomic mass 197, atomic number 79) is remarkably brighter than a particle consisting of carbon (atomic mass 12, atomic number 6). The elemental concentration of the sample is determined by using the characteristic X-ray spectrum. The composition analysis is performed in a ‘‘spot mode’’ in which the beam is localized on a single area manually selected within the field of view. The energy dispersive spectroscopy detector is typically able to detect elements with atomic numbers of being equal to or greater than six [174]. The intensity of the peaks in the energy dispersive spectroscopy is not a quantitative measurement of elemental concentrations. However, from relative peak heights, relative amounts can be inferred.

5. RESULTS AND DISCUSSION

5.1. Experiments of biomass combustion

The values of the major parameters observed from all the biomass combustion experiments are depicted in *Table 5.1*. The outcomes of the three contaminated biomass incineration experiments conducted under the same operational conditions somehow demonstrate the reproducibility of the combustion experiments.

Table 5.1. Values of major parameters observed during the biomass combustion experiments.

Parameter	Unit	Experiments for reproducibility testing				Other different experiments			
		1	2	3	$Mean \pm SD$	$C10$	$C20$	$C30$	$N20$
Q	kW	12.6	13.1	12.7	12.8 ± 0.22	10.1	18.5	31.7	19.1
f	kg h^{-1}	4.9	4.9	4.9	4.9 ± 0.00	4.6	6.8	10.0	6.3
$\dot{V}$	L h^{-1}	195.4	191.2	176.3	187.6 ± 8.2	136.7	239.2	415.4	255.0
T_1	°C	15	18	18	17 ± 1.5	12	11	10	11
T_2	°C	61	61	65	62 ± 1.8	61	63	52	60
T_3	°C	70	77	80	75 ± 4.1	75	78	76	75
T_4	°C	129	131	94	118 ± 17.1	83	106	149	100
T_5	°C	154	152	127	144 ± 12.2	114	153	195	151
T_6	°C	549	585	623	586 ± 30.1	617	701	758	742
T_7	°C	580	692	719	664 ± 60.5	693	840	924	895
CO_2	vol %	6.1	5.2	8.7	6.7 ± 1.5	11.1	12.6	15.0	14.9
O_2	vol %	14.3	15.4	11.5	13.7 ± 1.6	7.7	6.9	5.5	4.6
CO	vol ppm	1751	1706	1122	1526 ± 287	4457	1946	2433	2899
NO_x	vol ppm	72.1	63.5	102.7	79.4 ± 16.8	118.9	50.6	175.4	65.7
Cooling	-	No	No	No	No	No	Yes	Yes	Yes

1, 2, and 3: Experiment number of the three contaminated biomass combustion experiments conducted under similar operational conditions for reproducibility testing; $Mean \pm SD$: Average value ± standard deviation of the three similar experiments 1, 2, and 3; $C10$, $C20$, $C30$: Contaminated biomass combustion experiment of 10, 20, and 30 kW respectively; $N20$: Normal biomass combustion experiment of 20 kW; Cooling: The flue gas is cooled down by going through an air heat exchanger.

Several parameters measured during the experiments were visualized in graphs. *Figure 5.1* shows an example of temperatures of water and flue gas at disparate positions in the system throughout the contaminated biomass combustion experiment $C20$; the measurement data of other experiments are presented in the Appendix. Based on the graph, the inlet water temperature (T_1) represented in blue color virtually did not change and stayed at 11 °C. Meanwhile, the other parameters increased and became stable once the boiler reached steady-state operational conditions. These parameters fluctuated around the critical values as follows:

T_2-63 °C (circulation water temperature), T_3-78 °C (water outlet temperature), T_4-106 °C (flue gas temperature in the stack), T_5-153 °C (temperature after the water heat exchanger), T_6-701 °C (temperature at the edge of the combustion chamber), T_7-840 °C (temperature in the middle of the combustion chamber). Suddenly, the plummets occurred at some points of the experiments, which are more tangible in terms of combustion temperatures identified by red and dark colors. That might be explained by the powders from the pellet accumulated, which temporarily cause congestion affecting the fuel supply and combustion process. It is the reason for the dramatic drops in temperatures.

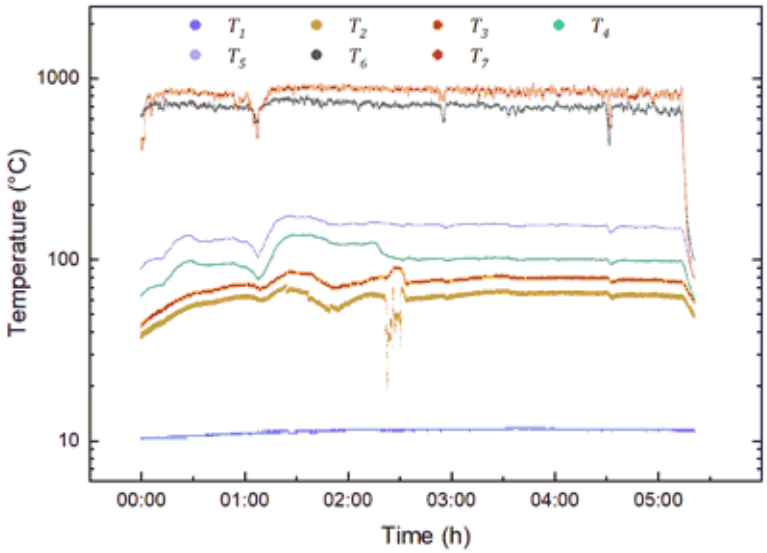

Figure 5.1. An example of observed temperatures during the contaminated biomass combustion experiment of 20 kW (see Table 4.2).

An instance of other variables including water flow rate, differential temperature, and heat removal during contaminated biomass combustion experiment $C20$ is presented in *Figure 5.2*. The volume flow rate of the water inlet was adjusted to a critical value of 239.2 L h^{-1}. This adjustment is aimed at ensuring the temperature prerequisites of the boiler (water outlet from 70–90 °C, the difference between outlet and return water from 10–25 °C). In the earlier stage of the experiments, differential temperature tended to rise, then it started to decline as the impacts of the climb in the water flow rate. This parameter reached the stable state of oscillating around 67 °C after the stabilization of the system. The same trend could be observed in the case of heat removal, its steady number is nearly 20 kW.

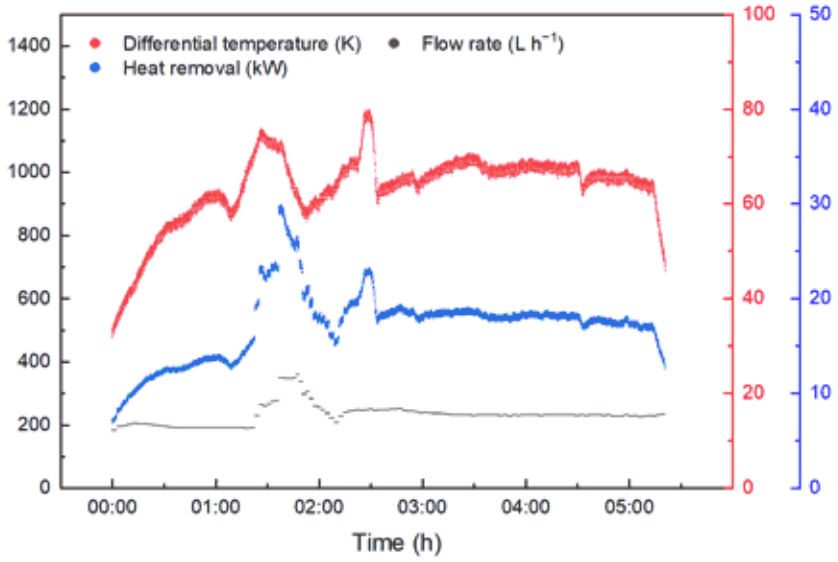

Figure 5.2. An example of differential temperature, removal heat, and water flow rate during the contaminated biomass combustion experiment of 20 kW.

In addition, the portable gas analyzer "Horiba" was utilized to dissect the composition of flue gas. An example of the flue gas composition measurement during the contaminated biomass combustion experiment $C20$ is depicted in *Figure 5.3*. The result shows the majority of carbon dioxide (CO_2), oxygen (O_2), and somehow carbon monoxide (CO). Meanwhile, the presence of nitrogen oxide (NO_x) is rather minor. Although the gas analysis does not sound directly relative to the research topic, that could be useful for further investigations or calculations.

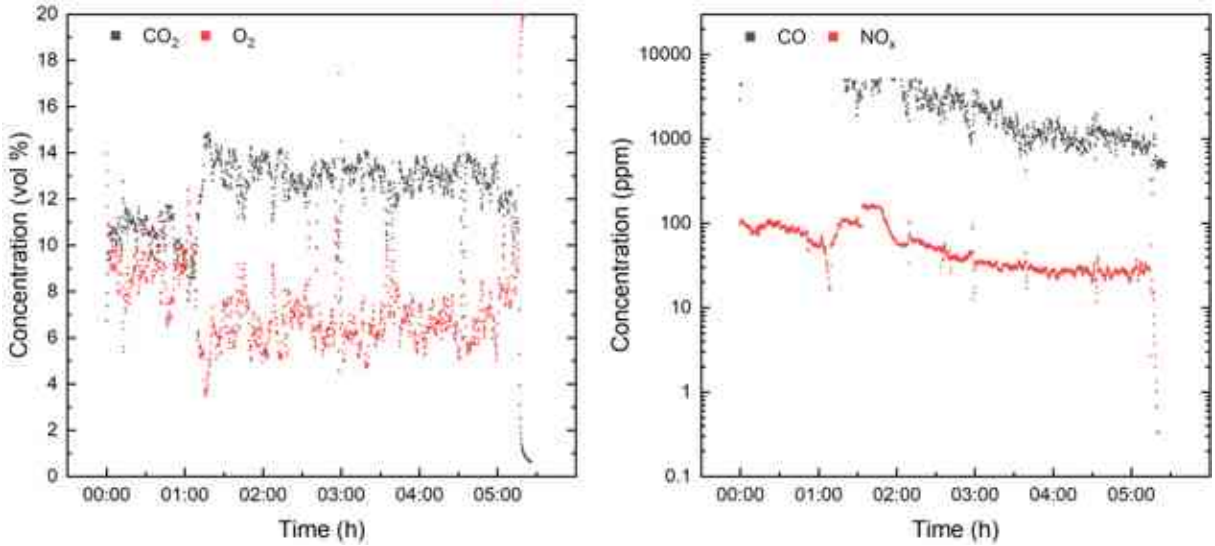

Figure 5.3. An example of flue gas composition measurement during the contaminated biomass combustion experiment of 20 kW.

5.2. The fate of metals and the reproducibility of combustion experiments

The ICP analytical outcomes of the solid samples are generally separated into two elemental groups. The first classification includes elements that are below the detection limit (BDL) in each sample. These elements consist of some NMs (Ir, Os, Pd, Pt, and Ru), several $REEs$ (Er, Eu, Ho, Pr, Tb, Tm, and Yb), and other metals (Th, U). No further investigation nor discussion was made for this metal group. The second chemical categorization comprises a few NMs (Ag, Au, and Rh), some $REEs$ (Ce, Dy, Gd, La, Nd, Sc, Sm, and Y), and other elements (Cd, Co, Cr, Cu, Fe, Mg, Mn, Ni, Pb, Ti, V, Zn) which are detectable in at least one sample. The second metal group was used for further investigations and calculations.

The metal concentrations of solid remains obtained from the three similar combustion experiments are given in *Table 5.2*. To thoroughly assess the reproducibility as well as for further evaluation and discussion, the average values of the outcomes together with their standard deviation are calculated and shown in *Table 5.3*, *Figure 5.4*, and *Figure 5.5*. According to the table and the graphs, the standard deviation values are not so high versus their average concentrations apart from deposited ash samples of Cr and Ni. The results of metal concentrations (*Table 5.2*) and combustion parameters (*Table 5.1*) demonstrate that the combustion experiments and their outcomes are reproducible.

A few NMs such as Ag, Au, and Rh were identified in the ash samples. Rhodium was solely detectable in the fly ash at the level of 0.28 mg kg^{-1}. This is a valuable finding from the scientific point of view since this element was rarely reported before. Other noble metals, including Ag and Au, were found in each ash sample. The highest concentrations of Ag (21.93 mg kg^{-1}) and Au (5.05 mg kg^{-1}) were observed in the fly ash. These numbers are 12 and 3 times greater than the metal grades in bottom ash for Ag and Au, respectively. Considerable concentrations of NMs observed in EA, DA, and FA indicate these metals are leaving the combustion chamber.

Several $REEs$ were found in the solid residues at considerable levels. The most significant outcomes were observed in the case of Nd, such as 33.57 mg kg^{-1} in BA, 20.57 mg kg^{-1} in EA, and 9.32 mg kg^{-1} in DA. On the other hand, Sc was scarcely detected in the combustion ashes. The concentrations of rare earth minerals in FA are either below the detection limits or not available. The behavior of these elements in the system shows a consistent trend, their concentrations follow the decreasing orders of $BA > EA > DA$ (*Figure 5.4*). The greater metal concentrations in BA versus other solid remains indicates the minor volatility of rare earth metal compounds during incineration.

Table 5.2. Concentrations of detectable metals in solid remains derived from the three contaminated biomass combustion experiments conducted under similar operational conditions (mg kg^{-1}).

Element	BA			EA			DA			FA		
	1	2	3	1	2	3	1	2	3	1	2	3
Ag	2.16	1.76	1.61	2.37	4.01	3.40	7.44	13.2	10.7	18.7	26.8	20.3
Au	<1	1.55	<1	<1	1.07	1.11	2.98	2.79	3.39	<10	5.05	<10
Rh	<1	<0.01	<1	<1	<0.01	<1	<2	<0.01	<4	<4	0.278	<8
Ce	6.59	7.22	6.35	6.29	5.71	3.77	4.21	3.81	4.37	-	-	-
Dy	1.50	2.16	1.66	<1	1.34	<1	<2	<2	<4	<7.5	<7.5	<10
Gd	6.26	5.30	4.30	4.03	4.35	2.91	<10	2.43	2.62	<3	<0.2	<4
La	4.72	5.25	4.25	4.04	4.16	2.53	2.61	2.20	2.06	-	-	-
Nd	37	35.8	27.9	18.8	23.9	19	8.73	9.30	9.94	-	-	-
Sc	0.290	0.416	0.304	0.344	0.309	<0.25	<0.5	<0.01	<1	-	-	-
Sm	3.49	5.04	2.30	1.64	2.18	1.22	<5	0.667	<2	<3	<0.2	<4
Y	2.93	3.35	2.79	2.39	2.64	1.60	1.57	1.45	1.51	-	-	-
Cd	3.07	2.87	3.81	39.9	44.9	67.2	120	169	163	138	142	160
Co	13.5	17.9	12.7	9.55	11.6	8.00	38.9	12.4	9.72	<2	<2	<3
Cr	30	35.2	30.1	39.4	35.1	25.6	2990	527	337	18.4	23.1	24.8
Cu	161	199	195	192	215	167	364	268	247	221	257	184
Fe	7490	7590	6630	13700	7410	6620	36100	12500	10000	-	-	-
Mg	34700	34900	30900	26500	28700	19000	19400	19100	20200	-	-	-
Mn	1690	1920	1700	1910	1490	1010	1580	1140	1130	35.1	35	32.2
Ni	25.42	32.55	26.07	22.17	28.41	18.69	1534	262	178	-	-	-
Pb	<5	<5	<5	11.7	11.4	12.2	56.1	83.4	77.4	211	222	207
Ti	150	199	156	195	145	93	216	111	111	-	-	-
V	4.74	4.07	3.26	5.05	3.88	2.61	26.9	6.66	5.20	-	-	-
Zn	941	995	1040	1830	2330	2340	7910	11500	10400	27265	26971	31163

"<": Below the detection limit; "-" Not available; BA, EA, DA, and FA: Bottom ash, after exchanger ash, deposited ash, and fly ash respectively; 1, 2, 3: Experiment number of the three contaminated combustion experiments conducted under similar operational conditions.

Table 5.3. Average concentrations of detectable metals in solid remains derived from the three contaminated biomass combustion experiments conducted under similar operational conditions.

Element	$Mean \pm SD$ (mg kg^{-1})			
	BA	EA	DA	FA
Ag	1.84 ± 0.23	3.26 ± 0.68	10.45 ± 2.36	21.93 ± 3.50
Au	1.55	1.09 ± 0.02	3.05 ± 0.25	5.05
Rh	<0.01	<0.01	<0.01	0.28
Ce	6.72 ± 0.37	5.26 ± 1.08	4.13 ± 0.24	-
Dy	1.77 ± 0.28	1.34	<2	<7.5
Gd	5.29 ± 0.80	3.76 ± 0.62	2.53 ± 0.10	<0.2
La	4.74 ± 0.41	3.58 ± 0.74	2.29 ± 0.23	-
Nd	33.57 ± 4.04	20.57 ± 2.36	9.32 ± 0.49	-
Sc	0.34 ± 0.06	0.33 ± 0.02	<0.01	-
Sm	3.61 ± 1.12	1.68 ± 0.39	0.67	<0.2
Y	3.02 ± 0.24	2.21 ± 0.44	1.51 ± 0.05	-
Cd	3.25 ± 0.40	50.67 ± 11.87	150.7 ± 21.82	146.7 ± 9.57
Co	14.70 ± 2.29	9.72 ± 1.47	20.34 ± 13.17	-
Cr	31.77 ± 2.43	33.37 ± 5.77	1285 ± 1208	22.10 ± 2.71
Cu	185.0 ± 17.05	191.3 ± 19.60	293.0 ± 50.93	220.7 ± 29.80
Fe	7237 ± 430.9	9243 ± 3168	19533 ± 11759	-
Mg	33500 ± 1840	24733 ± 4152	19567 ± 464.3	-
Mn	1770 ± 106.1	1470 ± 367.7	1283 ± 209.8	34.10 ± 1.34
Ni	28.01 ± 3.22	23.09 ± 4.02	658.2 ± 620.4	-
Pb	-	11.77 ± 0.33	72.30 ± 11.71	213.3 ± 6.34
Ti	168.3 ± 21.82	144.3 ± 41.64	146.0 ± 49.50	-
V	4.02 ± 0.61	3.85 ± 1.00	12.92 ± 9.90	-
Zn	992.0 ± 40.47	2167 ± 238.1	9937 ± 1502	28466 ± 1911

"<": Below the detection limit, "-" Not available; $Mean$: The average value; SD: Standard deviation; BA, EA, DA, and FA: Bottom ash, after exchanger ash, deposited ash, and fly ash, respectively.

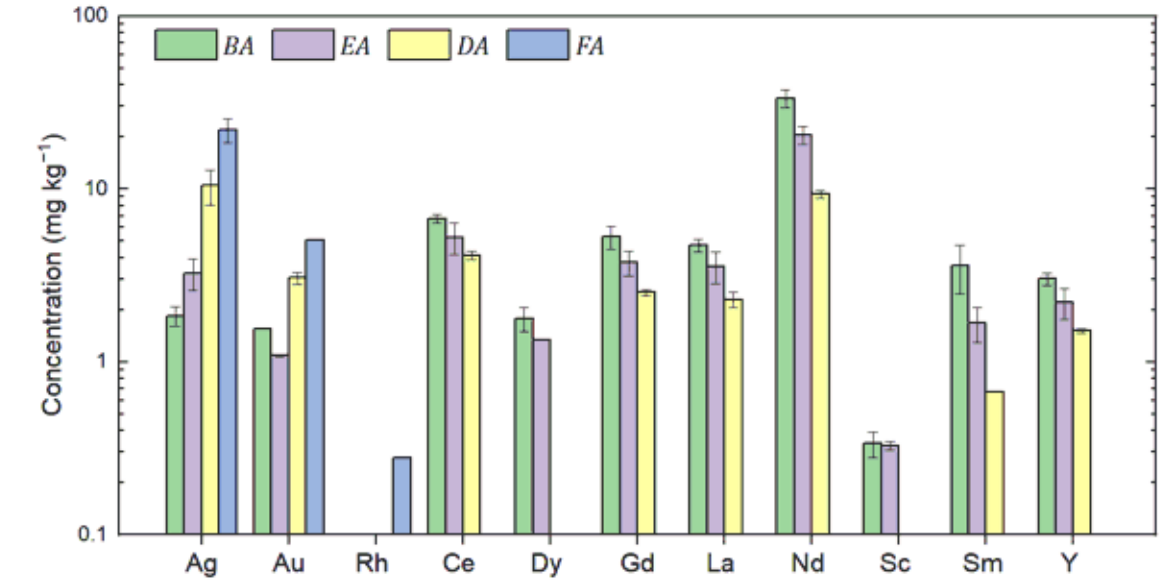

Figure 5.4. The average concentration of NMs and REEs in solid remains derived from three contaminated biomass combustion experiments conducted under similar operational conditions.

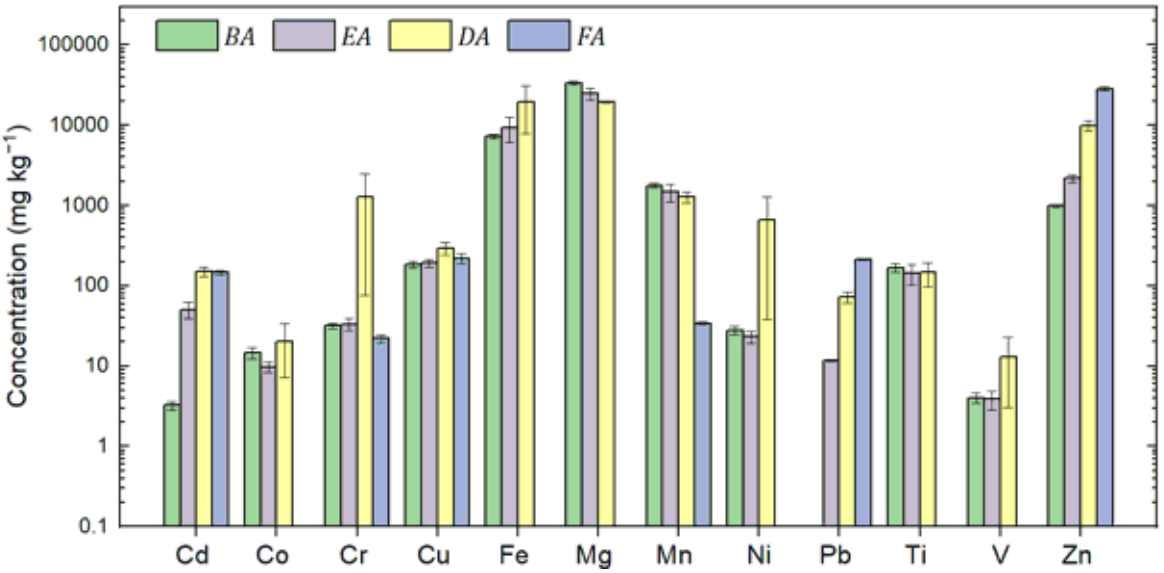

Figure 5.5. The average concentration of other metals in solid remains derived from three contaminated biomass combustion experiments conducted under similar operational conditions.

Other elements including heavy metals were also analyzed in this study for environmental purposes. Their concentrations in the solid samples varied in a vast range from less than one to thousands of mg kg^{-1} (*Figure 5.5*). The prominent results are the presence of 28466 mg kg^{-1} Zn in FA and 33500, 24733, 19567 mg kg^{-1} of Mg in BA, EA, DA respectively. The distributions of these other elements in the burning system differ from metal to metal. Cd, Zn, and Pb were

highly volatilized as their concentrations in EA, DA, and FA are remarkably greater compared to in BA. The levels of Cd and Zn in FA are 45 and 29 times greater than those in BA. While Pb is not detectable in the bottom ash, this element is significantly found in the other solid residuals. For less volatile elements such as Cu, Mg, Fe, Ti, Co, and V, there is no substantial disparity in metal concentration between the different ash samples. These outcomes are in good agreement with other studies [45], [54]. On the contrary, Mn was hardly volatilized as its presence in BA (1770 mg kg^{-1}) is much greater compared to in FA (34.1 mg kg^{-1}). The elements of Cr and Ni performed an atypical trend, their concentrations in the deposited ash samples are tremendously superior to other combustion ashes. Further theoretical and experimental analyses are necessary for a better understanding of the behavior of these two metals.

The identified elemental concentrations in after heat exchanger ash, deposited ash, and fly ash indicate that a noticeable amount of metals leaves the combustion chamber, which later ends up at other positions of the burning system and emits into the environment in large part. Based on the analytical outcomes, during the combustion process, a portion of the metal input in biomass stays in the combustion chamber and can be removed with bottom ash. The other part goes through the water heat exchanger and is partially found in the ash collected after the heat exchanger. The fly ash captured from flue gas contains a certain metal content. Another quantity of metals is detected in deposited ash, which is taken from the surface of the flue gas system. Eventually, the remaining metal proportion in both solid and volatile forms along with flue gas leaves the burning system.

5.3. Influence of combustion parameters and feedstocks on the behavior of metals including NMs and $REEs$ during biomass combustion

Basically, three contaminated biomass combustion experiments corresponding to three boiler performance levels of 10 kW ($C10$), 20 kW ($C20$), and 30 kW ($C30$) were conducted to study the influence of combustion parameters on the metal flows. The effect of feedstocks was investigated by comparing the results of the two experiments carried out under similar conditions (the firing rate is 20 kW) but using different feedstocks of contaminated pellet ($C20$) and common market pellet or normal pellet ($N20$). The concentrations of the detectable valuable metals in the solid samples collected from those experiments are given in *Table 5.4*.

Table 5.4. Concentrations of detectable metals in woody biomass and solid remains derived from different biomass combustion experiments.

Element	WB		BA				EA				DA				FA			
	CB	NB	$C10$	$C20$	$C30$	$N20$	$C10$	$C20$	$C30$	$N20$	$C10$	$C20$	$C30$	$N20$	$C10$	$C20$	$C30$	$N20$
Ag	<0.5	<0.5	3.87	2.94	2.01	1.32	5.13	8.44	11.4	1.78	12.4	15.4	23.6	3.46	24.3	19.2	13.1	2.94
Au	<0.05	<1	<1	<1	1.52	<1	2.64	<1	1.34	<1	1.9	3.04	2.98	<1	<9	3.52	<9	<9
Ce	0.526	<0.5	4.72	6.4	6.42	16.1	1.69	5.58	4.98	10	2.17	1.61	3.42	4.18	<4.5	<1.5	<4.5	<4.5
Dy	<1	<1	2.08	2.22	2.5	<1	<1	1.4	1.82	<1	<1	<1	<1	<1	<9	<3	<9	<9
Gd	0.026	<0.5	6.06	7.49	7.5	7.64	2	5.3	5.6	5.03	2.5	1.56	3.42	2.34	<4.5	<1.5	<4.5	<4.5
La	<0.25	<0.25	3.96	5.23	5.08	8.53	1.29	3.84	3.85	5.08	1.54	1.07	2.45	2.22	<3	<1	<3	<3
Nd	<0.5	<1	26.5	30.7	39.1	6.57	9.39	18.4	30.5	4.24	7.51	4.02	12.5	1.61	<9	<3	<9	<9
Sc	<0.01	<0.25	0.271	0.372	0.404	2.04	<0.25	0.38	0.384	1.26	<0.25	<0.25	<0.25	0.508	<3	<1	<3	<3
Sm	0.026	<0.5	2.59	3.12	5.79	1.55	<0.5	1.64	2.68	0.905	<0.5	<0.5	0.787	<0.5	<4.5	<1.5	<4.5	<4.5
Y	<0.25	<0.25	2.37	3.13	3.11	5.83	0.961	2.51	2.39	3.52	1.08	0.809	1.49	1.46	<3	<1	<3	<3
Cd	3.75	<0.5	57	15.4	2.64	0.581	95.6	106	151	39.8	93.2	104	322	18	132	82.9	123	5.81
Co	<0.25	<0.5	10.7	15.1	18.3	6.73	4.34	8.76	10.8	4.49	5.14	4.17	6.07	2.63	<4.5	<1.5	<4.5	<4.5
Cr	3.01	5.17	28	27.7	32.7	33.6	25.3	29.5	33.6	33.4	32.4	44.1	62.4	62.7	26.2	26.1	34.9	38.1
Cu	3.63	<1	160	162	203	166	184	189	199	191	636	2210	953	833	184	239	247	313
Fe	113	99.7	4390	5700	7420	10700	3940	5210	6260	11000	3470	4050	4590	6310	95.3	60.4	96.7	173
Mg	640	228	32700	36400	36600	38600	11700	29600	27200	26900	16700	12100	18100	14200	158	71.5	64	88.5
Mn	28.1	23.2	1450	1730	1680	3570	663	1450	1350	2830	974	1150	1190	1740	44.4	46.5	62.4	114
Ni	0.98	1.23	19.7	26.4	30.7	33	12.2	21.1	24.8	26.9	15.7	19.1	25.1	23.4	<9	<3	<9	<9
Pb	<5	<5	16.9	9.79	<5	<5	17.7	17.4	34	10.2	55.2	74.5	107	38.8	228	210	188	71.9
Ti	<10	<5	90	148	180	921	62	171	164	634	69.6	77.6	108	224	<15	<5	<15	<15
V	<1	<1	1.8	2.22	2.8	15.6	1.54	2.77	2.88	9.57	2.27	1.71	2.31	5.26	<9	<3	<9	<9
Zn	197	6.81	4180	2050	606	57.2	3380	4470	5500	922	9200	13500	16600	2260	34700	27400	26300	3020

"<": The concentration of the metal is below the detection limit; WB: Woody biomass, CB: Contaminated biomass, NB: Normal biomass or common market pellet; BA, EA, DA, and FA: Bottom ash, after heat exchanger ash, deposited ash, and fly ash, respectively; $C10$, $C20$, $C30$: Contaminated biomass combustion experiments of 10 kW, 20 kW, and 30 kW, respectively; $N20$: Combustion experiment of 20 kW utilizing normal pellets.

5.3.1. Influence of combustion parameters

The concentration of individual NMs and $REEs$ in the solid remains captured from the discrepant contaminated biomass combustion experiments is visualized in *Figure 5.6*.

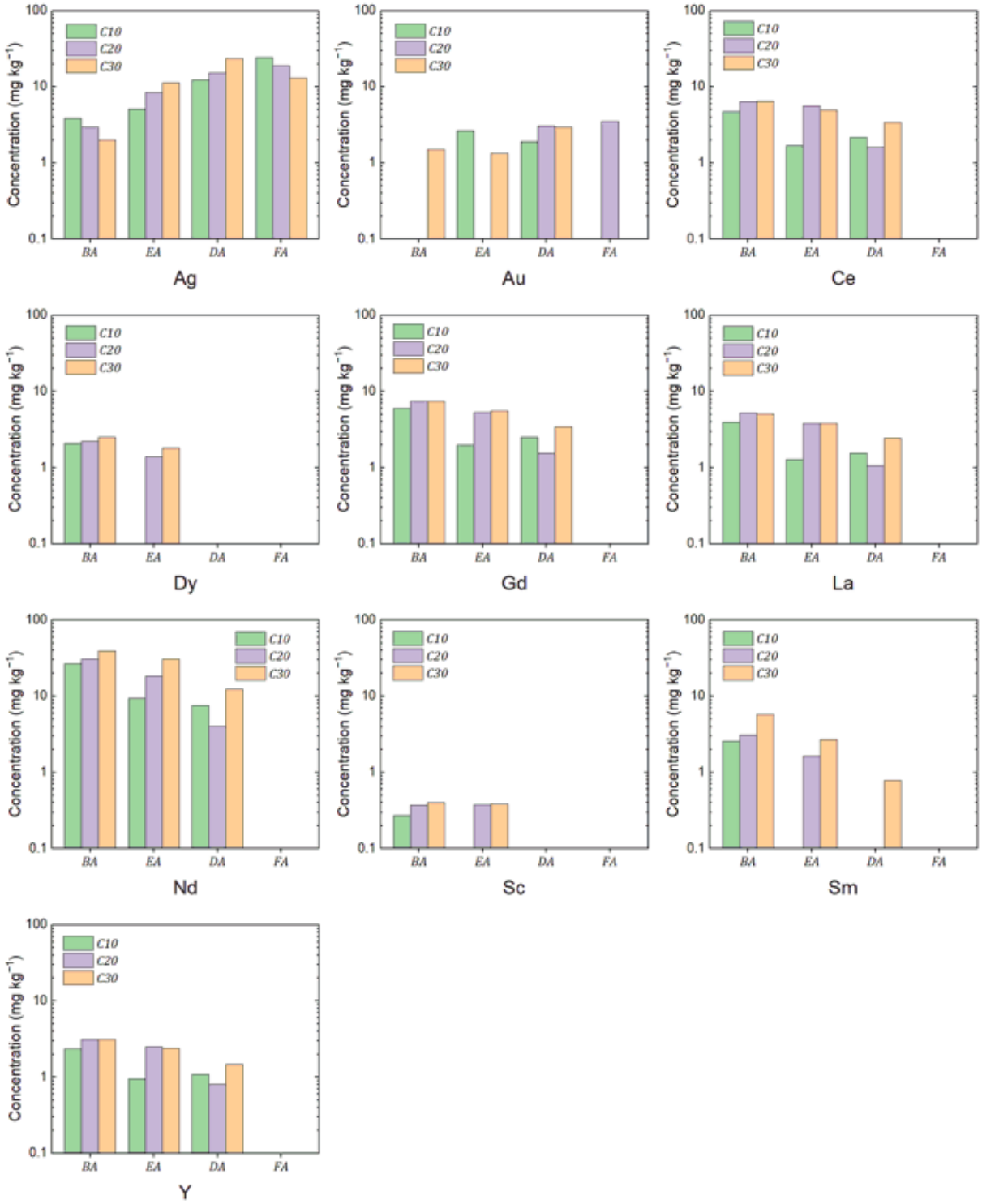

Figure 5.6. Concentrations of NMs and $REEs$ in ashes derived from different contaminated biomass combustion experiments of 10 kW ($C10$), 20 kW ($C20$), and 30 kW ($C30$).

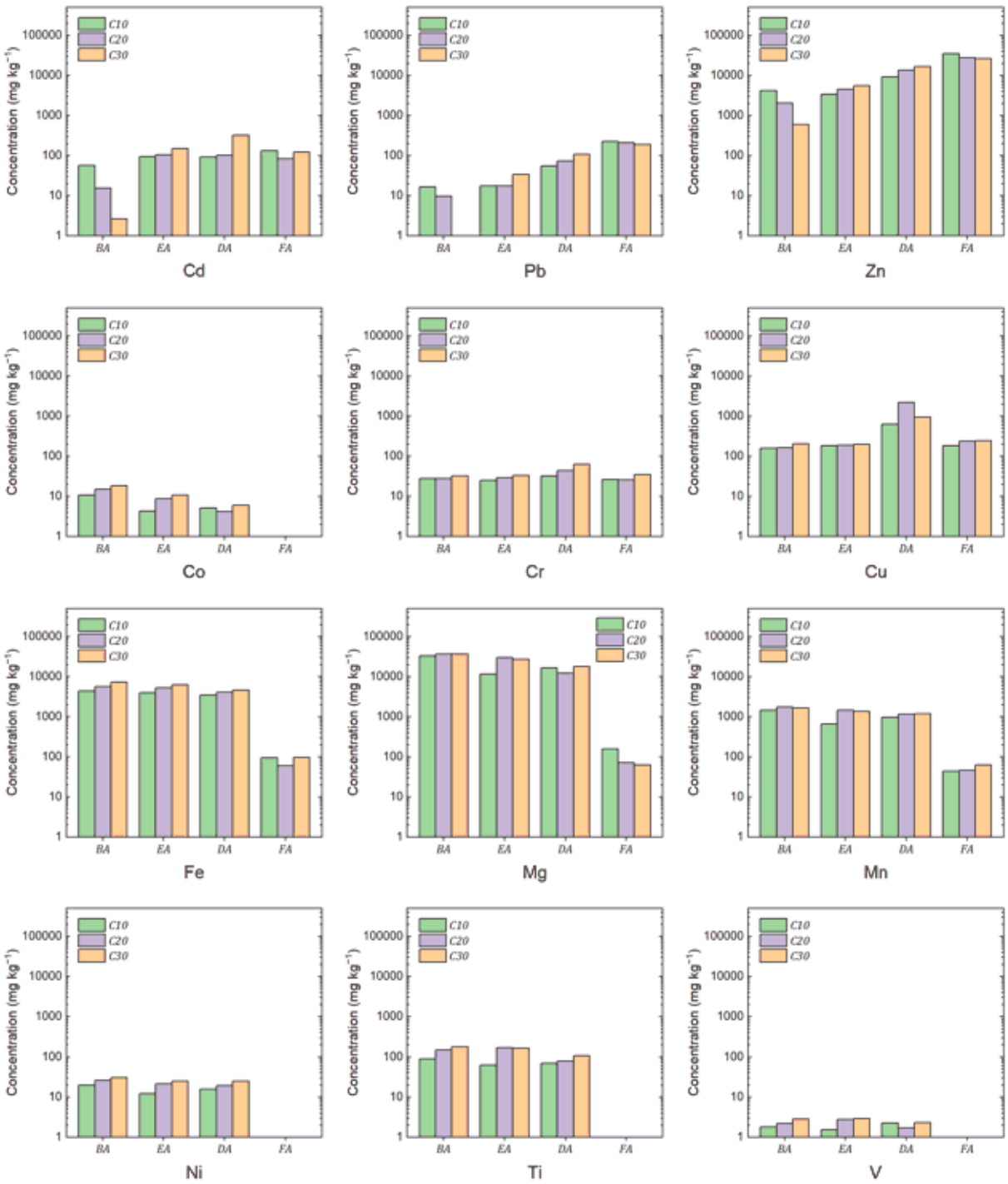

Figure 5.7. Concentrations of other elements in ashes derived from different contaminated biomass combustion experiments of 10 kW ($C10$), 20 kW ($C20$), and 30 kW ($C30$).

On the basis of *Figure 5.6*, the concentration of Ag in BA and FA collected from the contaminated biomass combustion experiment of 10 kW ($C10$) is significantly greater compared to the higher boiler performance levels. The opposite trend was observed in the case of EA and DA indicating a strong combustion parameter dependence. That could be explained by that Ag is highly volatile, thus the higher combustion temperature or firing rate results in

less Ag concentration in BA. On the other hand, low flue gas temperature (< 100 °C) in the low-performance experiment enhances the fallout of metals leading to higher Ag levels in FA.

In the case of Au, the dependence is minor and uncertain, further theoretical and experimental analyses are necessary for a better understanding of the behavior of this element.

$REEs$ show a consistent trend during contaminated biomass incineration as seen in *Figure 5.6*. Because $REEs$ are low volatile metals, their concentrations in BA, EA, and DA tend to increase with the performance of the boiler. Rare earth elements are below detection limits in all fly ash samples. High-performance levels or high combustor temperatures have an advantage for the enrichment of $REEs$ from biomass into solid residuals.

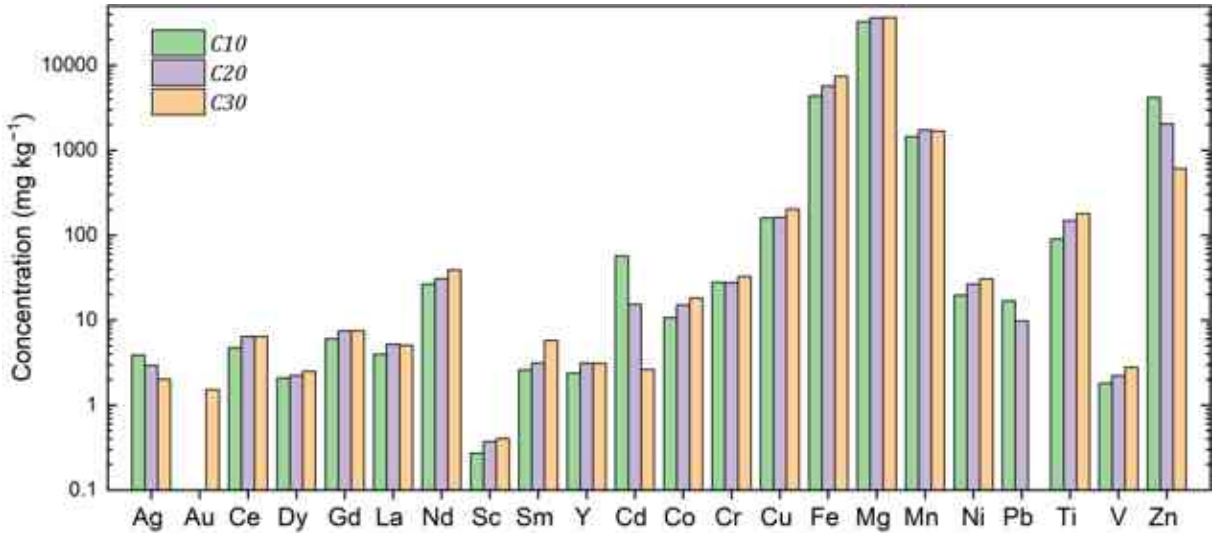

Figure 5.8. The concentration of metals in BA under different conditions of contaminated biomass combustion.

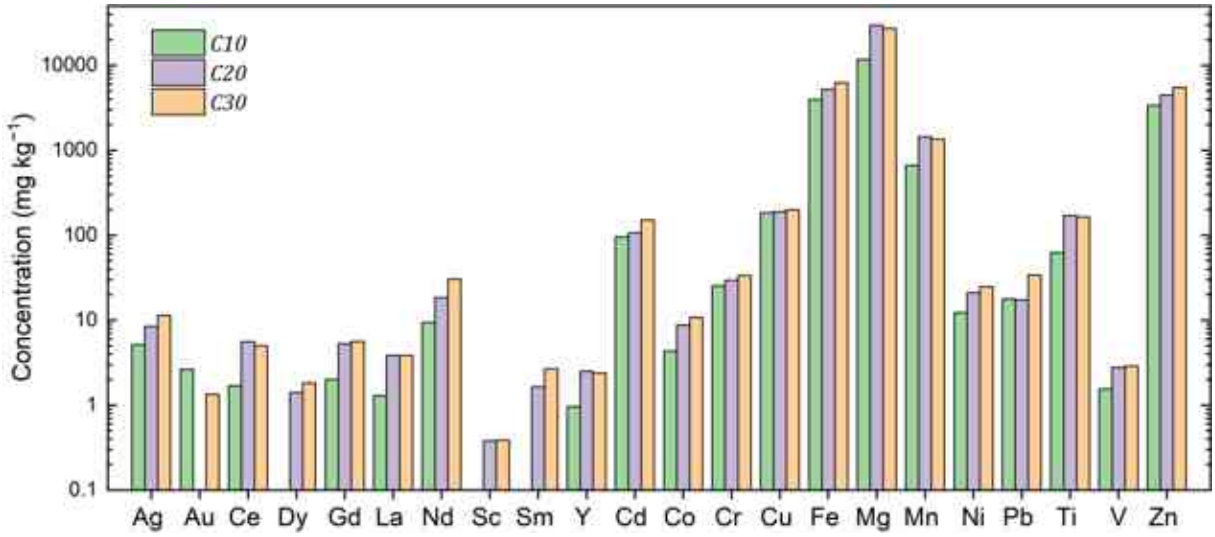

Figure 5.9. The concentration of metals in EA under different conditions of contaminated biomass combustion.

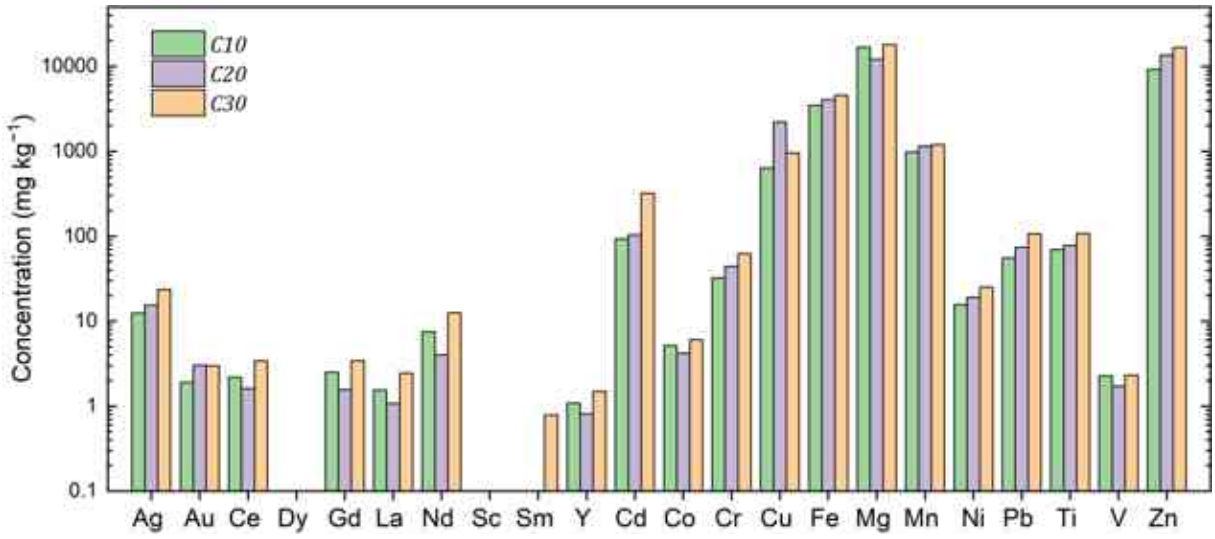

Figure 5.10. The concentration of metals in DA under different conditions of contaminated biomass combustion.

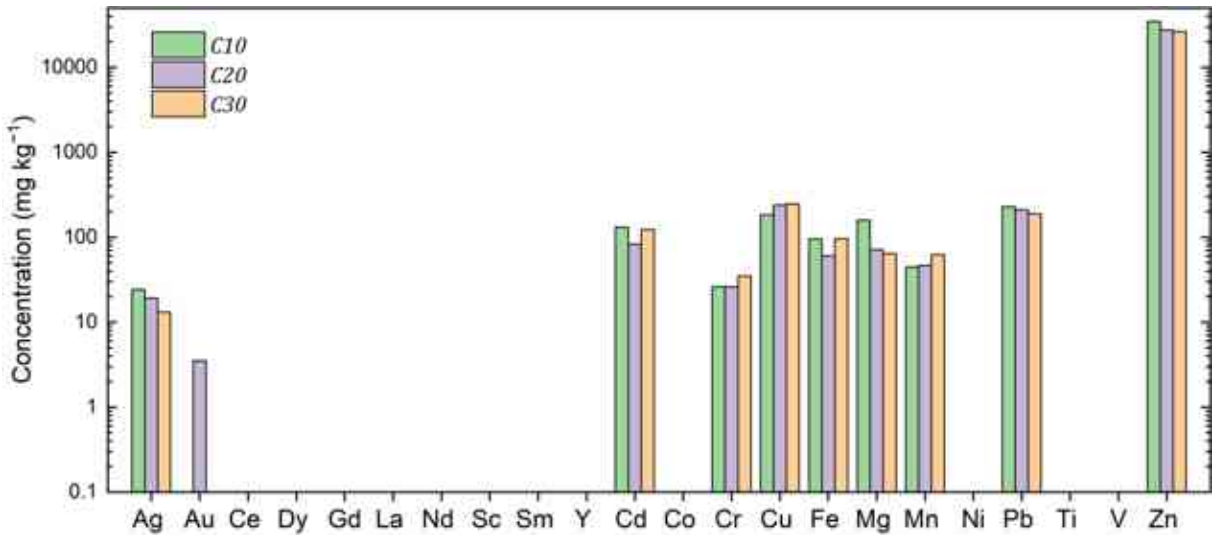

Figure 5.11. The concentration of metals in FA under different conditions of contaminated biomass combustion.

Similar to Ag, the concentrations in BA and FA of the greatly volatile elements such as Cd, Pb, and Zn considerably decrease under higher-level performance experiments. Meanwhile, a different trend was observed in the case of EA and DA *Figure 5.7*. For less volatile elements such as Co, Cr, Cu, Fe, Mg, Mn, Ni, Ti, and V, higher performance levels largely result in greater metal concentrations in BA, EA, and DA. The influence is minor in the case of FA, metal grades in this solid remain show disparate trends.

On the whole, under lower-performance experiments, the concentrations in BA and FA of highly volatile elements such as Ag, Cd, Pb, and Zn are remarkably greater versus higher-performance cases (*Figure 5.8* and *Figure 5.11*). Low flue gas temperatures (<100 °C) are in

favor of enhancing the fall-out of metals in the fly ash. For less volatile elements of $REEs$ and Co, Cr, Cu, Fe, Mg, Mn, Ni, Ti, and V, their concentrations in the bottom ash increase with the performance of the boiler. On the other hand, higher performance levels largely lead to greater concentrations in EA, and DA for most metals as seen in *Figure 5.9* and *Figure 5.10*. High-performance levels or high combustor temperatures have an advantage for the enrichment of low volatile elements including $REEs$ from biomass into solid remains.

5.3.2. Influence of feedstocks

The chemical analysis results of the solid samples obtained from the two similar condition experiments of 20 kW utilizing different materials of contaminated biomass ($C20$) and normal biomass ($N20$) are compared. The comparison aims to investigate the effect of feedstocks on the distribution of metals during biomass incineration. Based on *Table 5.4*, concentrations of NMs in solid samples of the contaminated biomass combustion are substantially greater compared to that of the common biomass combustion. Silver levels fold approximately 2, 5, 4, and 7 times in BA, EA, DA, and FA, respectively. Gold is below the detection limit in all solid samples of the common biomass experiment, but this element is found in the ashes of contaminated biomass combustion. The superior concentrations of NMs in contaminated solid samples indicate that the harvested polluted biomass is favorable for the investigation of precious metals. Developing NM hyperaccumulators are also necessary to increase the concentrations of NMs in biomass ashes.

The behavior of metal comprising NMs and $REEs$ during both contaminated biomass combustion and common biomass combustion performs the similarity as seen in *Table 5.4*. The concentrations of NMs in EA, DA, and FA are greater versus in BA. On the contrary, the levels of $REEs$ consistently follow the decreasing orders of $BA > EA > DA > WB$. These outcomes are in complete agreement with the results of the previous experiments described in section 5.2. The distributions of the other metals including heavy metals in the burning system differed from metal to metal. Cadmium, zinc, and lead were highly volatilized as their concentrations in EA, FA, and FA are remarkably greater compared to in BA. For less volatile elements such as Co, Cr, Ni, and V, there is no substantial disparity in metal concentrations between the different ash samples. On the contrary, Fe, Mg, Mn, and Ti were hardly volatilized as their presence in BA is much greater compared to in FA. Copper performed an atypical trend, its concentrations in the deposited ash samples are tremendously superior to other combustion ashes.

The enrichment factor (EF) is defined as the quotient of metal concentration in ashes to that in woody biomass as seen in the equation below. This is used to describe the effectiveness of the enrichment process in enhancing metal levels.

$$Enrichment\ factor\ (EF) = \frac{Metal\ concentration\ in\ ash}{Metal\ concentration\ in\ biomass} \quad (4)$$

Table 5.5. The enrichment factor of contaminated biomass combustion experiment ($C20$) and common market biomass combustion experiment ($N20$).

Element	BA		EA		DA		FA	
	$C20$	$N20$	$C20$	$N20$	$C20$	$N20$	$C20$	$N20$
Ag	5.9*	2.6*	16.9*	3.6*	30.8*	6.9*	38.4*	5.9*
Au	-	-	-	-	60.8*	-	70.4*	-
Ce	12.2	32.2*	10.6	20.0*	3.1	8.4*	-	-
Dy	2.2*	-	1.4*	-	-	-	-	-
Gd	288.1	15.3*	203.8	10.1*	60.0	4.7*	-	-
La	20.9*	34.1*	15.4*	20.3*	4.3*	8.9*	-	-
Nd	61.4*	6.6*	36.8*	4.2*	8.0*	1.6*	-	-
Sc	37.2*	8.2*	38.0*	5.0*	-	2.0*	-	-
Sm	120.0	3.1*	63.1	1.8*	-	-	-	-
Y	12.5*	23.3*	10.0*	14.1*	3.2*	5.8*	-	-

"*": Minimum enrichment factor; BA, EA, DA, and FA: Bottom ash, after exchanger ash, deposited ash, and fly ash, respectively; $C20$ and $N20$: Biomass combustion experiments of 20 kW utilizing contaminated pellets and common market pellets (normal biomass).

All NMs and most $REEs$ were below the detection limits in the woody biomass samples. However, as a result of the combustion process, their concentrations became high enough to be found in at least one ash sample. Their enrichment factors in this case are calculated based on the detection limits, which are the minimum values or the worst-case scenario. The enrichment factors of NMs and $REEs$ from both contaminated biomass combustion ($C20$) and common market biomass combustion ($N20$) are shown in *Table 5.5*. The higher index values were typically found in the contaminated one, which might stem from the difference of the two biomass feedstocks (*Table 4.1*, *Table 5.4*). The enrichment factors vary in a wide range from more than one to nearly 300. The outstanding results were observed in the case of Gd

($EF\text{-}BA$ = 288.1, $EF\text{-}EA$ = 203.8, $EF\text{-}DA$ = 60) and Sm ($EF\text{-}BA$ = 120, $EF\text{-}EA$ = 63.1) for the contaminated biomass combustion. Additionally, the minimum enrichment factors of NMs are relatively high in terms of DA and FA obtained from the contaminated biomass combustion experiment (Ag: $EF\text{-}DA$ = 30.8, $EF\text{-}FA$ = 38.4; Au: $EF\text{-}DA$ = 60.8, $EF\text{-}FA$ = 70.4). Meanwhile, in the case of common market biomass combustion, Ce ($EF\text{-}BA$ = 32.2, $EF\text{-}EA$ = 20, $EF\text{-}DA$ = 8.4) and La ($EF\text{-}BA$ = 34.1, $EF\text{-}EA$ = 20.3, $EF\text{-}DA$ = 8.9) show the highest minimum EF outcomes. Conclusively, the enrichment factor is significant, indicating the efficiency of the combustion process in concentrating valuable metals from biomass into solid residues. That is a benefit for the further stage of extraction to reclaim NMs and $REEs$ from solid remains.

5.4. The efficiency of the leaching process

The three-stage leaching process effectively enriched gold, as 12.1 mg kg^{-1} Au was detected in the leached bottom ash folding 8 times the gold level in bottom ash. Additionally, the residues obtained from the leaching of bottom ash and after heat exchanger ash contain 14.2 and 21.5 mg kg^{-1} Ag, respectively, which are 7 and 2 times higher than the Ag concentration in the corresponding ashes. The greater level of silver in the leaching residual indicates that the leaching process effectively enriches this noble metal. Leaching also has proven efficient in heightening rare earth metal contents. For instance, 39.1 mg kg^{-1} Nd in the bottom ash was enhanced to 54.9 mg kg^{-1} Nd after leaching.

The integration of the combustion and leaching approach substantially enriches the NM and REE contents. Silver concentrations in the leaching residuals such as the bottom ash-derived residue and the after exchanger ash-derived residue fold at least 28 and 43 times, respectively, compared to its levels in the biomass. The concentration of neodymium in the leached bottom ash is at least 110 times higher, compared to that in the contaminated plants. Most notably, after the combustion and leaching treatment, the level of gold was increased by more than 242 times. The combined approach of combustion and leaching lays a solid foundation for the recovery of high-value metals from bio-ores.

5.5. Formation of valuable metals in biomass combustion solid remains

Gold was found in all the contaminated bottom ashes via SEM analysis, even in the samples where Au was below the detection limit. *Figure 5.12* is an imaging example of gold in bottom ash obtained from contaminated biomass combustion experiments with a particle size of around 12 μm. Gold was observed in the bottom ash virtually in pure particle form having minor

elemental associations as the examined particle contains more than 95% of Au. Many similar particles were detected (*Figure 5.13*) preliminarily indicating that gold clearly appears as neat particles in the bottom ash. Gold forming pure particles in biomass bottom ash is a valuable finding from the scientific point of view.

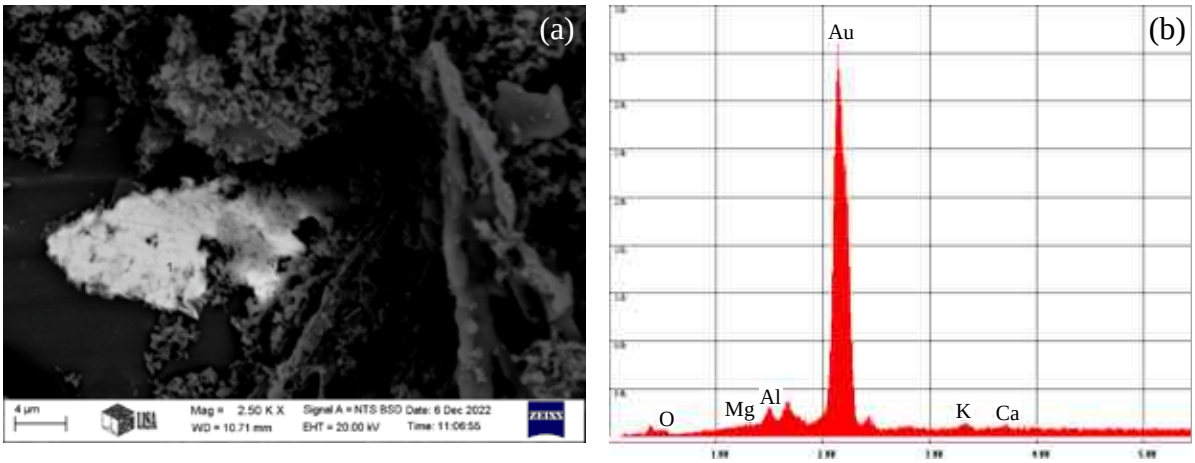

Figure 5.12. Appearance of gold in bottom ash. (a) SEM image, (b) EDS spectrum, >95% Au.

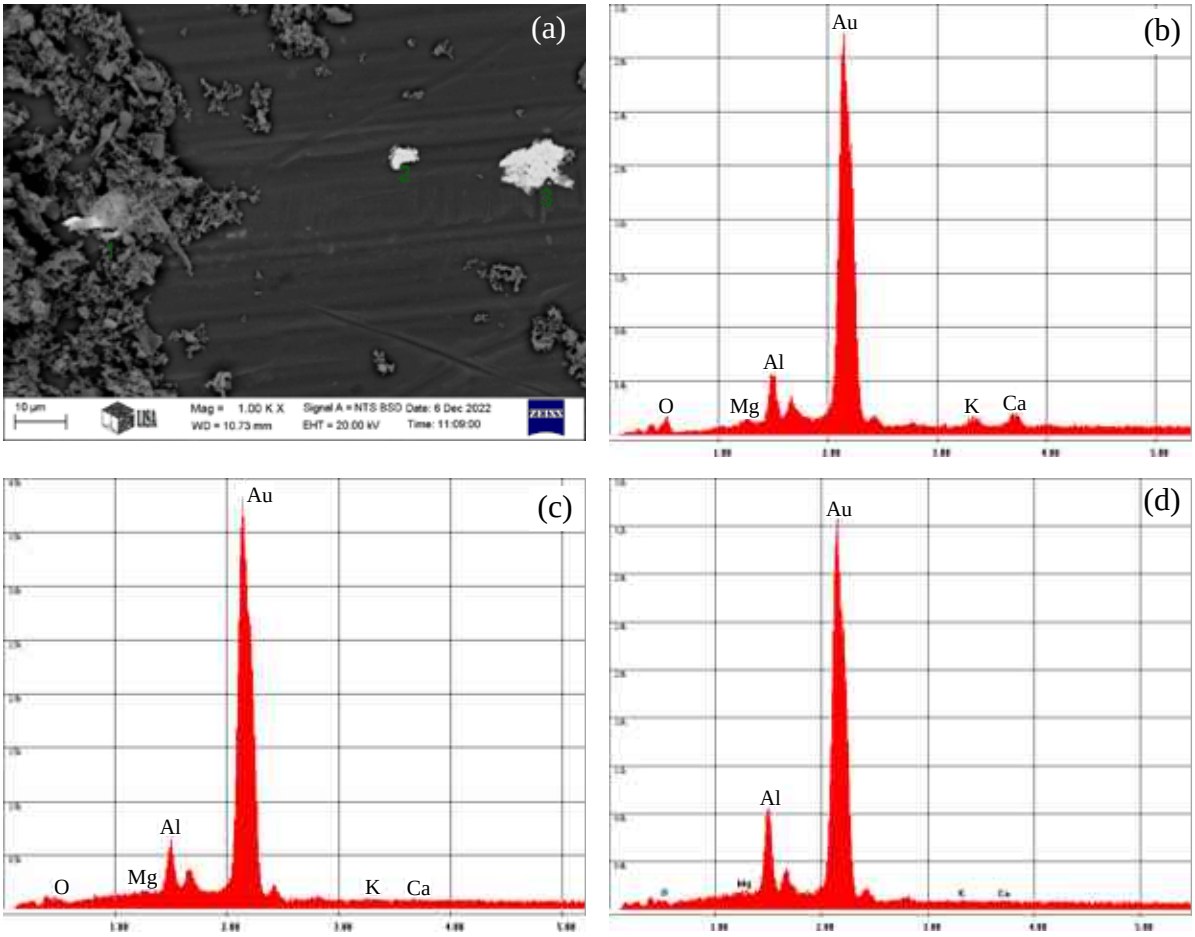

Figure 5.13. Another example of Au in bottom ash. (a) SEM image, (b) EDS spectrum point 1, c) EDS spectrum point 2, d) EDS spectrum point 3.

While the most significant gold particles by size appear in the bottom ash, a considerable amount of Au escapes the combustion chamber with the upward flowing flue gas, which has the ability of catching and transporting particles by its aerodynamical properties. It is supposed that Au particle sizes bigger than that found in the bottom ash won't appear in any subsequent parts of the combustion system. Therefore, the gold appearing in the sampling point of after heat exchanger ash should contain only smaller gold particles. This fact is supported by the SEM analysis, an example is shown in *Figure 5.14*, where tiny gold particles are attached to the surface of a bigger particle. Various scenarios describe the origin of such gold particles: 1) the particle is originated from the plant as is, however, the shape of the particle may vary depending on the residence time in the firing zone together with the temperature of combustion; 2) a bigger gold particle was broken into smaller fragments due to the lamellar structure and resulting in a smaller sized gold particle enough for escaping the combustion chamber; 3) the gold particle can melt as it flies through the high temperature zone due to the relatively small size resulting near droplet shaped forms; 4) the combination of the 1–3 scenarios.

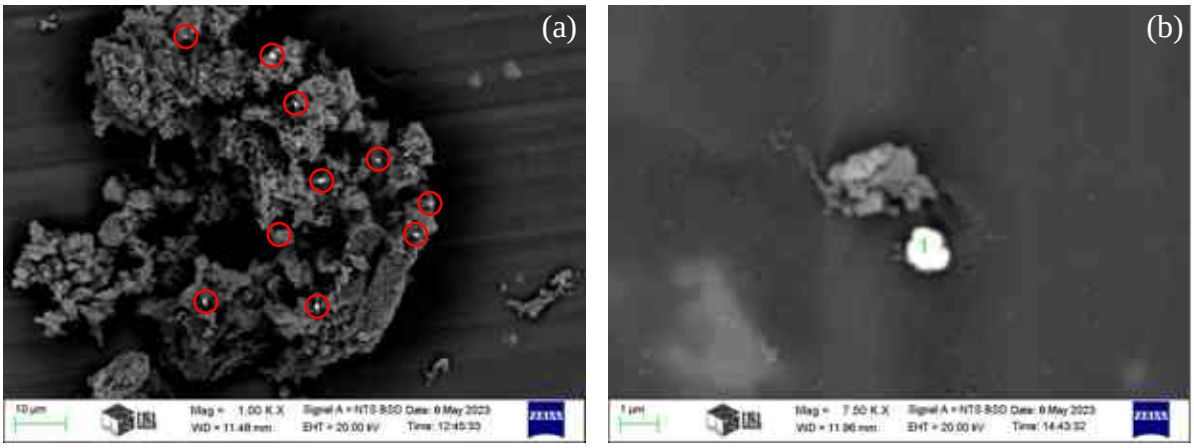

Figure 5.14. SEM image examples of Au in after heat exchanger ash. a) the gold is attached to a bigger ash particle (indicated by the circles), b) the gold appears in neat form independently.

The next sampling point in the combustion system is the wall of the air heat exchanger, which is considered a source of deposited ash. Although individual 1–2 µm gold particles were found in the after heat exchanger ash, the results show that deposited ash contained Au associated with other compounds indicating that the gold rather appears as coating on another ash particle. *Figure 5.15* shows an example of such finding, including the EDS spectrum, where mostly K (21.6%), S (4.5%), O (20.6%), and Al (9.4%) elements were also detected.

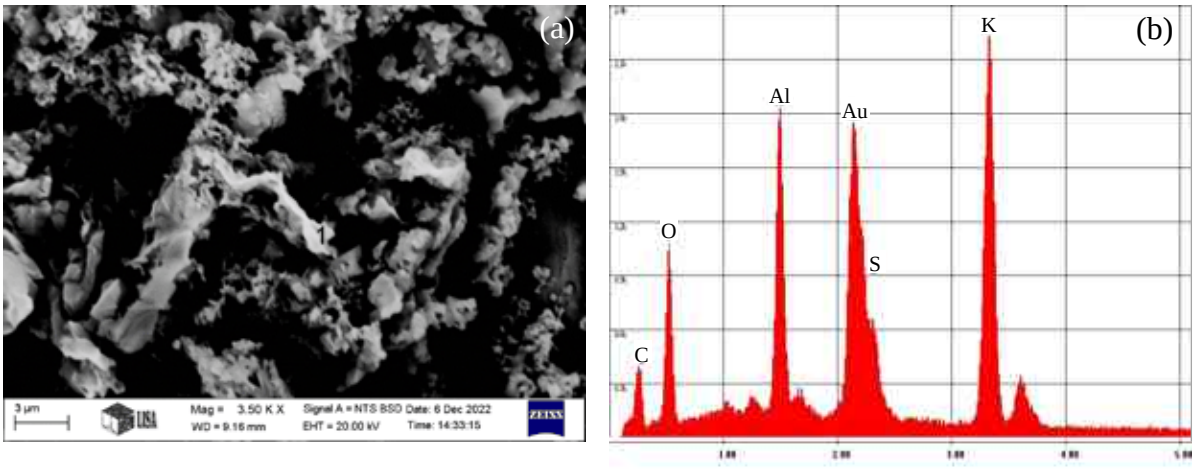

Figure 5.15. Example of Au in deposited ash. (a) SEM image, (b) EDS spectrum.

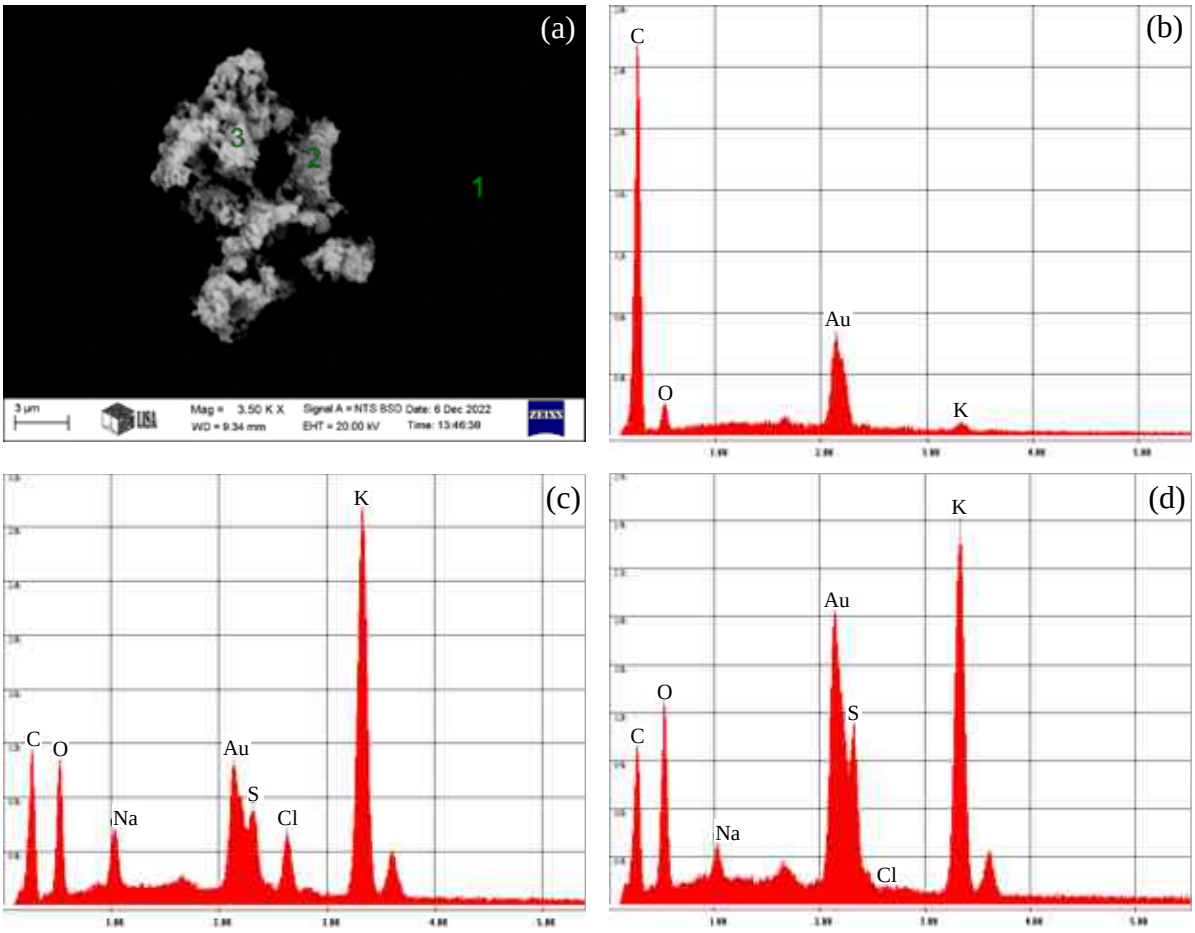

Figure 5.16. Example of Au in fly ash. (a) SEM image, (b) EDS spectrum point 1, (c) EDS spectrum point 2, (d) EDS spectrum point 3.

The SEM analysis of fly ash suggests similar behavior to the deposited ash, as the gold appears as a coating on a particle with different material structures containing K, Na, S, and O elements in all the cases during fly ash examination. One example is shown in *Figure 5.16*, where number 1 highlighted in the SEM image denotes the background primarily contenting

carbon. Meanwhile, number 2 (containing 17.9% Au and 25.5% K, 3.4% Na, 4.2% S, 21.3% O) and number 3 (consisting of 30.9% Au and 20.2% K, 1.4% Na, 6.8% S, 21.6% O) represent the occurrence of Au in the fly ash particles. The coating-like structure suggests that the gold in melted or partially melted form present in the combustion chamber should hit another appropriate particle, during which the gold creates a thin layer on the surface. A certain amount of gold escapes the combustion chamber by this pathway, which can be considered as gold loss if fly ash is not treated. Additionally, since bottom ash contains the most amount of gold, including particles in the tenth of microns by size, followed by the after heat exchanger ash with 1–2 micron particles, fly ash might also contain neat gold particles as well in the system utilized in this study, but supposingly at the nanometer scale.

Silver was detected only in the contaminated fly ash sample via SEM-EDS analysis. This element is typically associated with potassium sulphate as well in the form of a coating on the surface of the particle as seen in *Figure 5.17*. Its behavior is similar to the formation of gold in fly ash.

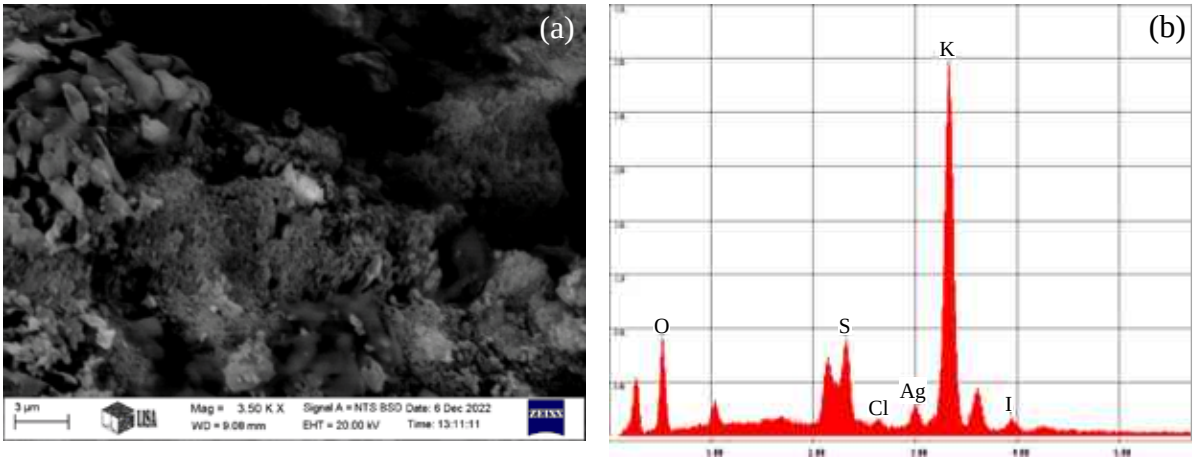

Figure 5.17. Example of Ag in fly ash. (a) SEM image, (b) EDS spectrum.

In addition to NMs, SEM-EDS examination showed $REEs$ in the contaminated residues. Examples of $REEs$ in the solid remains can be seen in *Figure 5.18*. In which, Ce and Nd are observed as coatings on a particle surface on a bottom ash particle surface primarily associated with calcium, oxygen, and potassium (*Figure 5.18a, b*). Meanwhile, in the ash collected after the heat exchanger ash, some $REEs$ such as Er, Nd, and Pr are found as integral parts of the solid particles (*Figure 5.18c, d*). The presence of $REEs$ in contaminated biomass ashes is difficult to be discovered. That might arise from these elements are associated or intermixed with other substances becoming a surface phenomenon or an integral part of solid particles. The

question about the occurrence of $REEs$ is in limbo, which requires further theoretical and experimental studies.

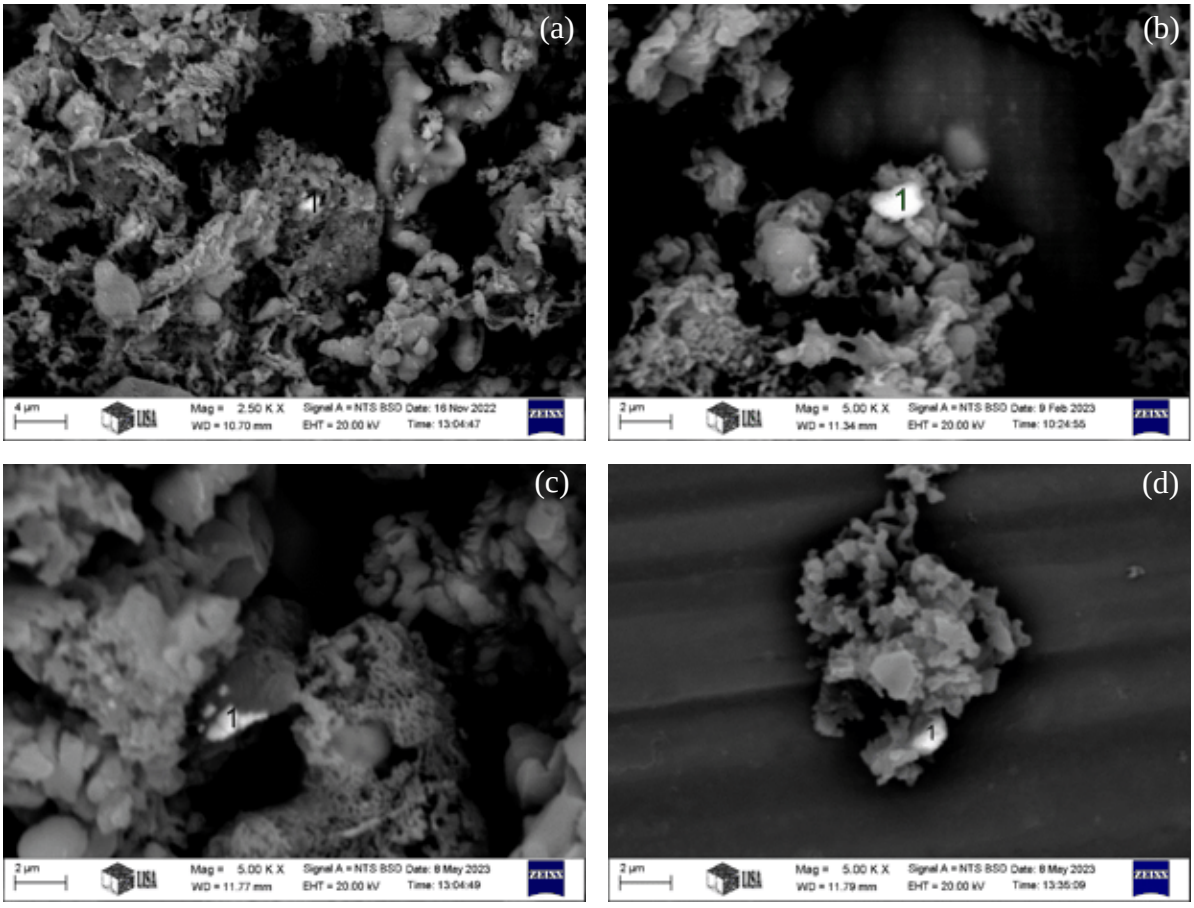

Figure 5.18. SEM image examples of REEs in ashes. (a) Ce in bottom ash, (b) Nd in bottom ash, (c) Er in after heat exchanger ash, (b) Nd and Pr in after heat exchanger ash.

In short, SEM-EDS analysis provides the images of NMs and $REEs$ in contaminated biomass ashes as well as the elemental composition information. The SEM-EDS results are consistent with the ICP measurement confirming the reliability of the chemical analysis. Gold virtually forms individual pure particles in the bottom ashes and the after heat exchanger ashes obtained from contaminated biomass combustion experiments. Meanwhile, in the fly ash and the deposited ash, this precious metal is seen as a coating or laminar morphology. Silver is discovered only in contaminated fly ash samples. Similar to gold, silver is also typically associated with potassium sulphate in the form of a coating on the surface of the fly ash particle. Rare earth elements are barely found via SEM-EDS examination. Rare earth metals such as cerium and neodymium are detected in bottom ash primarily associated with calcium, oxygen, and potassium. Erbium, neodymium, and praseodymium are observed as integral parts of the

solid particles in the after heat exchanger ash. The SEM-EDS findings are valuable to understanding the formation of high-value metals during the incineration of polluted biomass.

5.6. Formation of valuable metals in leaching residues

The leached ash samples have the benefit of having more discoverable gold and other valuable metal particles during the SEM analysis as most of the ballast material is removed. *Figure 5.19a* shows an example of a gold structure found in the leached bottom ash sample. The surface of this particle was analyzed by EDS, which shows that the particle is evidently in neat gold form containing >98% Au (*Figure 5.19b*). The shape and the lamellar structure suggest that the particle was present in the plant in the same or similar form as seen in the picture. It is hypothesized that the particle falls down into the ashtray in a relatively short period of time due to its size and dense manner, meaning that the residence time of this particle in the heating zone is small; therefore, signs of heat treatment cannot be seen.

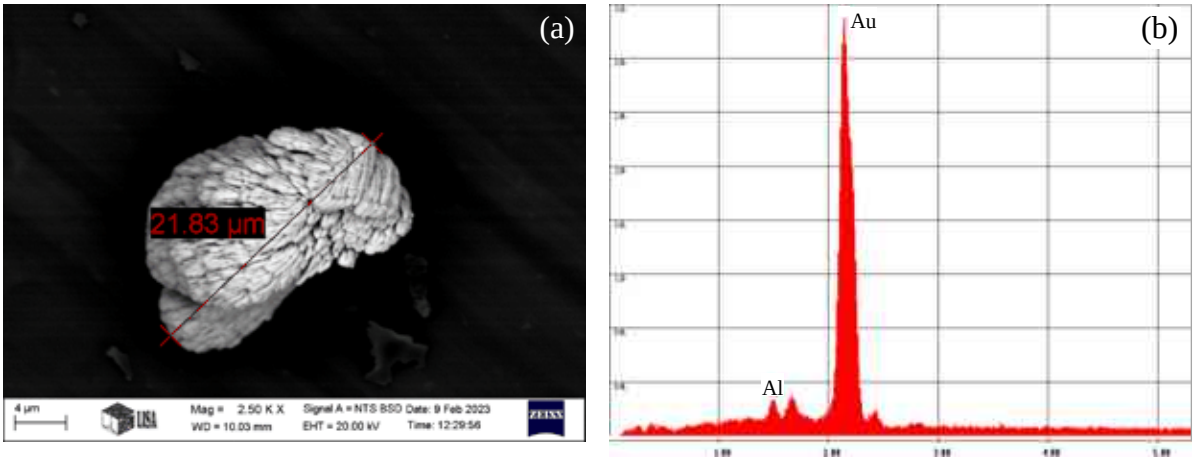

Figure 5.19. Appearance of gold in leached bottom ash. a) SEM image, b) EDS spectrum, >98% Au.

An example of another scenario can be seen in *Figure 5.20a*, where the size and shape of the particle reveal that it was subjected to heat enough to partially melt the gold, which practically eliminates the lamellar structure but is insufficient to create droplet-like forms. Based on EDS analysis, this particle also consists of gold only (>99% Au, *Figure 5.20b*). *Figure 5.19* and *Figure 5.20* typically show the two borders of the overall appearance spectrum. Anything in between is the most general in the bottom ash samples, i.e. partial heat treatment can be observed on such particles combined with significantly smaller particles attached to the body surface (*Figure 5.21*). The shape of these particles can be described as porous, irregular, and rounded with low sphericity. In comparison, they have only minor elemental associations as the

examined leached bottom ash gold particles consist of more than 98% Au. Other SEM image examples of Au in leached bottom ash is shown in *Figure 5.22*.

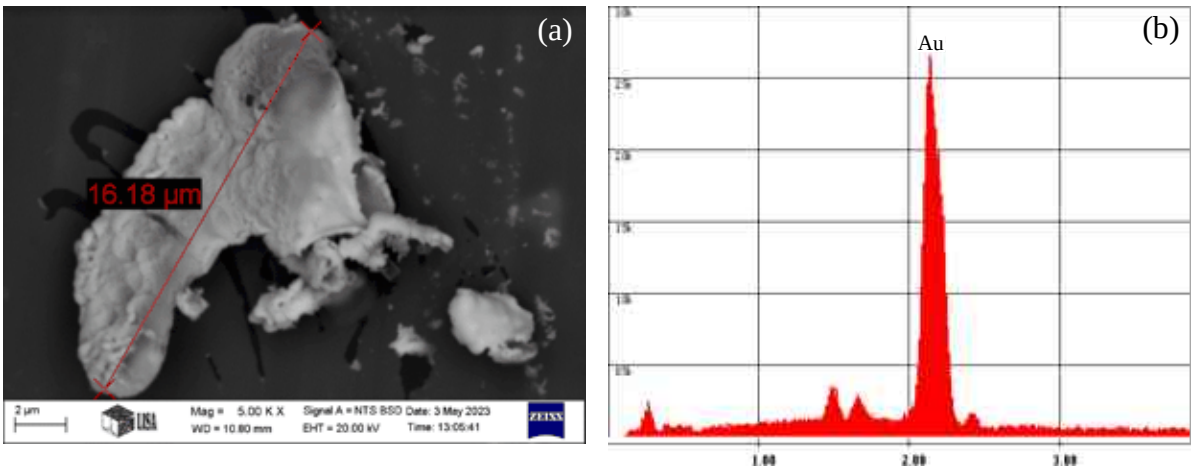

Figure 5.20. Appearance of gold in leached bottom ash. a) SEM image, b) EDS spectrum, >99% Au.

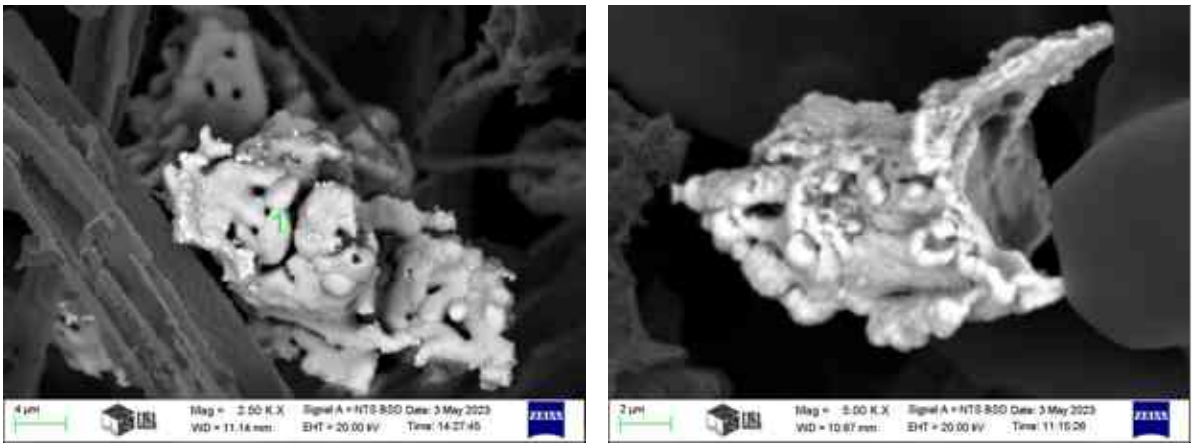

Figure 5.21. Appearance of gold in leached bottom ash.

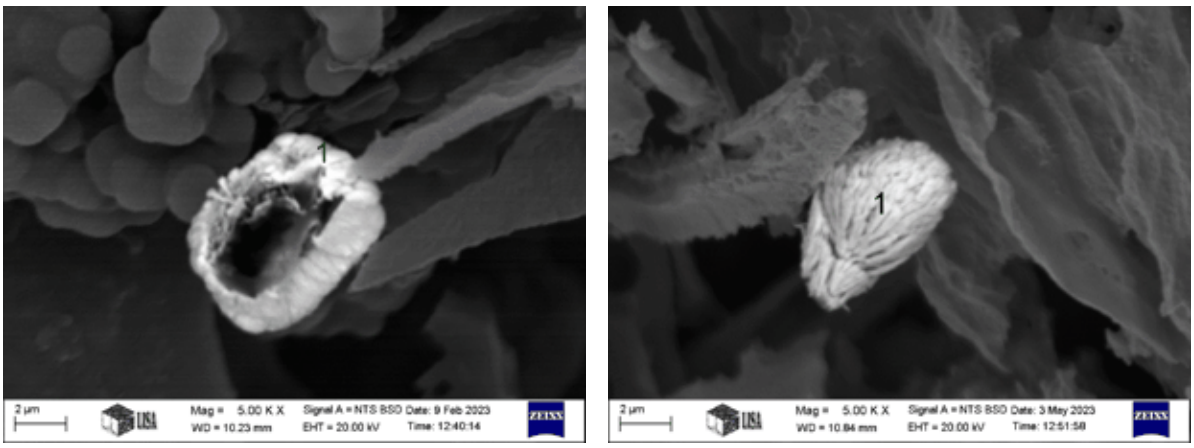

Figure 5.22. Other SEM image examples of Au in leached bottom ash.

SEM-EDS analysis was not able to find the presence of Ag in bottom ashes (section 5.5). However, as a result of the leaching process, this element was enriched and detected in the obtained residual. *Figure 5.23* is an example of Ag in the bottom ash leaching residue where the particle consists of 48.37% Ag, 36.26% Sn, 14.13% Al, and 1.24% Si. Silver was found as an integral part of the solid particle primarily intermixed with tin and aluminum.

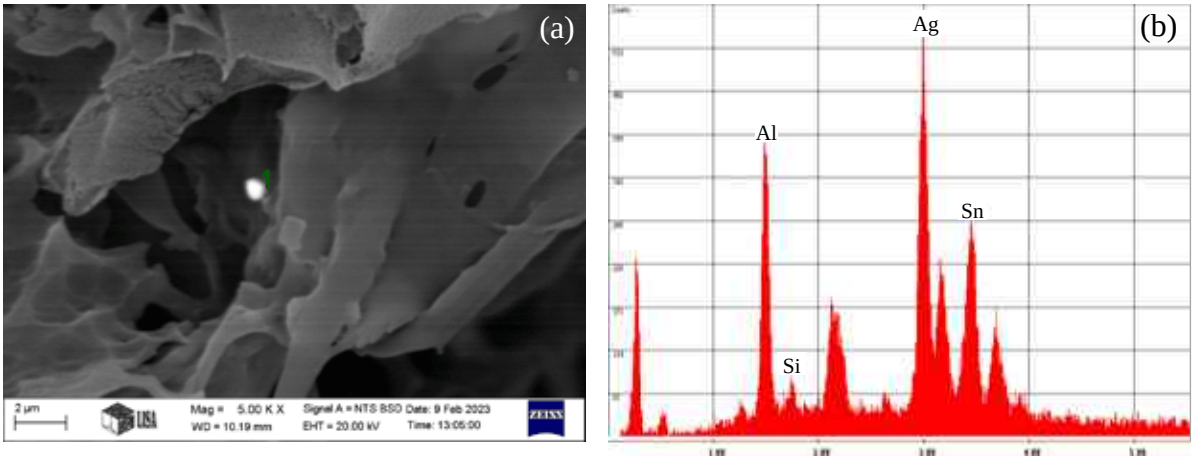

Figure 5.23. Example of Ag in leached bottom ash. (a) SEM image, (b) EDS spectrum.

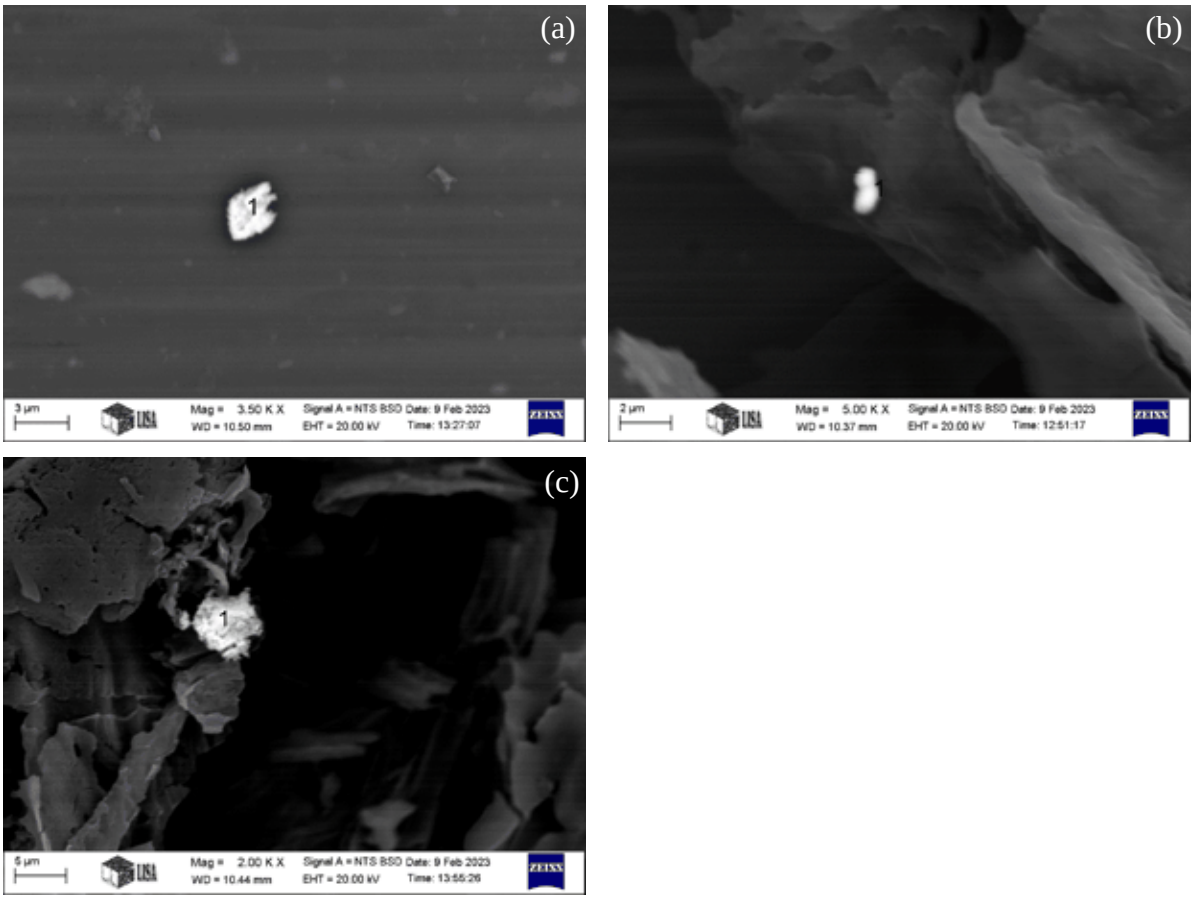

Figure 5.24. SEM image examples of REEs in leached bottom ash. (a) Er, (b) Nd, (c) Pr.

In addition to NMs, the presence of $REEs$ also is easier to be observed in solid samples derived from the leaching of bottom ashes. The formations of rare earth metals in these materials perform different trends. Erbium was found in leaching residues in the form of individual particles as the particle shown in *Figure 5.24a* contains nearly 70% Er. Neodymium was associated with other substances such as Fe and Al becoming an integral part of the residue solid particle (consisting of > 45% Nd as seen in *Figure 5.24b*). Meanwhile, praseodymium was seen as a thin coating on the surface of leaching residue particles mainly associated with neodymium, iron, and oxygen (*Figure 5.24c*).

6. CONCLUSION AND OUTLOOK

In this era of industrialization, the world is confronting a range of challenges including environmental pollution, climate change, and the exhaustion of natural resources such as fossil fuels and metal reserves. These ongoing issues have spurred the utilization of biomass for energy generation and compelled the globe to recover metals from secondary mineral sources. My PhD topic "The Behavior of Noble Metals and Rare Earth Elements During Biomass Combustion" contributes to addressing the aforementioned global concerns, its impacts extend to various industries comprising waste management, energy production, and metal recovery. The primary objective of my doctoral research is to develop a viable combustion and flue gas system specifically designed for pelletized polluted biomass in order to investigate the fate of NMs and $REEs$ during incineration. The experimental setup aims to capture NMs and $REEs$ in solid remains, facilitating their extraction and reducing their emission. Additionally, leaching of the combustion solid residues is another interest of this study which paves the way for reclaiming valuable metals.

A contaminated location situated in Gyöngyösoroszi (Hungary) was chosen as the source of biomass utilized in this study based on the chemical analysis outcomes of plants gathered from different locations. The polluted plants harvested from the selected land were incinerated in a fixed-grate pilot-scale boiler, while solid remains from various positions in the combustion and flue gas system were captured and analyzed. The results show that the levels of NMs comprising Au and Ag in FA, DA, and EA are higher than in BA. Considerable concentrations of NMs observed in EA, DA, and FA indicate these metals are leaving the combustion chamber. The behavior of $REEs$ in the burning system shows a consistent trend, their concentrations follow the decreasing orders of $BA > EA > DA > FA$. The greater metal concentrations in BA versus other solid remains demonstrate the minor volatility of rare earth metal compounds during incineration. Other elements including heavy metals perform different trends; Cd, Zn, and Pb are highly volatilized, while Co, Cr, Cu, Fe, Mg, Mn, Ni, Ti, and V are found less volatile during biomass incineration.

The enrichment factor is significant demonstrating the effectiveness of the combustion process in concentrating valuable metals from biomass into ashes. The highest numbers are found in the case of Gd ($EF\text{-}BA$ = 288.1, $EF\text{-}EA$ = 203.8, $EF\text{-}DA$ = 60). Noble metals such as Ag and Au also have relatively high enrichment factors (Ag: $EF\text{-}DA$ = 30.8, $EF\text{-}FA$ = 38.4; Au: $EF\text{-}DA$ = 60.8, $EF\text{-}FA$ = 70.4). Elevated levels of NMs and $REEs$ in biomass combustion

solid remains are an advantage for the further stage of extraction to reclaim these valuable metals from unconventional resources.

Combustion parameters and feedstocks have substantial influences on the fate of metals during contaminated biomass combustion. For Ag and highly volatile elements such as Cd, Pb, and Zn, the greater firing rate (or combustion temperature or flue gas temperature) results in less concentrations in BA and FA, but higher levels in EA and DA. Meanwhile, the concentrations of less volatile elements consisting of $REEs$, Co, Cr, Cu, Fe, Mg, Mn, Ni, Ti, and V in all the biomass combustion solid remains tend to increase with the boiler performance. Under similar operational conditions, the concentrations of NMs in the ashes captured from the contaminated biomass combustion experiment are remarkably greater than that of the common biomass combustion experiment. It indicates the cruciality of the harvested contaminated biomass for phytomining.

Biomass-derived ashes were furtherly subjected to a three-stage leaching process of water leaching, acid leaching (10% HCl), and alkaline leaching (5% NaOH). The leaching process efficiently enriched NMs and $REEs$, as 1.52 mg kg^{-1} Au, 2.01 mg kg^{-1} Ag, and 39.1 mg kg^{-1} Nd in the bottom ash were enhanced to 12.1, 14.2, and 54.9 mg kg^{-1}, respectively, in the leached bottom ash. The integration of the combustion and leaching process could significantly enrich the concentrations of NMs and $REEs$ from the woody biomass into the leaching residuals. The leached ash samples also have the advantage of having more discoverable gold and other valuable metal particles during the SEM scanning as most of the ballast material is eliminated.

The SEM-EDS outcomes are consistent with the ICP analyses. Gold was found in all the combustion ashes, but the formation associated with gold depends on the location of sampling. The gold particles are presented in neat form in the bottom ash with the purity of higher than 98%. Additionally, the size of a gold particle is significantly higher in bottom ash compared to other solid residues, which is elucidated by the fact that the relatively heavy gold particles cannot be transported out of the combustion chamber by the flue gas flow. Pure gold particles in the size of 1–2 µm were observed in the ash collected in the chamber after the heat exchanger, meanwhile, gold and silver in fly ash appear as a coating on a particle containing potassium, sodium, sulfur, and oxygen. The SEM findings assist in better understanding the formation of gold and other valuable metals and strengthen the feasibility of recovering these elements from unconventional resources.

To the best knowledge, this is the first comprehensive research on the combustion of contaminated biomass containing NMs and $REEs$. It is worth noting that the incineration of

polluted plants containing these valuable metals is common. However, it is neither investigated nor known. In this research, a suitable experimental system for pelletized polluted biomass was developed and the fate of metals (including NMs and $REEs$) as well as the influence factors on the metal flows were investigated. This study verified the viability of combustion technology for contaminated biomass contributing to the success of the overall phytomining concept to recover these valuable metals from unconventional resources.

In the following stage, high-value metals will be subsequently extracted and recovered from the leaching residues. It will be the last brick to complete the entire phytomining pathway for reclaiming NMs and $REEs$ from secondary minerals. The PhD study has proven the efficiency of combustion technology in enriching valuable metals from contaminated biomass into solid remains and has opened new insights into NM and REE phytomining. The combustion technique and somehow the holistic phytoextraction-enrichment-extraction chain can be applied to other material inputs of contaminated biomass coming from different brownfields.

7. NEW SCIENTIFIC RESULTS

1st Claim

The highest concentration of silver in the solid remains gathered from the combustion of pelletized woody biomass (including logs, branches, and leaves) in a fixed-grate pilot-scale boiler within the firing range of 10–30 kW_{th} is presented in the fly ash sampled from the stack at 83–149 °C. This follows the solid residue sampled after the water heat exchanger of the boiler, while the lowest concentration can be detected in the bottom ash. On the other side, the concentration of rare earth elements follows a different tendency, meaning that bottom ash gives the highest concentration, followed by the ash gathered after the heat exchanger.

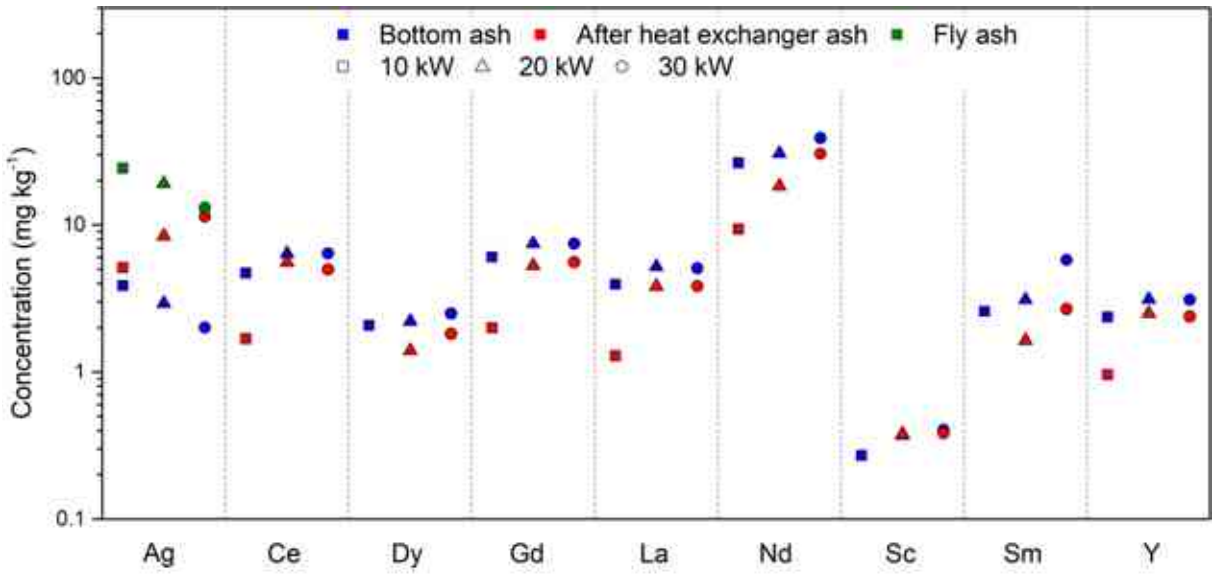

Figure of the first thesis point. Concentrations of silver and rare earth elements in solid remains derived from contaminated biomass combustion experiments.

2nd Claim

The boiler performance has a significant impact on the metal concentration of the bottom ash derived from the combustion of pelletized woody biomass (including logs, branches, and leaves) in a fixed-grate pilot-scale boiler within the firing range of 10–30 kW_{th}. The concentration of silver in the bottom ash tends to decrease by 48% when the thermal power of the boiler is increased from 10 kW to 30 kW, while the concentration of rare earth elements including Ce, Dy, Gd, La, Nd, Sc, Sm and Y increases with the boiler performance by 44% on

an average. Higher boiler performance or combustion temperature has a benefit for the enrichment of rare earth elements from biomass into bottom ash.

3rd Claim

The gold appears in pure form in all solid burning residues obtained from the combustion of pelletized woody biomass (including logs, branches, and leaves) in a fixed-grate pilot-scale boiler within the firing range of 10–30 kW_{th}. The formation associated with gold depends on the location of sampling. The gold particles are presented in neat form in the bottom ash with purity of higher than 95%, which particles are originated from the plant source used as fuel. Additionally, the size of a gold particle is significantly higher in bottom ash compared to other solid residues, which is elucidated by the fact that the relatively heavy gold particles cannot be transported out of the combustion chamber by the flue gas flow. Pure gold particles in the size of 1–2 μm are presented in the ash collected in the chamber after the heat exchanger, meanwhile, gold and silver in fly ash appear as a coating on a particle containing potassium, sodium, sulfur, and oxygen.

4th Claim

Noble metals and rare earth elements present in the initial woody biomass fuel can be enriched during biomass combustion. The enrichment factor (EF) is defined as the quotient of metal concentration in solid residues to that in woody biomass, which is used to describe the efficiency of the enrichment process. In the case of metals below detection limits in woody biomass, the enrichment factors are computed using the detection limits, which represent the worst-case scenarios or the lowest possible values. During the combustion of pelletized woody biomass (including logs, branches, and leaves) in a fixed-grate pilot-scale boiler with a firing range of 20 kW_{th}, the minimum enrichment factors of noble metals are relatively high in terms of deposited ash gathered from the stack surface (EF = 31 and 61 for Ag and Au, respectively) and fly ash (EF = 38 and 70 for Ag and Au, respectively). However, the most outstanding enrichment factor results are observed in the case of Gd (EF = 288, 204, and 60 for bottom ash, the ash gathered after heat exchanger and deposited ash gathered from the stack surface, respectively) and Sm (EF = 120 and 63 for bottom ash and the ash gathered after heat exchanger, respectively).

LIST OF PUBLICATIONS

Journal Papers

J.1. Truong Dinh, Zsolt Dobo, Helga Kovacs, "Phytomining of noble metals – A review", *Chemosphere 286*, paper 131805, 2022, doi: https://doi.org/10.1016/j.chemosphere.2021.131805, **IF = 8.943 (D1)**

J.2. Truong Dinh, Zsolt Dobo, Helga Kovacs, "Phytomining of rare earth elements – A review", *Chemosphere 297*, paper 134259, 2022, doi: https://doi.org/10.1016/j.chemosphere.2022.134259, **IF = 8.943 (D1)**

J.3. Truong Dinh, Helga Kovacs, Zsolt Dobo, "The fate of noble metals and rare earth elements during pelletized biomass combustion", *Heliyon*, 2023 doi: https://doi.org/10.1016/j.heliyon.2023.e23546, **IF = 4.0 (Q1)**

J.4. Zsolt Dobo, Truong Dinh, Tibor Kulcsár, "A Review on Recycling of Spent Lithium-Ion Batteries", *Energy Reports*, vol. 9, 2023, doi: https://doi.org/10.1016/j.egyr.2023.05.264, **IF = 5.2 (Q1)**

J.5. Truong Phi Dinh, Helga Kovács, Zsolt Dobó, "Behavior and treatment of metals in burning system during biomass combustion - literature review", *Materials Science and Engineering: A Publication of The University of Miskolc*, vol. 45, no. 1, pp. 63–76, 2020, doi: 10.32974.mse.2020.006

J.6. Truong Phi Dinh, Helga Kovács, Zsolt Dobó, "Distribution of metals within different plant parts of biomass gathered from a brownfield land located in Gyöngyösoroszi, Hungary", *Materials Science and Engineering: A Publication of The University of Miskolc*, vol. 46, no. 1, pp. 14–22, 2021, doi: 10.32974/mse.2021.002

J.7. Truong Dinh, Zsolt Dobó, Helga Kovács, "Enrichment of rare earth elements from contaminated biomass prior to extraction", *Analecta Technica Szegedinensia*, vol. 16, no. 1, pp. 77–82, 2022, doi: https://doi.org/10.14232/analecta.2022.1.77-82

J.8. T Dinh, Z Dobó, H Kovács, "The Overall Concept of Phytomining of Noble Metals", *PhD Students Almanach*: A publication of the University of Miskolc, Faculty of Materials and Chemical Engineering, vol. 1, pp. 224–230, 2022

J.9. Truong Dinh, Zsolt Dobó, Helga Kovács, "Elemental Analysis of Contaminated Biomass Ashes for Phytomining of Rare Earth Elements", *Analecta Technica Szegedinensia*, vol. 17, no. 3, pp. 26–32, 2023, doi: https://doi.org/10.14232/analecta.2023.3.26-32

J.10. T Dinh, Z Dobó, H Kovács, "Experimental system for combustion of contaminated biomass", *PhD Students Almanach*: A publication of the University of Miskolc, Faculty of Materials and Chemical Engineering, vol. 1, pp. 220–226, 2023

Publications in Conference Proceedings

P.1. T Dinh, Z Dobó, H Kovács, "The overall concept of phytomining of rare earth elements", *ME TKP2020-NKA conference*, pp. 113–120, 2022

P.2. HELGA KOVACS, TRUONG PHI DINH, ZSOLT DOBÓ, "Enrichment of Noble Metals and Rare Earth Elements from Contaminated Biomass before Extraction", *IASTEM* international conference, pp. 13–16, 2022

P.3. T. Dinh, Z. Dobo, H. Kovacs, "Enrichment of valuable metals from contaminated biomass into combustion solid remains", *11th EUROPEAN COMBUSTION MEETING 2023*, pp. 1–5, 2023

Oral and Poster Presentations

O.1. Truong Phi Dinh, "Theoretical Background of NM and REE Extraction from Biomass Ashes, Miskolc, Hungary", *Raw materials university day*, Miskolc, Hungary, 20/10/2020, poster presentation

O.2. Truong Phi Dinh, "Chemical Analysis of Biomass Ashes for Phytomining of REEs", *Raw materials university day*, Miskolc, Hungary, 20/10/2020, poster presentation

O.3. Phi Truong Dinh, Zsolt Dobó, Helga Kovács, "Elemental Analysis of Contaminated Biomass Ashes for Phytomining of Rare Earth Elements", *Science Cannot Wait: New Horizons*, Košice, Slovakia, 29/11/2021, oral presentation

O.4. Phi Truong Dinh, Zsolt Dobó, Helga Kovács, "Enrichment of Rare Earth Elements from Contaminated Biomass Prior to Extraction", *ICOSTEE 2022 - International Conference on Science, Technology, Engineering and Economy*, Szeged, Hungary, 2022/03/24, poster presentation

O.5. T. Dinh, Z. Dobo, H. Kovacs, "Enrichment of valuable metals from contaminated biomass into combustion solid remains", *ECM 2023 – 11th European Combustion Meeting 2023*, Rouen, France, April 26–28 2023, poster presentation

LIST OF REFERENCES

[1] U.S. Energy and I. Administration, "DOE-EIA International Energy Outlook 2019," 2019, [Online]. Available: www.eia.gov/ieo

[2] V. Smil, *Energy transitions: global and national perspectives*. ABC-CLIO, 2016.

[3] T. B. Johansson, A. P. Patwardhan, N. Nakićenović, and L. Gomez-Echeverri, *Global energy assessment: toward a sustainable future*. Cambridge University Press, 2012.

[4] P. C. Abhilash, R. K. Dubey, V. Tripathi, P. Srivastava, J. P. Verma, and H. B. Singh, "Remediation and management of POPs-contaminated soils in a warming climate: challenges and perspectives," *Environ. Sci. Pollut. Res.*, vol. 20, no. 8, pp. 5879–5885, Aug. 2013, doi: 10.1007/s11356-013-1808-5.

[5] S. Alker, V. Joy, P. Roberts, and N. Smith, "The Definition of Brownfield," *J. Environ. Plan. Manag.*, vol. 43, no. 1, pp. 49–69, Jan. 2000, doi: 10.1080/09640560010766.

[6] P. Panagos, M. Van Liedekerke, Y. Yigini, and L. Montanarella, "Contaminated sites in Europe: Review of the current situation based on data collected through a European network," *Journal of Environmental and Public Health*, vol. 2013. 2013. doi: 10.1155/2013/158764.

[7] W.-S. Liu *et al.*, "Water, sediment and agricultural soil contamination from an ion-adsorption rare earth mining area," *Chemosphere*, vol. 216, pp. 75–83, Feb. 2019, doi: 10.1016/j.chemosphere.2018.10.109.

[8] H. Zhang *et al.*, "Chronic Toxicity of Rare-Earth Elements on Human Beings : Implications of Blood Biochemical Indices in REE-high Regions, South Jiangxi," *Biol. Trace Elem. Res.*, vol. 73, no. 1, pp. 1–18, 2000, doi: 10.1385/BTER:73:1:1.

[9] K. Bauddh, J. Korstad, and P. Sharma, Eds., *Phytorestoration of Abandoned Mining and Oil Drilling Sites*. Elsevier, 2021. doi: 10.1016/C2019-0-02457-0.

[10] I. Martínez-Alcalá and R. Clemente, "Phytoremediation of Metalloid-contaminated Soil," in *Metalloids in Plants*, Wiley, 2020, pp. 27–46. doi: 10.1002/9781119487210.ch3.

[11] R. L. Chaney *et al.*, "Phytoremediation of soil metals," *Curr. Opin. Biotechnol.*, vol. 8, no. 3, pp. 279–284, Jun. 1997, doi: 10.1016/S0958-1669(97)80004-3.

[12] A. van der Ent, A. J. M. Baker, G. Echevarria, M.-O. Simonnot, and J. L. Morel, Eds., *Agromining: Farming for Metals*. Cham: Springer International Publishing, 2021. doi: 10.1007/978-3-030-58904-2.

[13] V. Sheoran, A. S. Sheoran, and P. Poonia, "Phytomining: A review," *Miner. Eng.*, vol.

22, no. 12, pp. 1007–1019, Oct. 2009, doi: 10.1016/j.mineng.2009.04.001.

[14] D. E. Salt *et al.*, “Phytoremediation: A Novel Strategy for the Removal of Toxic Metals from the Environment Using Plants,” *Nat. Biotechnol.*, vol. 13, no. 5, pp. 468–474, May 1995, doi: 10.1038/nbt0595-468.

[15] A. van der Ent, A. J. M. Baker, R. D. Reeves, A. J. Pollard, and H. Schat, “Hyperaccumulators of metal and metalloid trace elements: Facts and fiction,” *Plant Soil*, vol. 362, no. 1–2, pp. 319–334, 2013, doi: 10.1007/s11104-012-1287-3.

[16] H. Kovacs, K. Szemmelveisz, and A. B. Palotas, “Solubility analysis and disposal options of combustion residues from plants grown on contaminated mining area,” *Environ. Sci. Pollut. Res.*, vol. 20, no. 11, pp. 7917–7925, Nov. 2013, doi: 10.1007/s11356-013-1673-2.

[17] J. He *et al.*, “Cadmium tolerance in six poplar species,” *Environ. Sci. Pollut. Res.*, vol. 20, no. 1, pp. 163–174, Jan. 2013, doi: 10.1007/s11356-012-1008-8.

[18] W. Zhenggui *et al.*, “Rare earth elements in naturally grown fern Dicranopteris linearis in relation to their variation in soils in South-Jiangxi region (Southern China),” *Environ. Pollut.*, vol. 114, no. 3, pp. 345–355, 2001, doi: 10.1016/S0269-7491(00)00240-2.

[19] L. Miao, Y. Ma, R. Xu, and W. Yan, “Environmental biogeochemical characteristics of rare earth elements in soil and soil-grown plants of the Hetai goldfield, Guangdong Province, China,” *Environ. Earth Sci.*, vol. 63, no. 3, pp. 501–511, 2011, doi: 10.1007/s12665-010-0718-9.

[20] W. O. Robinson, “The occurrence of rare earths in plants and soils,” *Soil Science*, vol. 56, no. 1. pp. 1–6, 1943. doi: 10.1097/00010694-194307000-00001.

[21] R. B. Anderson, Christopher W N Stewart, F. N. Moreno, C. T. J. Wreesmann, J. L. Gardea-Torresdey, B. H. Robinson, and J. A. Meech, “Gold phytomining. Novel developments in a plant-based mining system,” 2003.

[22] J. Borovička, Z. Řanda, E. Jelínek, P. Kotrba, and C. E. Dunn, “Hyperaccumulation of silver by Amanita strobiliformis and related species of the section Lepidella,” *Mycol. Res.*, vol. 111, no. 11, pp. 1339–1344, 2007, doi: 10.1016/j.mycres.2007.08.015.

[23] B. D. Krisnayanti, C. W. N. Anderson, S. Sukartono, Y. Afandi, H. Suheri, and A. Ekawanti, “Phytomining for artisanal gold mine tailings management,” *Minerals*, vol. 6, no. 3, pp. 1–11, 2016, doi: 10.3390/min6030084.

[24] C. Anderson, F. Moreno, and J. Meech, “A field demonstration of gold phytoextraction technology,” *Miner. Eng.*, vol. 18, no. 4, pp. 385–392, 2005, doi:

10.1016/j.mineng.2004.07.002.

[25] D. Walton, “The phytoextraction of gold and palladium from mine tailings: this thesis is presented in fulfilment of the requirements for the degree of Master of Philosophy.” Massey University, 2002.

[26] T. Nemutandani, D. Dutertre, L. Chimuka, E. Cukrowska, and H. Tutu, “The potential of Berkheya coddii for phytoextraction of nickel, platinum, and palladium contaminated sites,” *Toxicol. Environ. Chem.*, vol. 88, no. 2, pp. 175–185, 2006, doi: 10.1080/02772240600585842.

[27] H. M. Aquan, “Phytoextraction of palladium and gold from Broken Hill gossan: a thesis presented in partial fulfilment of the requirements for the degree of Master of Environmental Management at Massey University, Manawatū, New Zealand.” Massey University, 2015.

[28] B. H. Robinson, R. R. Brooks, A. W. Howes, J. H. Kirkman, and P. E. H. Gregg, “The potential of the high-biomass nickel hyperaccumulator Berkheya coddii for phytoremediation and phytomining,” *J. Geochemical Explor.*, vol. 60, no. 2, pp. 115–126, Dec. 1997, doi: 10.1016/S0375-6742(97)00036-8.

[29] C. W. . Anderson *et al.*, “Phytomining for nickel, thallium and gold,” *J. Geochemical Explor.*, vol. 67, no. 1–3, pp. 407–415, Dec. 1999, doi: 10.1016/S0375-6742(99)00055-2.

[30] B. ROBINSON, “Soil Amendments Affecting Nickel and Cobalt Uptake by Berkheya coddii: Potential Use for Phytomining and Phytoremediation,” *Ann. Bot.*, vol. 84, no. 6, pp. 689–694, Dec. 1999, doi: 10.1006/anbo.1999.0970.

[31] R. R. Brooks, “Copper and cobalt uptake byHaumaniastrum species,” *Plant Soil*, vol. 48, no. 2, pp. 541–544, Nov. 1977, doi: 10.1007/BF02187261.

[32] R. Reeves and A. Baker, “Metal-accumulating plants. Phytoremediation of Toxic Metals: Using Plants to Clean Up the Environment,” *John Wiley*, vol. 6, Jan. 2000.

[33] V. Bert, I. Bonnin, P. Saumitou-Laprade, P. de Laguerie, and D. Petit, “Do Arabidopsis halleri from nonmetallicolous populations accumulate zinc and cadmium more effectively than those from metallicolous populations?,” *New Phytol.*, vol. 155, no. 1, pp. 47–57, Jul. 2002, doi: 10.1046/j.1469-8137.2002.00432.x.

[34] F. Malaisse, R. R. Brooks, and A. J. M. Baker, “Diversity of vegetation communities in relation to soil heavy metal content at the Shinkolobwe copper/cobalt/uranium mineralization, Upper Shaba, Zaïre,” *Belgian J. Bot.*, pp. 3–16, 1994.

[35] S. . Xue, Y. . Chen, R. D. Reeves, A. J. . Baker, Q. Lin, and D. R. Fernando, “Manganese uptake and accumulation by the hyperaccumulator plant Phytolacca acinosa Roxb. (Phytolaccaceae),” *Environ. Pollut.*, vol. 131, no. 3, pp. 393–399, Oct. 2004, doi: 10.1016/j.envpol.2004.03.011.

[36] T. Mizuno, K. Emori, and S. Ito, “Manganese hyperaccumulation from non-contaminated soil in Chengiopanax sciadophylloides Franch. et Sav. and its correlation with calcium accumulation,” *Soil Sci. Plant Nutr.*, vol. 59, no. 4, pp. 591–602, Aug. 2013, doi: 10.1080/00380768.2013.807213.

[37] X.-H. Zhang, J. Liu, H.-T. Huang, J. Chen, Y.-N. Zhu, and D.-Q. Wang, “Chromium accumulation by the hyperaccumulator plant Leersia hexandra Swartz,” *Chemosphere*, vol. 67, no. 6, pp. 1138–1143, Apr. 2007, doi: 10.1016/j.chemosphere.2006.11.014.

[38] L. Q. Ma, K. M. Komar, C. Tu, W. Zhang, Y. Cai, and E. D. Kennelley, “A fern that hyperaccumulates arsenic,” *Nature*, vol. 411, no. 6836, pp. 438–438, May 2001, doi: 10.1038/35078151.

[39] P. Visoottiviseth, K. Francesconi, and W. Sridokchan, “The potential of Thai indigenous plant species for the phytoremediation of arsenic contaminated land,” *Environ. Pollut.*, vol. 118, no. 3, pp. 453–461, Aug. 2002, doi: 10.1016/S0269-7491(01)00293-7.

[40] M. Ghosh and S. P. Singh, “A review on phytoremediation of heavy metals and utilization of it’s by products,” *Asian J Energy Env.*, vol. 6, no. 4, p. 18, 2005.

[41] H. Kovacs and K. Szemmelveisz, “Disposal options for polluted plants grown on heavy metal contaminated brownfield lands – A review,” *Chemosphere*, vol. 166, pp. 8–20, Jan. 2017, doi: 10.1016/j.chemosphere.2016.09.076.

[42] A. Sas-Nowosielska, R. Kucharski, E. Małkowski, M. Pogrzeba, J. M. Kuperberg, and K. Kryński, “Phytoextraction crop disposal - An unsolved problem,” *Environ. Pollut.*, vol. 128, no. 3, pp. 373–379, 2004, doi: 10.1016/j.envpol.2003.09.012.

[43] T. Dinh, Z. Dobo, and H. Kovacs, “Phytomining of noble metals – A review,” *Chemosphere*, vol. 286, p. 131805, Jan. 2022, doi: 10.1016/j.chemosphere.2021.131805.

[44] T. Dinh, Z. Dobo, and H. Kovacs, “Phytomining of rare earth elements – A review,” *Chemosphere*, vol. 297, p. 134259, Jun. 2022, doi: 10.1016/j.chemosphere.2022.134259.

[45] H. Kovacs, Z. Dobo, T. Koos, A. Gyimesi, and G. Nagy, “Influence of the Flue Gas Temperature on the Behavior of Metals during Biomass Combustion,” *Energy and Fuels*, vol. 32, no. 7, pp. 7851–7856, 2018, doi: 10.1021/acs.energyfuels.8b00796.

[46] S. V. Vassilev, D. Baxter, and C. G. Vassileva, “An overview of the behaviour of

biomass during combustion: Part II. Ash fusion and ash formation mechanisms of biomass types," *Fuel*, vol. 117, no. PART A. pp. 152–183, 2014. doi: 10.1016/j.fuel.2013.09.024.

[47] H. Kovacs, K. Szemmelveisz, and T. Koós, "Theoretical and experimental metals flow calculations during biomass combustion," *Fuel*, vol. 185, pp. 524–531, 2016, doi: 10.1016/j.fuel.2016.08.007.

[48] I. Obernberger, F. Biedermann, W. Widmann, and R. Riedl, "Concentrations of inorganic elements in biomass fuels and recovery in the different ash fractions," *Biomass and Bioenergy*, vol. 12, no. 3. pp. 211–224, 1997. doi: 10.1016/S0961-9534(96)00051-7.

[49] T. Valmari, E. I. Kauppinen, J. Kurkela, J. K. Jokiniemi, G. Sfiris, and H. Revitzer, "Fly ash formation and deposition during fluidized bed combustion of willow," *J. Aerosol Sci.*, vol. 29, no. 4, pp. 445–459, 1998, doi: 10.1016/S0021-8502(97)10021-0.

[50] H. Kovacs, K. Szemmelveisz, and A. B. Palotas, "Environmentally Sound Combustion of Ligneous Plants Grown in Heavy Metal-Contaminated Soil," pp. 261–277, 2015, doi: 10.1007/978-3-319-14526-6_14.

[51] A. Nzihou and B. Stanmore, "The fate of heavy metals during combustion and gasification of contaminated biomass-A brief review," *Journal of Hazardous Materials*, vol. 256–257. pp. 56–66, 2013. doi: 10.1016/j.jhazmat.2013.02.050.

[52] L. Li, C. Yu, J. Bai, Q. Wang, and Z. Luo, "Heavy metal characterization of circulating fluidized bed derived biomass ash," *Journal of Hazardous Materials*, vol. 233–234. pp. 41–47, 2012. doi: 10.1016/j.jhazmat.2012.06.053.

[53] O. Dahl, H. Nurmesniemi, R. Pöykiö, and G. Watkins, "Comparison of the characteristics of bottom ash and fly ash from a medium-size (32 MW) municipal district heating plant incinerating forest residues and peat in a fluidized-bed boiler," *Fuel Processing Technology*, vol. 90, no. 7–8. pp. 871–878, 2009. doi: 10.1016/j.fuproc.2009.04.013.

[54] M. Narodoslawsky and I. Obernberger, "From waste to raw material - The route from biomass to wood ash for cadmium and other heavy metals," *J. Hazard. Mater.*, vol. 50, no. 2–3, pp. 157–168, 1996, doi: 10.1016/0304-3894(96)01785-2.

[55] B. Jally, B. Laubie, Y.-T. Tang, and M.-O. Simonnot, "Processing of Plants to Products: Gold, REEs and Other Elements," 2021, pp. 63–74. doi: 10.1007/978-3-030-58904-2_4.

[56] R. L. Chaney, "Phytoextraction and phytomining of soil nickel," in *Nickel in Soils and*

Plants, CRC Press, 2018, pp. 341–374.

[57] S. Cotton, *Chemistry of precious metals*. Springer Science & Business Media, 1997.

[58] W. M. Haynes, *Handbook of chemistry and physics*. CRC Press, 2016.

[59] N. Krishnamurthy and C. K. Gupta, *Extractive metallurgy of rare earths*. CRC press, 2015.

[60] W. Dastyar, A. Raheem, J. He, and M. Zhao, "Biofuel Production Using Thermochemical Conversion of Heavy Metal-Contaminated Biomass (HMCB) Harvested from Phytoextraction Process," *Chem. Eng. J.*, vol. 358, no. August 2018, pp. 759–785, 2019, doi: 10.1016/j.cej.2018.08.111.

[61] "Institute of rare earths and strategic metals." https://en.institut-seltene-erden.de/

[62] "London metal exchange." https://www.lme.com/

[63] "OSMIUM." https://www.osmium-preis.com/

[64] "Johnson Matthey." https://matthey.com/

[65] "World Gold Council." https://www.gold.org/

[66] "The Silver Institute." https://www.silverinstitute.org/

[67] D. Schüler, M. Buchert, R. Liu, S. Dittrich, and C. Merz, "Study on rare earths and their recycling," *Öko-Institut eV Darmstadt*, vol. 49, pp. 30–40, 2011.

[68] S. B. Castor and J. B. Hedrick, "Rare earth elements," *Ind. Miner. Rocks*, pp. 769–792, 2006.

[69] V. Balaram, "Rare earth elements: A review of applications, occurrence, exploration, analysis, recycling, and environmental impact," *Geosci. Front.*, vol. 10, no. 4, pp. 1285–1303, Jul. 2019, doi: 10.1016/j.gsf.2018.12.005.

[70] X. Pang, D. Li, and A. Peng, "Application of rare-earth elements in the agriculture of china and its environmental behavior in soil," *J. Soils Sediments*, vol. 1, no. 2, pp. 124–129, Jun. 2001, doi: 10.1007/BF02987718.

[71] K. Redling, "Rare earth elements in agriculture with emphasis on animal husbandry." lmu, 2006.

[72] D. Yan, S. Ro, O. Sunam, and S. Kim, "On the Global Rare Earth Elements Utilization and Its Supply-Demand in the Future," *IOP Conf. Ser. Earth Environ. Sci.*, vol. 508, p. 012084, Jul. 2020, doi: 10.1088/1755-1315/508/1/012084.

[73] S. Massari and M. Ruberti, "Rare earth elements as critical raw materials: Focus on international markets and future strategies," *Resour. Policy*, vol. 38, no. 1, pp. 36–43, Mar. 2013, doi: 10.1016/j.resourpol.2012.07.001.

[74] G. Gunn, Ed., *Critical Metals Handbook*. Oxford: John Wiley & Sons, 2014. doi: 10.1002/9781118755341.

[75] D.-R. DERA, "European Commission,'Critical Raw Materials Resilience: Charting a Path towards Greater Security and Sustainability,'" COM/2020/474 final (Brussels, 2020), https://eur-lex. europa. eu/legal …, 2021.

[76] E. C. E. Commission, "Critical Raw materials for the EU. Report of the Ad-hoc Working Group on defining critical raw materials." European Commission Brussels, 2010.

[77] C. W. N. Anderson, R. B. Stewart, F. N. Moreno, J. L. Gardea-torresdey, B. H. Robinson, and J. a Meech, "Gold phytomining . Novel Developments in a Plant-based Mining System," *Proc. Gold 2003 Conf. New Ind. Appl. Gold*, no. 2, pp. 35–45, 2003.

[78] A. van der Ent *et al.*, "Exceptional Uptake and Accumulation of Chemical Elements in Plants: Extending the Hyperaccumulation Paradigm," 2021, pp. 99–131. doi: 10.1007/978-3-030-58904-2_6.

[79] N. Feichtmeier and K. Leopold, "Bioavailability of Platinum Group Elements to Plants—A Review BT - Platinum Metals in the Environment," F. Zereini and C. L. S. Wiseman, Eds. Berlin, Heidelberg: Springer Berlin Heidelberg, 2015, pp. 311–338. doi: 10.1007/978-3-662-44559-4_20.

[80] F. A. Msuya, R. R. Brooks, and C. W. N. Anderson, "Chemically-induced uptake of gold by root crops: Its significance for phytomining," *Gold Bull.*, vol. 33, no. 4, pp. 134–137, 2000, doi: 10.1007/BF03215491.

[81] X. Xu, W. Zhu, Z. Wang, and G.-J. Witkamp, "Distributions of rare earths and heavy metals in field-grown maize after application of rare earth-containing fertilizer," *Sci. Total Environ.*, vol. 293, no. 1–3, pp. 97–105, Jul. 2002, doi: 10.1016/S0048-9697(01)01150-0.

[82] L. Brioschi *et al.*, "Transfer of rare earth elements (REE) from natural soil to plant systems: implications for the environmental availability of anthropogenic REE," *Plant Soil*, vol. 366, no. 1–2, pp. 143–163, May 2013, doi: 10.1007/s11104-012-1407-0.

[83] G. Tyler, "Rare earth elements in soil and plant systems - A review," *Plant Soil*, vol. 267, no. 1–2, pp. 191–206, Dec. 2004, doi: 10.1007/s11104-005-4888-2.

[84] A. E. Lamb, C. W. N. Anderson, and R. G. Haverkamp, "The induced accumulation of gold in the plants Brassica juncea, Berkheya coddii and chicory," *Chemistry in New Zealand*, vol. 65, no. 2. pp. 34–36, 2001.

[85] V. Wilson-Corral, C. Anderson, M. Rodriguez-Lopez, M. Arenas-Vargas, and J. Lopez-

Perez, “Phytoextraction of gold and copper from mine tailings with Helianthus annuus L. and Kalanchoe serrata L.,” *Miner. Eng.*, vol. 24, no. 13, pp. 1488–1494, 2011, doi: 10.1016/j.mineng.2011.07.014.

[86] K. Krzciuk and A. Gałuszka, “Prospecting for hyperaccumulators of trace elements: a review,” *Crit. Rev. Biotechnol.*, vol. 35, no. 4, pp. 522–532, Oct. 2015, doi: 10.3109/07388551.2014.922525.

[87] C. W. N. Anderson, R. R. Brooks, R. B. Stewart, and Robyn Simcock, “Harvesting a crop of gold in plants,” *Nature*, vol. 395, no. October, p. 553, 1998.

[88] R. C. R. Piccinin, S. D. Ebbs, S. M. Reichman, S. D. Kolev, I. E. Woodrow, and A. J. M. Baker, “A screen of some native Australian flora and exotic agricultural species for their potential application in cyanide-induced phytoextraction of gold,” *Miner. Eng.*, vol. 20, no. 14, pp. 1327–1330, 2007, doi: 10.1016/j.mineng.2007.07.005.

[89] R. G. Haverkamp, A. T. Marshall, and D. Van Agterveld, “Pick your carats: Nanoparticles of gold-silver-copper alloy produced in vivo,” *J. Nanoparticle Res.*, vol. 9, no. 4, pp. 697–700, 2007, doi: 10.1007/s11051-006-9198-y.

[90] E. Handayanto, N. Muddarisna, and B. D. Krisnayanti, “Induced phytoextraction of mercury and gold from cyanidation tailings of small-scale gold mining area of west Lombok, Indonesia,” *Adv. Environ. Biol.*, vol. 8, no. 5, pp. 1277–1284, 2014.

[91] E. González-Valdez *et al.*, “Induced accumulation of Au, Ag and Cu in Brassica napus grown in a mine tailings with the inoculation of Aspergillus niger and the application of two chemical compounds,” *Ecotoxicol. Environ. Saf.*, vol. 154, no. February, pp. 180–186, 2018, doi: 10.1016/j.ecoenv.2018.02.055.

[92] A. Sagiroglu, A. Sasmaz, and Ö. Sen, “Hyperaccumulator plants of the Keban mining district and their possible impact on the environment,” *Polish J. Environ. Stud.*, vol. 15, no. 2, pp. 317–325, 2006.

[93] A. T. Harris and R. Bali, “On the formation and extent of uptake of silver nanoparticles by live plants,” *J. Nanoparticle Res.*, vol. 10, no. 4, pp. 691–695, 2008, doi: 10.1007/s11051-007-9288-5.

[94] W. A. Fuchs and A. W. Rose, “The geochemical behavior of platinum and palladium in the weathering cycle in the Stillwater Complex, Montana,” *Econ. Geol.*, vol. 69, no. 3, pp. 332–346, 1974, doi: 10.2113/gsecongeo.69.3.332.

[95] E. L. Kothny, “Palladium in plant ash,” *Plant Soil*, vol. 53, no. 4, pp. 547–550, 1979.

[96] Z. A. S. Harumain, “Phytomining of precious metals from mine wastes.” University of

York, 2016.

[97] Z. A. S. Harumain *et al.*, “Toward Financially Viable Phytoextraction and Production of Plant-Based Palladium Catalysts,” *Environ. Sci. Technol.*, vol. 51, no. 5, pp. 2992–3000, Mar. 2017, doi: 10.1021/acs.est.6b04821.

[98] M. Kolodziej, I. Baranowska, and A. Matyja, “Determination of platinum in plant samples by voltammetric analysis,” *Electroanalysis*, vol. 19, no. 15, pp. 1585–1589, 2007, doi: 10.1002/elan.200703876.

[99] D. B. Diehl and Z. E. Gagnon, “Interactions between essential nutrients with platinum group metals in submerged aquatic and emergent plants,” *Water. Air. Soil Pollut.*, vol. 184, no. 1–4, pp. 255–267, 2007, doi: 10.1007/s11270-007-9414-0.

[100] K. Kińska and J. Kowalska, “Comparison of Platinum , Rhodium , and Palladium Bioaccumulation by Sinapis alba and their Influence on Phytochelatin Synthesis in Plant Tissues,” vol. 28, no. 3, pp. 1735–1740, 2019, doi: 10.15244/pjoes/89507.

[101] G. Bonanno, “Trace element accumulation and distribution in the organs of Phragmites australis (common reed) and biomonitoring applications,” *Ecotoxicol. Environ. Saf.*, vol. 74, no. 4, pp. 1057–1064, 2011, doi: 10.1016/j.ecoenv.2011.01.018.

[102] W. O. Robinson, R. Whetstone, and B. F. Scribner, “THE PRESENCE OF RARE EARTHS IN HICKORY LEAVES,” *Science (80-.).*, vol. 87, no. 2264, pp. 470–470, May 1938, doi: 10.1126/science.87.2264.470.

[103] W. O. Robinson, H. Bastron, and K. J. Murata, “Biogeochemistry of the rare-earth elements with particular reference to hickory trees,” *Geochim. Cosmochim. Acta*, vol. 14, no. 1–2, pp. 55–67, Aug. 1958, doi: 10.1016/0016-7037(58)90093-0.

[104] W. A. Thomas, “Accumulation of rare earths and circulation of cerium by mockernut hickory trees,” *Can. J. Bot.*, vol. 53, no. 12, pp. 1159–1165, 1975, doi: 10.1177/1087054713488438.

[105] H. Ichihashi, H. Morita, and R. Tatsukawa, “Rare earth elements (REEs) in naturally grown plants in relation to their variation in soils,” *Environ. Pollut.*, vol. 76, no. 2, pp. 157–162, 1992, doi: 10.1016/0269-7491(92)90103-H.

[106] M. Yuan *et al.*, “Accumulation and fractionation of rare earth elements (REEs) in the naturally grown Phytolacca americana L. in southern China,” *Int. J. Phytoremediation*, vol. 20, no. 5, pp. 415–423, Apr. 2018, doi: 10.1080/15226514.2017.1365336.

[107] M. Mohsin *et al.*, “Phytoextraction and recovery of rare earth elements using willow (Salix spp.),” *Sci. Total Environ.*, vol. 809, p. 152209, Feb. 2022, doi:

10.1016/j.scitotenv.2021.152209.

[108] T. Ozaki, S. Enomoto, Y. Minai, S. Ambe, and Y. Makide, “A Survey of Trace Elements in Pteridophytes,” *Biol. Trace Elem. Res.*, vol. 74, no. 3, pp. 259–274, 2000, doi: 10.1385/BTER:74:3:259.

[109] Y. Lai, Q. Wang, W. Yan, L. Yang, and B. Huang, “Preliminary study of the enrichment and fractionation of REEs in a newly discovered REE hyperaccumulator Pronephrium simplex by SEC-ICP-MS and MALDI-TOF/ESI-MS,” *J. Anal. At. Spectrom.*, vol. 20, no. 8, pp. 751–753, 2005, doi: 10.1039/b501766a.

[110] Y. Lai, Q. Wang, L. Yang, and B. Huang, “Subcellular distribution of rare earth elements and characterization of their binding species in a newly discovered hyperaccumulator Pronephrium simplex,” *Talanta*, vol. 70, no. 1, pp. 26–31, Aug. 2006, doi: 10.1016/j.talanta.2005.12.062.

[111] A. L. L. de Araújo, E. A. De Nadai Fernandes, M. A. Bacchi, and E. J. De França, “Bioaccumulation pattern of lanthanides in pteridophytes and magnoliophytes species from Atlantic Forest,” *J. Radioanal. Nucl. Chem.*, vol. 291, no. 1, pp. 187–192, Jan. 2012, doi: 10.1007/s10967-011-1283-8.

[112] N. Grosjean, D. Blaudez, M. Chalot, E. M. Gross, and M. Le Jean, “Identification of new hardy ferns that preferentially accumulate light rare earth elements: a conserved trait within fern species,” *Environ. Chem.*, vol. 17, no. 2, p. 191, 2020, doi: 10.1071/EN19182.

[113] Y. Q. Wang, J. X. Sun, H. M. Chen, and F. Q. Guo, “Determination of the contents and distribution characteristics of REE in natural plants by NAA,” *J. Radioanal. Nucl. Chem.*, vol. 219, no. 1, pp. 99–103, May 1997, doi: 10.1007/BF02040273.

[114] X. Shan *et al.*, “Accumulation and uptake of light rare earth elements in a hyperaccumulator Dicropteris dichotoma,” *Plant Sci.*, vol. 165, no. 6, pp. 1343–1353, Dec. 2003, doi: 10.1016/S0168-9452(03)00361-3.

[115] L. F. Wang, H. B. Ji, K. Z. Bai, L. B. Li, and T. Y. Kuang, “Photosynthetic characterization of the plant Dicranopteris dichotoma Bernh. in a rare earth elements mine,” *J. Integr. Plant Biol.*, vol. 47, no. 9, pp. 1092–1100, 2005, doi: 10.1111/j.1744-7909.2005.00138.x.

[116] Z. Chour *et al.*, “Recovery of rare earth elements from Dicranopteris dichotoma by an enhanced ion exchange leaching process,” *Chem. Eng. Process. - Process Intensif.*, vol. 130, pp. 208–213, Aug. 2018, doi: 10.1016/j.cep.2018.06.007.

[117] B. Laubie, Z. Chour, Y.-T. Tang, J.-L. Morel, M.-O. Simonnot, and L. Muhr, "REE Recovery from the Fern D. Dichotoma by Acid Oxalic Precipitation After Direct Leaching with EDTA," 2018, pp. 2659–2667. doi: 10.1007/978-3-319-95022-8_224.

[118] W.-S. Liu *et al.*, "Co-deposition of silicon with rare earth elements (REEs) and aluminium in the fern Dicranopteris linearis from China," *Plant Soil*, vol. 437, no. 1–2, pp. 427–437, Apr. 2019, doi: 10.1007/s11104-019-04005-0.

[119] B. Qin *et al.*, "Vacuum pyrolysis method for reclamation of rare earth elements from hyperaccumulator Dicranopteris dichotoma grown in contaminated soil," *J. Clean. Prod.*, vol. 229, pp. 480–488, Aug. 2019, doi: 10.1016/j.jclepro.2019.05.031.

[120] Z. Chour, B. Laubie, J. L. Morel, Y.-T. Tang, M.-O. Simonnot, and L. Muhr, "Basis for a new process for producing REE oxides from Dicranopteris linearis," *J. Environ. Chem. Eng.*, vol. 8, no. 4, p. 103961, Aug. 2020, doi: 10.1016/j.jece.2020.103961.

[121] C. Zhiqiang and C. Zhibiao, "Clipping strategy to assist phytoremediation by hyperaccumulator Dicranopteris dichotoma at rare earth mines," *Int. J. Phytoremediation*, vol. 22, no. 10, pp. 1038–1047, Aug. 2020, doi: 10.1080/15226514.2020.1725870.

[122] C. Liu *et al.*, "Element Case Studies: Rare Earth Elements," 2021, pp. 471–483. doi: 10.1007/978-3-030-58904-2_24.

[123] W.-S. Liu *et al.*, "Variation in rare earth element (REE), aluminium (Al) and silicon (Si) accumulation among populations of the hyperaccumulator Dicranopteris linearis in southern China," *Plant Soil*, Jan. 2021, doi: 10.1007/s11104-021-04835-x.

[124] B. Jally *et al.*, "A new method for recovering rare earth elements from the hyperaccumulating fern Dicranopteris linearis from China," *Miner. Eng.*, vol. 166, p. 106879, Jun. 2021, doi: 10.1016/j.mineng.2021.106879.

[125] H. V. Warren and R. E. Delavault, "Gold and silver content of some trees and horsetails in British Columbia," *Bull. Geol. Soc. Am.*, vol. 61, no. 2, pp. 123–128, 1950, doi: 10.1130/0016-7606(1950)61[123:GASCOS]2.0.CO;2.

[126] C. A. Girling and P. J. Peterson, "Gold in plants," *Gold Bull.*, vol. 13, no. 4, pp. 151–157, 1980, doi: 10.1007/BF03215461.

[127] V. Sheoran, A. S.Sheoran, and P. Poonia, "Phytomining of gold: A review," *J. Geochemical Explor.*, vol. 128, pp. 42–50, 2013, doi: 10.1016/j.gexplo.2013.01.008.

[128] V. Wilson-Corral, C. W. N. Anderson, and M. Rodriguez-Lopez, "Gold phytomining. A review of the relevance of this technology to mineral extraction in the 21st century," *J.*

Environ. Manage., vol. 111, pp. 249–257, 2012, doi: 10.1016/j.jenvman.2012.07.037.

[129] E. Herincs, M. Puschenreiter, W. Wenzel, and A. Limbeck, "A novel flow-injection method for simultaneous measurement of platinum (Pt), palladium (Pd) and rhodium (Rh) in aqueous soil extracts of contaminated soil by ICP-OES," *J. Anal. At. Spectrom.*, vol. 28, no. 3, pp. 354–363, 2013, doi: 10.1039/c3ja30367e.

[130] J. Singh and A. S. Kalamdhad, "Concentration and speciation of heavy metals during water hyacinth composting," *Bioresource Technology*, vol. 124. pp. 169–179, 2012. doi: 10.1016/j.biortech.2012.08.043.

[131] M. D. Hetland, J. R. Gallagher, D. J. Daly, D. J. Hassett, and L. V Heebink, "Processing of plants used to phytoremediate lead-contaminated sites.," in *Sixth international in situ and on site bioremediation symposium*, 2001, pp. 129–136.

[132] G. Yu, H. Lei, T. Bai, Z. Li, Q. Yu, and X. Song, "In-situ stabilisation followed by ex-situ composting for treatment and disposal of heavy metals polluted sediments," *Journal of Environmental Sciences*, vol. 21, no. 7. pp. 877–883, 2009. doi: 10.1016/S1001-0742(08)62357-8.

[133] P. Basu, *Biomass gasification and pyrolysis: practical design and theory*. Academic press, 2010.

[134] A. V. Bridgwater, D. Meier, and D. Radlein, "An overview of fast pyrolysis of biomass," *Org. Geochem.*, vol. 30, no. 12, pp. 1479–1493, Dec. 1999, doi: 10.1016/S0146-6380(99)00120-5.

[135] X. Hu and M. Gholizadeh, "Biomass pyrolysis: A review of the process development and challenges from initial researches up to the commercialisation stage," *J. Energy Chem.*, vol. 39, no. x, pp. 109–143, 2019, doi: 10.1016/j.jechem.2019.01.024.

[136] V. S. Sikarwar *et al.*, "An overview of advances in biomass gasification," *Energy Environ. Sci.*, vol. 9, no. 10, pp. 2939–2977, 2016, doi: 10.1039/c6ee00935b.

[137] A. Akhtar, V. Krepl, and T. Ivanova, "A Combined Overview of Combustion, Pyrolysis, and Gasification of Biomass," *Energy and Fuels*, vol. 32, no. 7, pp. 7294–7318, 2018, doi: 10.1021/acs.energyfuels.8b01678.

[138] L. Rosendahl, *Biomass combustion science, technology and engineering*. Elsevier, 2013.

[139] M. Lackner and Á. B. Palotás, *Combustion From Basics to Applications*. John Wiley & Sons, 2013.

[140] A. E. Lamb, C. W. N. Anderson, and R. G. Haverkamp, "The extraction of gold from plants and its application to phytomining," 2001.

[141] M.-O. Simonnot, J. Vaughan, and B. Laubie, “Processing of Bio-ore to Products BT - Agromining: Farming for Metals: Extracting Unconventional Resources Using Plants,” A. Van der Ent, G. Echevarria, A. J. M. Baker, and J. L. Morel, Eds. Cham: Springer International Publishing, 2018, pp. 39–51. doi: 10.1007/978-3-319-61899-9_3.

[142] W. J. Liu, W. W. Li, H. Jiang, and H. Q. Yu, “Fates of Chemical Elements in Biomass during Its Pyrolysis,” *Chem. Rev.*, vol. 117, no. 9, pp. 6367–6398, 2017, doi: 10.1021/acs.chemrev.6b00647.

[143] J. Koppejan and S. Van Loo, *The handbook of biomass combustion and co-firing*. Routledge, 2012.

[144] T. G. Ambaye, M. Vaccari, F. D. Castro, S. Prasad, and S. Rtimi, “Emerging technologies for the recovery of rare earth elements (REEs) from the end-of-life electronic wastes: a review on progress, challenges, and perspectives,” *Environ. Sci. Pollut. Res.*, vol. 27, no. 29, pp. 36052–36074, Oct. 2020, doi: 10.1007/s11356-020-09630-2.

[145] M. Firdaus, M. A. Rhamdhani, Y. Durandet, W. J. Rankin, and K. McGregor, “Review of High-Temperature Recovery of Rare Earth (Nd/Dy) from Magnet Waste,” *J. Sustain. Metall.*, vol. 2, no. 4, pp. 276–295, Dec. 2016, doi: 10.1007/s40831-016-0045-9.

[146] R. K. Jyothi, T. Thenepalli, J. W. Ahn, P. K. Parhi, K. W. Chung, and J.-Y. Lee, “Review of rare earth elements recovery from secondary resources for clean energy technologies: Grand opportunities to create wealth from waste,” *J. Clean. Prod.*, vol. 267, p. 122048, Sep. 2020, doi: 10.1016/j.jclepro.2020.122048.

[147] K. Binnemans *et al.*, “Recycling of rare earths: a critical review,” *J. Clean. Prod.*, vol. 51, pp. 1–22, Jul. 2013, doi: 10.1016/j.jclepro.2012.12.037.

[148] J. Cui and L. Zhang, “Metallurgical recovery of metals from electronic waste: A review,” *J. Hazard. Mater.*, vol. 158, no. 2–3, pp. 228–256, 2008, doi: 10.1016/j.jhazmat.2008.02.001.

[149] H. R. Watling, “The bioleaching of sulphide minerals with emphasis on copper sulphides — A review,” *Hydrometallurgy*, vol. 84, no. 1–2, pp. 81–108, Oct. 2006, doi: 10.1016/j.hydromet.2006.05.001.

[150] P. Rasoulnia, R. Barthen, and A.-M. Lakaniemi, “A critical review of bioleaching of rare earth elements: The mechanisms and effect of process parameters,” *Crit. Rev. Environ. Sci. Technol.*, vol. 51, no. 4, pp. 378–427, Feb. 2021, doi: 10.1080/10643389.2020.1727718.

[151] N. Das and D. Das, “Recovery of rare earth metals through biosorption: An overview,” *J. Rare Earths*, vol. 31, no. 10, pp. 933–943, Oct. 2013, doi: 10.1016/S1002-0721(13)60009-5.

[152] N. K. Gupta, A. Gupta, P. Ramteke, H. Sahoo, and A. Sengupta, “Biosorption-a green method for the preconcentration of rare earth elements (REEs) from waste solutions: A review,” *J. Mol. Liq.*, vol. 274, pp. 148–164, Jan. 2019, doi: 10.1016/j.molliq.2018.10.134.

[153] T. B. da Costa, M. G. C. da Silva, and M. G. A. Vieira, “Recovery of rare-earth metals from aqueous solutions by bio/adsorption using non-conventional materials: a review with recent studies and promising approaches in column applications,” *J. Rare Earths*, vol. 38, no. 4, pp. 339–355, Apr. 2020, doi: 10.1016/j.jre.2019.06.001.

[154] M. Wang, Q. Tan, J. F. Chiang, and J. Li, “Recovery of rare and precious metals from urban mines—A review,” *Front. Environ. Sci. Eng.*, vol. 11, no. 5, pp. 1–17, 2017, doi: 10.1007/s11783-017-0963-1.

[155] “High Concentrations of Rare Earth Elements Found in American Coal Basins | Department of Energy.” https://www.energy.gov/articles/high-concentrations-rare-earth-elements-found-american-coal-basins (accessed Dec. 17, 2021).

[156] J. E. Mungall and A. J. Naldrett, “Ore Deposits of the Platinum-Group Elements,” *Elements*, vol. 4, no. 4, pp. 253–258, Aug. 2008, doi: 10.2113/GSELEMENTS.4.4.253.

[157] S. Earle, *Physical geology*. BCcampus Open Education, 2019.

[158] M. L. Zientek, P. J. Loferski, H. L. Parks, R. F. Schulte, and R. R. Seal II, “Platinum-group elements,” Reston, VA, 2017. doi: 10.3133/pp1802N.

[159] R. D. Reeves, A. J. M. Baker, T. Jaffré, P. D. Erskine, G. Echevarria, and A. Ent, “A global database for plants that hyperaccumulate metal and metalloid trace elements,” *New Phytol.*, vol. 218, no. 2, pp. 407–411, Apr. 2018, doi: 10.1111/nph.14907.

[160] A. Bani, G. Echevarria, S. Sulçe, and J. L. Morel, “Improving the Agronomy of Alyssum murale for Extensive Phytomining: A Five-Year Field Study,” *Int. J. Phytoremediation*, vol. 17, no. 2, pp. 117–127, Feb. 2015, doi: 10.1080/15226514.2013.862204.

[161] X. Zhang, B. Laubie, V. Houzelot, E. Plasari, G. Echevarria, and M.-O. Simonnot, “Increasing purity of ammonium nickel sulfate hexahydrate and production sustainability in a nickel phytomining process,” *Chem. Eng. Res. Des.*, vol. 106, pp. 26–32, Feb. 2016, doi: 10.1016/j.cherd.2015.12.009.

[162] J. Tamás and E. Kovács, “Vegetation Pattern and Heavy Metal Accumulation at a Mine

Tailing at Gyöngyösoroszi, Hungary," *Zeitschrift für Naturforsch. C*, vol. 60, no. 3–4, pp. 362–368, Apr. 2005, doi: 10.1515/znc-2005-3-421.

[163] B. Horvath and K. Gruiz, "Impact of metalliferous ore mining activity on the environment in Gyongyosoroszi, Hungary," *Sci. Total Environ.*, vol. 184, no. 3, pp. 215–227, May 1996, doi: 10.1016/0048-9697(96)05104-2.

[164] G. Mathe-Gaspar, E. Sipter, T. Szili-Kovacs, T. Takacs, P. Mathe, and A. Anton, "Environmental Impact of Soil Pollution with Toxic Elements from the Lead And Zinc Mine at Gyöngyösoroszi (Hungary)," *Commun. Soil Sci. Plant Anal.*, vol. 40, no. 1–6, pp. 294–302, Mar. 2009, doi: 10.1080/00103620802647173.

[165] MBH Hungarian Biomass Recycling Co, "Technical data sheet for MBH VULCAN 30 pellet boiler."

[166] D. Ltd, "DEKATI ® PM10 IMPACTOR FOR ISO23210 MEASUREMENTS ISO 23210 description," 2009, [Online]. Available: www.dekati.fi

[167] G. Wu *et al.*, "Enrichment and occurrence form of rare earth elements during coal and coal gangue combustion," *Environ. Sci. Pollut. Res.*, vol. 29, no. 29, pp. 44709–44722, Jun. 2022, doi: 10.1007/s11356-022-18852-5.

[168] N. Lavrik and P. Henning, "Gold in ash and slag material of the Primorsk hydroelectric power," *E3S Web Conf.*, vol. 192, p. 03011, Sep. 2020, doi: 10.1051/e3sconf/202019203011.

[169] L. Wu, L. Ma, G. Huang, J. Li, and H. Xu, "Distribution and Speciation of Rare Earth Elements in Coal Fly Ash from the Qianxi Power Plant, Guizhou Province, Southwest China," *Minerals*, vol. 12, no. 9, p. 1089, Aug. 2022, doi: 10.3390/min12091089.

[170] A. V Taskin, I. S. Ivannikov, and O. S. Danilov, "Concentrating precious metals from ash and slag waste of Far Eastern energy enterprises," *IOP Conf. Ser. Earth Environ. Sci.*, vol. 87, no. 4, p. 042024, Oct. 2017, doi: 10.1088/1755-1315/87/4/042024.

[171] W. Franus, M. M. Wiatros-Motyka, and M. Wdowin, "Coal fly ash as a resource for rare earth elements," *Environ. Sci. Pollut. Res.*, vol. 22, no. 12, pp. 9464–9474, Jun. 2015, doi: 10.1007/s11356-015-4111-9.

[172] R. L. Thompson *et al.*, "Analysis of rare earth elements in coal fly ash using laser ablation inductively coupled plasma mass spectrometry and scanning electron microscopy," *Spectrochim. Acta Part B At. Spectrosc.*, vol. 143, pp. 1–11, May 2018, doi: 10.1016/j.sab.2018.02.009.

[173] S. V. Vassilev and C. G. Vassileva, "Methods for Characterization of Composition of

Fly Ashes from Coal-Fired Power Stations: A Critical Overview," *Energy & Fuels*, vol. 19, no. 3, pp. 1084–1098, May 2005, doi: 10.1021/ef049694d.

[174] B. G. Kutchko and A. G. Kim, "Fly ash characterization by SEM–EDS," *Fuel*, vol. 85, no. 17, pp. 2537–2544, 2006, doi: https://doi.org/10.1016/j.fuel.2006.05.016.

APPENDICES

Appendix 1. The major technical parameters of the boiler [166].

Parameters	Value	Unit
Nominal capacity	31	kW
Minimum capacity	9	kW
The maximum temperature that can be set	85	°C
The maximum permitted operating water pressure	2.5	bar
Pellet storage capacity	~ 130	kg
Weight of the boiler	320	kg
Efficiency	> 91	%
The maximum electric power consumption during ignition	350	W
The maximum electric power consumption during operation	50	W
Pellet consumption at maximum load	6.4	kg h^{-1}
Pellet consumption at minimum load	1.9	kg h^{-1}
Self-sustained uptime at maximum load	17	h
Self-sustained uptime at minimum load	58	h
Flue pipe diameter	80	mm
Height	1736	mm
Width	910	mm
Depth	655	mm

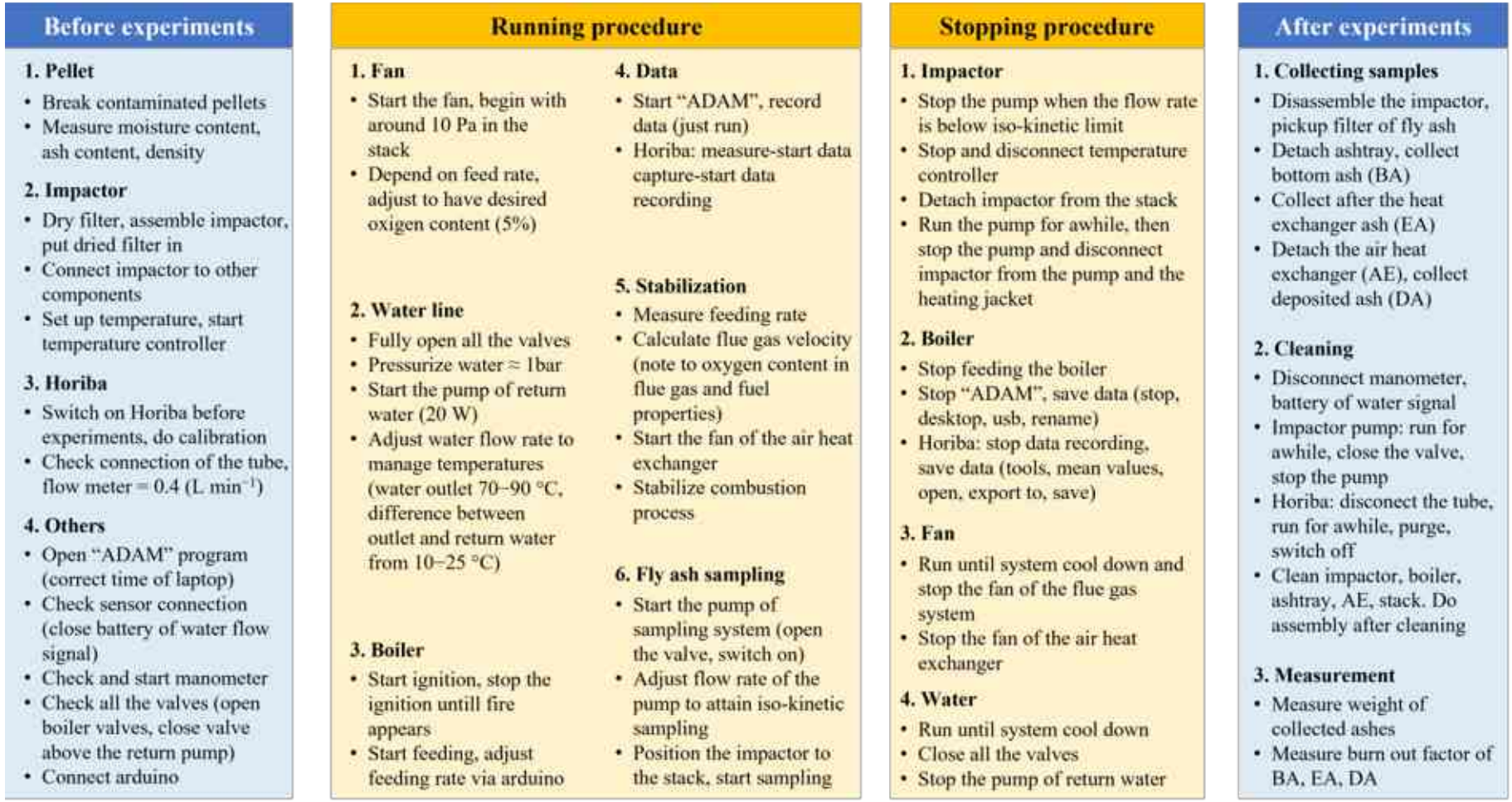

Appendix 2. The entire procedure of biomass combustion experiments.